

MULTIPLE ACTIVITIES OF ASPARTATE TRANSCARBAMOYLASE IN *Burkholderia*
cepacia: REQUIREMENT FOR AN ACTIVE DIHYDROOROTASE FOR ASSEMBLY
INTO THE DODECAMERIC HOLOENZYME

Hyunju Kim, B.S.

Dissertation Prepared for the Degree of
DOCTOR OF PHILOSOPHY

UNIVERSITY OF NORTH TEXAS

December 2010

APPROVED:

Gerard A. O'Donovan, Major Professor
Robert C. Benjamin, Committee Member
Rebecca Dickstein, Committee Member
Debrah A. Beck, Committee Member
John Knesek, Committee Member
Art J. Goven, Chair of the Department of
Biological Sciences
James D. Meernik, Acting Dean of the Robert
B. Toulouse School of Graduate Studies

Kim, Hyunju. *Multiple Activities of Aspartate Transcarbamoylase in Burkholderia cepacia: Requirement for an Active Dihydroorotase for Assembly into the Dodecameric Holoenzyme*. Doctor of Philosophy (Molecular Biology), December 2010, 161 pp., 7 tables, 55 figures, references, 148 titles.

The aspartate transcarbamoylase (ATCase) was purified from *Burkholderia cepacia* 25416. In the course of purification, three different ATCase activities appeared namely dodecameric 550 kDa holoenzyme, and two trimeric ATCases of 140 kDa (consists of 47 kDa PyrB subunits) and 120 kDa (consists of 40 kDa PyrB subunits) each. The 120 kDa PyrB polypeptide arose by specific cleavage of the PyrB polypeptide between Ser74 and Val75 creating an active polypeptide short by 74 amino acids. Both the 40 and 47 kDa polypeptides produced active trimers. To compare the enzyme activity of these trimers, an effector assay using nucleotides was performed. The 140 kDa trimer showed inhibition while the 120 kDa polypeptide showed less inhibition. To verify the composition of the *pyrBC* holoenzyme complex, *B. cepacia* dihydroorotase (DHOase, subunit size of 45 kDa) was purified by the pMAL protein fusion and purification system and holoenzyme reconstruction was performed using purified ATCase and DHOase. Both the 140 kDa and the 120 kDa trimers could produce holoenzymes of 550 kDa and 510 kDa, respectively. The reconstructed ATCase holoenzyme from cleaved ATCase showed better reconstruction compared to that from uncleaved ATCase in the conventional ATCase activity gel assay. To characterize the relationship between pyrimidine pathway and virulence factor production, motility tests and biofilm assays were conducted using

pyrC mutant. Even though no significant difference in growth rates was observed, there were significant differences between the wild type and mutant in the production of biofilm and virulence factors.

This study will help us to understand the structure and regulation of ATCase holoenzyme with DHOase, and facilitate the use of *B. cepacia* as an applicable bio-tool. Additionally, we can potentially pursue more efficient drug targets for *B. cepacia*.

Copyright 2010

by

Hyunju Kim

ACKNOWLEDGEMENTS

Dr. Gerard O'Donovan has been a great mentor. Without him I would not have finished the PhD program. He has always guided and trusted me, but when my research was moving from log phase to stationary phase, it was his feedback pushed me back into the log phase. Not only supporting my research, Dr. O'Donovan and Dr. Beck have been tremendous supporters of my family as we worked through the challenges of living in a foreign country. I still remember how nervous I was in Dr. Dickstein's Biochemistry course. This was the first course I took in the U.S. With her encouragement and knowledge from including two other advanced courses I became more confident and knew I could succeed. Dr. Benjamin has helped fill the 10 year gap between my college graduation and the start of my PhD program very quickly. Dr. Knesek, his cloning lab class was a great experience for me. He taught me many skills in Molecular Biology one-on-one, and always with a smile.

The support of my family has been invaluable. I thank my mother for believing in me from Korea. I also appreciate my sister and brother for being true friends when I needed. Seongcheol Kim, my best supporter and husband, has been a constant supporter while I have been doing this program. I also want to share this happiness with my lovely children, Stephanie and Anthony. They entitled me as a great mother and inspired me to be a good-effort Ph.D candidate. I also would like to share my happiness with all lab members Sara, Todd, Amy, Niazy, and Arwa, who have been good colleagues throughout the years and wish them success in their future.

TABLE OF CONTENTS

	Page
ACKNOWLEDGEMENTS-----	iii
LIST OF TABLES-----	v
LIST OF FIGURES-----	vi
CHAPTER	
1. INTRODUCTION-----	1
2. MATERIALS AND METHODS-----	35
3. RESULTS-----	75
4. DISCUSSION-----	125
REFERENCES-----	139

LIST OF TABLES

Table	Page
Table 1. The <i>Burkholderia</i> strains capable of degrading recalcitrant xenobiotics----	4
Table 2. <i>Burkholderia cepacia</i> complex species and strains with their genome sequences finished-----	10
Table 3. Potential virulence determinants of <i>B. cepacia</i> complex-----	17
Table 4. Classes of bacterial ATCases-----	28
Table 5. Bacterial strains and plasmids-----	36
Table 6. PCR primers used in this study-----	37
Table 7. Proposed new class of ATCase, class D, for <i>B.cepacia</i> -----	138

LIST OF FIGURES

1. Amino acid alignment of the <i>B. cepacia</i> PyrC sequence with other species of <i>Pseudomonas</i> -----	8
2. Scanned electron micrograph of <i>B. cepacia</i> 25416-----	9
3. Schematic diagram of biofilm formation in epithelial cells-----	12
4. Pyrimidine biosynthetic pathway-----	20
5. Salvage pathway of <i>P. aeruginosa</i> -----	26
6. Salvage pathway of <i>B. cepacia</i> -----	27
7. Map of pUC18 plasmid-----	46
8. Map of pMAL-c2E plasmid-----	49
9. Schematic diagram of the construction of pMAL- <i>B. cepacia pyrC</i> fusion plasmid-----	50
10. Schematic diagram of DHOase purification from pMAL-fusion protein purification system-----	52
11. Map of pGEX2T plasmid-----	57
12. Map of pEX18Gm plasmid-----	64
13. Transferring DNA from gel to nitrocellulose membrane-----	68
14. DNA sequence alignments of PyrC from <i>Burkholderia</i> spp.-----	76
15. Design of forward and reverse primers to amplify gene containing <i>B. cepacia pyrC</i> gene-----	77
16. PCR reaction to amplify <i>B. cepacia pyrC</i> -contained gene-----	78
17. Schematic diagram of construction of pHKeBC plasmid from inserting gene containing <i>B. cepacia pyrC</i> gene into pUC18 plasmid-----	79
18. Restriction digestion of pHKeBC plasmid-----	80
19. PCR reaction to amplify <i>B. cepacia pyrC</i> gene-----	81

20. Schematic diagram of construction of pHKeBC plasmid from inserting <i>B. cepacia pyrC</i> gene into pUC18 plasmid-----	82
21. Restriction digestion of pHKBC plasmid-----	83
22. Identified sequence of <i>B. cepacia pyrC</i> gene-----	85
23. Deposit of identified <i>B. cepacia pyrC</i> gene-----	86
24. Gene BLAST using NCBI data base-----	87
25. Complementation test-----	88
26. Schematic diagram of construction of pMHKBC plasmid from inserting <i>B. cepacia pyrC</i> gene into pMAL-c2E plasmid-----	89
27. Restriction digestion of pMHKBC plasmid-----	90
28. Purification of <i>B. cepacia</i> DHOase using pMAL protein fusion and purification system-----	92
29. Purification of highly purified <i>B. cepacia</i> DHOase by anion exchange chromatography-----	93
30. Enzyme kinetics of purified <i>B. cepacia</i> DHOases-----	95
31. Schematic diagram of construction of pSK2T plasmid from inserting <i>B. cepacia pyrB</i> gene into pGEX2T plasmid-----	96
32. Purification of <i>B. cepacia</i> ATCase using Glutathione S-transferase Gene Fusion System-----	97
33. ATCase activity gel assay-----	98
34. ATCase activity assay using purified uncleaved and cleaved <i>B. cepacia</i> ATCase-----	100
35. Effector assay of purified ATCases-----	102
36. Refolding of ATCase holoenzyme using purified <i>B. cepacia</i> ATCase and DHOase-----	103
37. Schematic diagram of construction of pEXHKBC plasmid from inserting <i>B. cepacia pyrC</i> gene into pEX18Gm plasmid-----	105

38. Restriction digestion of pEXHKBC plasmid-----	106
39. Schematic diagram of construction of pEXHKBCX plasmid from inserting <i>B. cepacia pyrC</i> gene into pEX18Gm plasmid-----	107
40. Restriction digestion of pEXHKBCX plasmid-----	108
41. PCR reaction to confirm the construction of <i>pyrC</i> knock out <i>B. cepacia</i> -----	109
42. PCR reaction to synthesize the probe to detect the deleted part of <i>pyrC</i> gene for Southern blot analysis-----	111
43. Restriction digestion of genomic DNA of wild type and <i>pyrC</i> knock out <i>B. cepacia</i> with <i>EcoRI</i> and <i>BamHI</i> enzymes-----	113
44. DIG-dUTP Hybridized Southern blot of <i>B. cepacia</i> wild type and <i>pyrC</i> mutant-----	114
45. Growth curve of <i>B. cepacia</i> wild type and <i>pyrC</i> mutant-----	116
46. Twitching motility assay-----	118
47. Swarming motility assay-----	119
48. Swimming motility assay-----	120
49. Microtiter plate biofilm assay-----	122
50. Air-liquid interface coverslip assay of 24 h cultured cells-----	123
51. Air-liquid interface coverslip assay of 48 h cultured cells-----	124
52. Feasible combination of DHOase and ATCase to make a ATCase holoenzyme-	133
53. Amino acids alignment of <i>B.cepacia</i> PyrC with Pseudomonad PyrC-----	134
54. Analysis of amino acids alignment of <i>B. cepacia</i> PyrC with Pseudomonad PyrC using Biology WorkBench-----	135
55. Expected locus of <i>B. cepacia pyrC</i> -----	136

CHAPTER 1

INTRODUCTION

What better microbial challenge to unite agricultural and medical microbiologists than an organism that reduces an onion to a macerated pulp, protects other crops from bacterial and fungal disease, devastates the health and social life of cystic fibrosis patients, and not only is resistant to the most famous of antibiotics, penicillin, but can use it as a nutrient!

J. R. W. Govan (Govan and Vandamme 1998)

Burkholderia cepacia was first described as the plant pathogen responsible for onion soft rot known as slippery skin during harvest and provided an appropriate species epithet (Latin: *cepa* = onion) by Burkholder in 1948 (Burkholder 1948).

Little was known about this organism until it emerged as an important opportunistic human pathogen in the early 1980s especially for cystic fibrosis patients. Cystic fibrosis (CF) is the most common genetic disease with approximately 1 in 2,500 Caucasians (carrier frequency of 1 in 25). The condition is characterized by defective ion channels, resulting in multiorgan dysfunction, most notably affecting the respiratory tract. The morbidity and mortality are greatly increased if the CF patient is infected with *B. cepacia* because many develop what is known as cepacia syndrome, which is a fatal necrotizing pneumonia. (Isles et al. 1984). The majority of CF is caused by *Pseudomonas aeruginosa* (*P. aeruginosa*). Infection with *B. cepacia* often occurs in patients who are already colonized with *P. aeruginosa*. In the United States, the median survival for CF patients infected with *B. cepacia* is 15.6 years, compared with 27.8 years for those

infected with *P. aeruginosa* (FitzSimmons 1998). Treatment of such infections is extremely difficult due to their high innate resistance to many antibiotics (Mahenthiralingam et al. 2005). The pathogenicity of *B. cepacia* is not limited to CF. Other groups, such as individuals with chronic granulomatous disease and immunocompromised patients are vulnerable and it has caused disease in healthy individuals.

Meanwhile, the organism has been developed as a biopesticide, and has seen potential as a bioremediation agent for breaking down recalcitrant herbicides and pesticides. Originally *B. cepacia* was known as a plant pathogen, but many *Burkholderia* species produce antimicrobial compounds which eliminate many soil-borne pathogens so it can protect plants from disease, particularly against fungal diseases (Holmes et al. 1998). Fungal pathogens such as *Fusarium*, *Pythium*, *Rhizoctonia*, *Cylindrocarpum*, and *Botrytis*, are known to cause widespread harm to the forestry industry. Those pathogenic fungi damage seedling grown in nurseries and stunt the growth of transplanted seedlings. A specific strain of *B. cepacia* has been developed as a successful seed and root inoculants that can inhibit these fungi on a variety of conifers (Reddy 1997). Other *Burkholderia* strains have been shown to be plant growth-promoting rhizobacteria (Thompson et al. 1997) and also nitrogen fixation is a common property in the genus *Burkholderia* (el-Banna and Winkelmann 1998). Recently, there is evidence suggesting that the members of *Burkholderia* genus are an ancient nitrogen-fixing symbiont of mimosa legumes adapted to acidic infertile soils (Bontemps et al. 2010).

In addition to all these features, *Burkholderia* species are capable of using over

200 organic compounds as carbon and energy sources (Fiore et al. 2001). This extraordinary nutritional versatility has led to the use of *Burkholderia* strains for biodegradation of environmental pollutants (Estrada-De Los Santos et al. 2001) as well as allowed their adaptation to a wide range of environments. Certain species of *Burkholderia* have already proved to be very efficient in biocontrol, bioremediation, and plant growth promotion. For example, *B. xenovorans* strain LB400 is one of the most highly effective polychlorinated biphenyl (PCB) degraders known (Chain et al. 2006). A summary of *Burkholderia* strains capable of degrading recalcitrant xenobiotics is available at the Biodegradative Strain Database (Table 1).

Although *B. cepacia* has an important environmental role in the agriculture and biotechnology industries, the use of *Burkholderia* strains in commercial applications has been strictly limited by the US Environmental Protection Agency as *Burkholderia* species have also emerged as opportunistic pathogens of humans, particularly in patients with CF (Parke and Gurian-Sherman 2001; Vandamme et al. 2007; Mahenthiralingam et al. 2008) or chronic granulomatous disease, as well. The selection of strains "safe" for environmental application is not presently possible phenotypically or genotypically.

Even "safe" strains could quickly develop into human pathogens due to their exceptional capacity of mutability. Therefore, their use represents a potential clinical risk to susceptible members of the community (Holmes et al. 1998). The microbiologists have described *B. cepacia* as "*Burkholderia cepacia*-Friend or Foe?" (Vidaver et al., *ASM News*, September 1999, p. 587) and "Killing fields--a Bacterial Pesticide May Threaten Human Life" Day, *New Scientist*, 23 May 1998, p. 5).

Table 1 The *Burkholderia* strains capable of degrading recalcitrant xenobiotics

Strain	Genus and species	Substrates
8	<i>Burkholderia cepacia</i>	benzoate; 4-fluorobenzoate; 4-hydroxybenzoate
AC1100	<i>Burkholderia cepacia</i>	2,3,4,6-tetrachlorophenol; 2,4,5-trichlorophenoxyacetate; pentachlorophenol (PCP)
G4	<i>Burkholderia cepacia</i>	benzene; meta-cresol; ortho-cresol; para-cresol; phenol; toluene; trichloroethylene (TCE)
KZ2	<i>Burkholderia cepacia</i>	2-chlorobenzoate
MB2	<i>Burkholderia cepacia</i>	2-methylbenzoate; 3-chloro-2-methylbenzoate
LB400	<i>Burkholderia fungorum</i>	biphenyl; polychlorinated biphenyls (PCBs)
KP23	<i>Burkholderia kururiensis</i>	trichloroethylene (TCE)
712	<i>Burkholderia</i> sp.	2,4-dichlorophenoxyacetate (2,4-D)
CBS3	<i>Burkholderia</i> sp.	4-chlorobenzoate; 2-nitrobenzoate; 3-nitrobenzoate; 4-nitrobenzoate; 3-nitrochlorobenzene; 2-nitrophenol; 3-nitrophenol; 4-nitrophenol; 2,4,6-trinitrotoluene
EML1549	<i>Burkholderia</i> sp.	2,4-dichlorophenoxyacetate (2,4-D)
JS150	<i>Burkholderia</i> sp.	benzene; benzoate; 1,2-dichlorobenzene; 1,4-dichlorobenzene; 2,5-dichlorophenol; 2-chlorophenol; 3-chlorophenol; meta-cresol; ortho-cresol; ethylbenzene; naphthalene; nitrobenzene; 2-nitrotoluene; 3-nitrotoluene; 4-nitrotoluene; phenol; salicylate; toluene; trichloroethylene (TCE)
RASC	<i>Burkholderia</i> sp.	2,4-dichlorophenoxyacetate (2,4-D)
RP007	<i>Burkholderia</i> sp.	benzoate; naphthalene; phenanthrene
TFD2	<i>Burkholderia</i> sp.	2,4-dichlorophenoxyacetate (2,4-D)
TFD39	<i>Burkholderia</i> sp.	2,4-dichlorophenoxyacetate (2,4-D)
TFD6	<i>Burkholderia</i> sp.	2,4-dichlorophenoxyacetate (2,4-D)

(Biodegradative Strain Database)

Members of genus *Burkholderia*, belong to the β subdivision of the proteobacteria, were initially classified in the genus *Pseudomonas* (previously *Pseudomonas cepacia*, *P. multivorans*, *P. kingii*), but have been reassigned to the newly created genus *Burkholderia* (Yabuuchi et al. 1992) on the basis of rRNA sequence analysis. Several reports have shown that *B. cepacia* is biologically quite distinct from *P. aeruginosa*. This is also supported by the present study, amino acid alignment of the *B. cepacia* PyrC sequence with other species of *Pseudomonas* has about 60% amino acid identity (Figure 1).

The general characteristics of *B. cepacia* include the following: Gram-negative rod, non-spore-forming, aerobe with a respiratory metabolism and catalase- positive and oxidase-positive; various nonfluorescent pigments may be produced and the optimal temperature for growth is 30- 35°C (Figure 2). Advances in molecular taxonomic analysis including whole-cell protein profiles, DNA-rRNA hybridization, DNA-DNA hybridization, fatty-acid analyses establish that the genus *Burkholderia* consists of several genomovars, which refers to a group of strains that is phenotypically similar but genotypically different (Coenye et al. 2001). The recent study has extended the complex to approximately 40 species, which comprises at least 17 distinct species (Vanlaere et al. 2008; Vanlaere et al. 2009). The bacterial strain used in this study is *B. cepacia* ATCC 25416, isolated in the 1940s by the American microbiologist Francis Burkholder from a decayed onion. Originally *B. cepacia* was considered a plant pathogen, but later it was also found in the sputum of a CF patient in the UK (Govan 2000). The genome of *B. cepacia* ATCC 25416, which belongs to genomovar I, is 8.1 Mb in length and is known

to have four circular replicons. (Rodley et al. 1995). Its genomic sequence has not been released so far. Most of the genomovars of the *B. cepacia* complex have been assigned a binomial species name and their genomic sequence is still very limited (Table 2). These bacteria are called the “*Burkholderia cepacia* complex” (Bcc) (Vandamme and Mahenthiralingam 2003; Huber et al. 2004; Baldwin et al. 2005). These organisms have been isolated from a wide range of ecological niches where they can have a range of beneficial properties. Strains from each of these species have been isolated from soil, water (including marine water), plants (particularly rhizosphere) (Payne et al. 2006), insects, fungi, and industrial settings (Coenye and Vandamme 2003; Mahenthiralingam and Vandamme 2005; Mahenthiralingam et al. 2008). Also, all species of *B. cepacia* complex have been isolated from patients with CF (Baldwin et al. 2007) and currently no prediction of the pathogenic potential of strains on the basis of its phylogenetic status is possible. This is obviously an area of interest between medicine and agriculture.

The ecological versatility of *Burkholderia* and capacity to propagate as environmental microbes and as opportunistic pathogens may be due to their unusually large genomes (twice that of *E. coli*). Many species contain one to five megaplasmids, and all species have circular chromosomes. The genome of *B. cepacia* consists of two to four chromosomes with an overall genome size of 5-9 Mb, which is rich in insertion sequences (Lessie et al. 1996; Wigley and Burton 2000). The genome comprises multiple replicons, allows unusual adaptability and easily facilitates the horizontal transfer of virulence genes from other pathogenic bacteria and, perhaps, the evolution of more virulent human pathogens (Govan et al. 1996). The evolution of multiple

chromosomes can be explained by three different mechanisms: by the split of a single chromosome, by chromosome duplication, or by acquisition of a large plasmid with essential genes. One replicon is typically larger, contains more essential genes than the others, and is considered the primary chromosome (Couturier and Rocha 2006).

A recent bioinformatics study suggested that the genes located on the secondary chromosomes exhibit a weaker codon usage bias than those located on the primary chromosome, being subject to a faster evolutionary rate (Cooper et al. 2010). The recent reports explained that the versatility of *B. cepacia* is reflected in the species' genome. For example, there are wide arrays of genomic islands variably represented across different *B. cepacia* strains that give each strain different characteristics.

These genomic islands were acquired via horizontal gene transfer from other soil saprophytes, consistent with a life in diverse environments outside of a host (Sim *et al.* 2008; Tuanyok *et al.* 2008; Tumapa *et al.* 2008), demonstrating that the genomes are adapted to different environmental conditions.

A few other bacterial species of agricultural and medical importance also have multiple chromosomes: *Brucella melitensis*, *B. abortus*, *B. suis*, *B. bovis*, *Sinorhizobium meliloti*, *Rhodobacter sphaeroides*, and *Agrobacterium tumefaciens* (Allardet-Servent *et al.* 1993; Michaux *et al.* 1993). Studying these organisms may give insight into the origin of multiple chromosomes in higher organism.

The specific virulence determinants utilized by *B. cepacia* during the course of infection are poorly understood compared to *P. aeruginosa*. One of the major problems associated with Bcc infection is their intrinsic resistance to most of the clinically

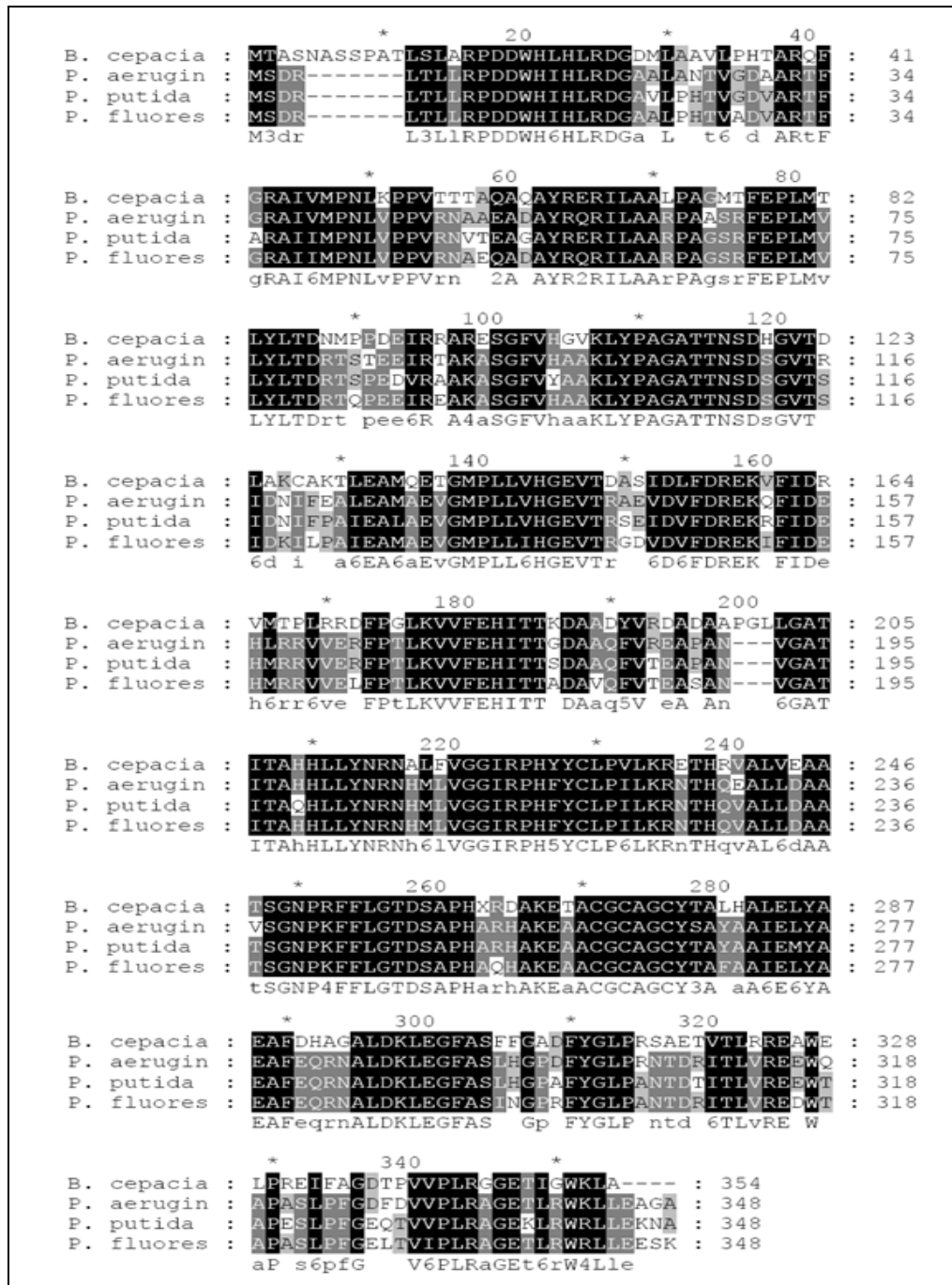


Fig. 1 Amino acid alignment of the *B. cepacia* PyrC sequence with other species of *Pseudomonas*.

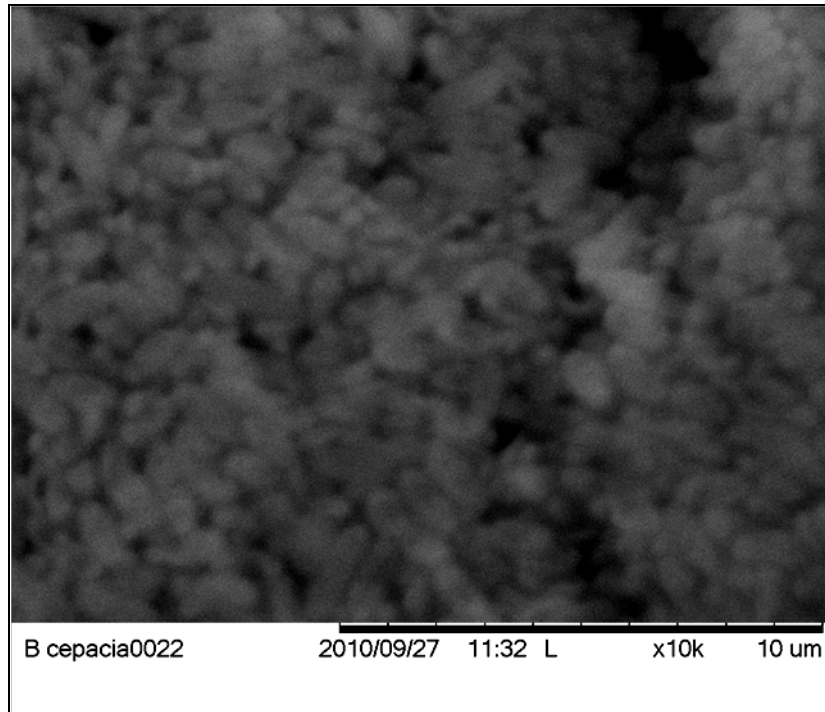


Fig. 2 Scanned electron micrograph of *B. cepacia* 25416. Image was taken by X10,000 total magnification.

Table 2 *Burkholderia cepacia* complex species and strains with their genome sequences completed.

Bcc Species	Strains sequenced
<i>B. cepacia</i>	
<i>B. ambifaria</i>	AMMD, MC40-6, MEX-5, IOP40-10
<i>B. multivorans</i>	ATCC17616
<i>B. cenocepacia</i>	J2315, MC0-3, AU1054, HI2424
<i>B. lata</i>	383
<i>B. mallei</i>	ATCC 23344, NCTC 10229, NCTC 10247, SAVP 1
<i>B. phymatum</i>	STM815
<i>B. pseudomallei</i>	1106a, 1710b, 668, K96243
<i>B. vietnamiensis</i>	G4
<i>B. dolosa</i>	
<i>B. glumae</i>	BGR1
<i>B. plantarii</i>	
<i>B. mana</i>	
<i>B. unamae</i>	
<i>B. oklahomensis</i>	
<i>B. phytofirmans</i>	PsJN
<i>B. tuberum</i>	
<i>B. ubonensis</i>	
<i>B. xenovorans</i>	LB400
<i>B. graminis</i>	
<i>B. thailandensis</i>	E264, ATCC 700388
<i>Burkholderia</i> sp.	
<i>Burkholderia</i> UFLA 4-5-1	

(<http://www.burkholderia.com/viewAllGenomes.do>)

available antimicrobials, including aminoglycosides, quinolones, and β -lactams (Chernish and Aaron 2003). In this study, the construction of *pyrC* knockout mutants in *B. cepacia* 25416 is hampered by unavailable genome information and the inherent resistance of this strain to the most antibiotics used for genetic selection. The multidrug resistance of *B. cepacia* results from several mechanisms which including various efflux pumps, changes the permeability of the membrane to the antibiotics and formation of biofilms (George et al. 2009). Biofilms are microbial communities that exist on abiotic or biotic surfaces. The severity of *B. cepacia* infection is due in part to its formation of biofilms, which have greater resistance to antibiotics than do planktonic cells (Djordjevic et al. 2002).

The first steps in the infection by *B. cepacia* are penetration of the mucosal blanket and subsequent adherence to the epithelial cell surface (Figure 3). The initiation of a biofilm is dependent upon the organism's pili and flagella used for attachment as well as through lateral movement which enlarges the colony. Twitching motility by Type IV pili enables the organism to move on solid surfaces. Pili are surface appendages that enhance bacterial adhesion to epithelial surface and to mucin (Sajjan and Forstner 1992). *B. cepacia* and *P. aeruginosa* often co-exist as mixed biofilms in the lungs of patients suffering from CF. Researchers have shown that infection with *P. aeruginosa* enhances the subsequent adhesion by *B. cepacia* in the lung of patients with CF (Saiman et al. 1990).

B. cepacia is a motile bacterium ranging from 1.6- 3.2 μm , and its motility is mediated by polar flagella (Hayashi et al. 2000). Motility has been shown to play an

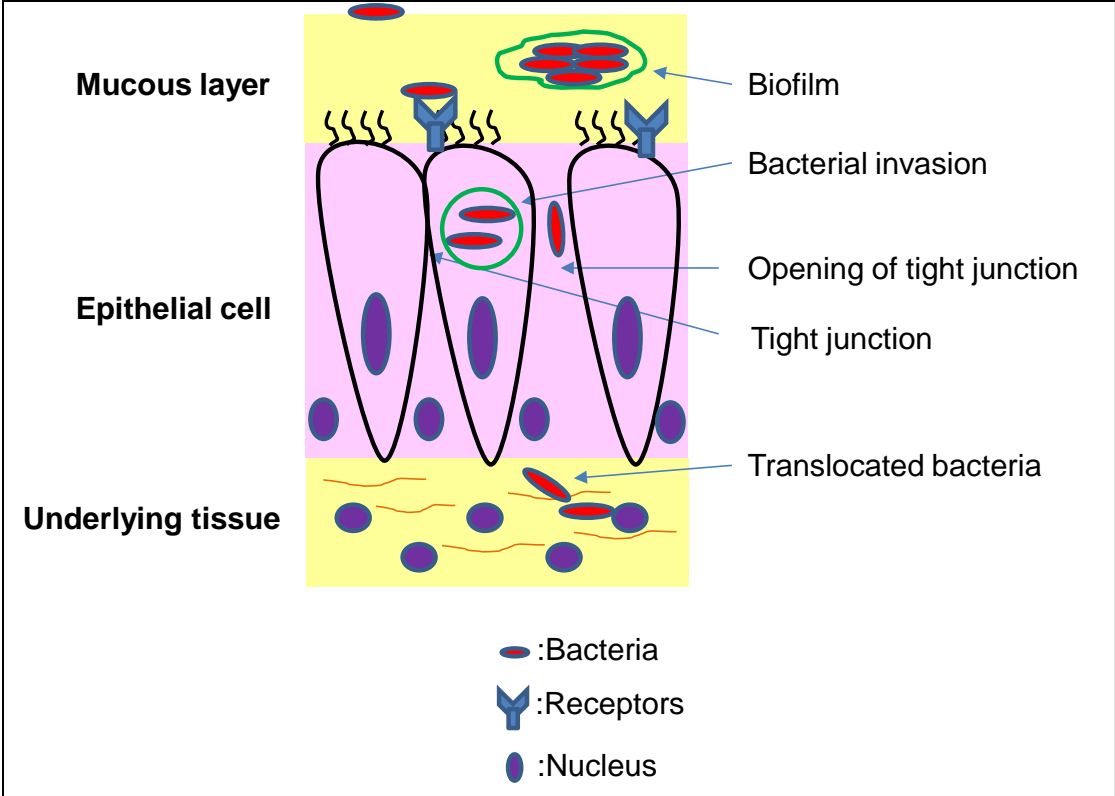


Fig. 3 Schematic diagram of biofilm formation in epithelial cells.

important role in the invasiveness of a number of bacterial pathogens. Mutations in genes encoding flagella have been shown to attenuate the virulence of several human pathogens, including *P. aeruginosa* and *Helicobacter pylori* (Eaton et al. 1992; Feldman et al. 1998). There is strong evidence that flagellum-mediated motility is a contributing factor in the ability of *B. cepacia* to invade respiratory epithelial cells (Tomich et al. 2002) . Thus, motility may be an important virulence determinant of *B. cepacia* for function in adhesion, the production of biofilms, and in the production of an inflammatory response in an infected host, overall enhancing the pathogenicity of the organism in the human host.

The beginning stages of infection have also been linked to the scavenging of iron. Iron is one of the most important nutrients for bacteria. However, oxygen and neutral pH oxidize Fe^{2+} to Fe^{3+} , which is not available to bacteria. Infection of the lung presents challenges to colonizing bacteria, not only due to the presence of alveolar macrophages, but also because this organ presents an iron restricted environment (Wang et al. 1996).

Therefore, the successful establishment of a niche within the lung requires an efficient means of iron capture. Bacteria have developed ways to scavenge iron with high affinity by producing siderophores, which are low-molecule-weight chelating molecules that sequester iron from other iron-containing molecules present in the surroundings. Members of the *B. cepacia* complex produce up to four different siderophores. *B. cepacia* 25416 is known to produce salicylic acid, pyochelin, ornibactin, and cepabactin.

Salicylic acid, or 2-hydroxybenzoic acid, serves as a precursor for the production of a variety of siderophores. It has iron-binding properties and appears to be able to

compete with transferring of iron and promote iron uptake as well as growth of many bacteria in iron-limiting conditions. Salicylic acid was previously reported to be produced by 88% of *B. cepacia* respiratory isolates from CF patients (Sokol et al. 1992; Visca *et al.* 1993).

Pyochelin is derived from the condensation of salicylic acid with two molecules of cysteine, which requires the presence of non-ribosomal peptide synthetases (NRPS) PchE and PchF. In a previous study of 43 *B. cepacia* isolates from CF patients from Toronto and Cleveland, 49% were found to produce pyochelin. The majority of pyochelin-positive strains were isolated from patients with severe pulmonary disease, with more than half of infections resulting in death (Sokol 1986).

Ornibactin appears to be the only siderophore produced by the *Burkholderia* and not made by fluorescent pseudomonads such as *P. aeruginosa* and cannot be utilized by them. (Meyer et al. 1995). It is a linear tetrapeptide derivative that chelates iron by providing three bidentate metal chelation groups (Stephan et al. 1993). It also appears to be the most prevalent siderophore among the *Burkholderia*, and is produced by a high proportion of clinical isolates. (Darling et al. 1998).

Cepabactin, 1-hydroxy-5-methoxy-6-methyl-2(1H)-pyridinone, is a cyclic hydroxamate. It was shown to have all the characteristics of a siderophore: biosynthesis of cepabactin occurred only under iron starvation conditions. There are no reports describing the production of cepabactin in clinical isolates of *B. cepacia* (Meyer et al. 1989).

Knockout of iron acquisition mechanisms has also been shown to attenuate the

virulence of many bacteria (Lawlor et al. 2007). Darling *et al.* reported that ornibactins and salicylic acid are the predominant siderophores produced by CF isolates and that pyochelin may also be an important siderophore for *B. cepacia*. Analysis of siderophores in *B. cepacia* and their effects to the cystic fibrosis should be performed in conjunction with a molecular typing method such as RAPD analysis with representative groups of strains prior to forming conclusions regarding their significance in particular patient populations (Darling et al. 1998).

The next step in pathogenesis is the invasion of lung epithelial cell and also translocation across the epithelium to the serosal side. Virulence factors that enhance its pathogenicity in epithelial cells include lipase, metalloproteases, and serine proteases. Lipases catalyze the hydrolysis and synthesis of esters of glycerol with long-chain fatty acids and play a role in the invasion of lung epithelial cells. Interestingly, lipase is now considered a candidate for biodiesel fuel production. Nouredini et al. (2005) used the transesterification of soybean oil with methanol, ethanol, and lipases from different microorganisms to determine which microorganism would yield the highest amount of alkyl esters which is another name for the molecules that are commonly referred to as biodiesel. They determined that the lipase from *B. cepacia* resulted in the highest yield of alkyl esters (Nouredini et al. 2005).

Metalloproteases also play an important role in the virulence of *B. cepacia* in lung tissue. ZmpA, a zinc metalloprotease, is one of the protease produced by *B. cepacia* 25416. The mature ZmpA is proteolytically active to type IV collagen, fibronectin, neutrophil alpha-1 protease inhibitor, alpha 2-macroglobulin, and gamma interferon

(Kooi et al. 2005).

Serine proteases have been shown to be a key factor in the intracellular invasion of lung tissue and also shown to be responsible for the ability of *B. cepacia* to utilize the ferritin as an iron source (Whitby et al. 2006). Ferritin concentrations are particularly high in the lungs of CF patients as compared to the non-CF lungs. Ferritin has not been shown to be an iron source for any other pathogenic bacteria thus far, which gives a significant advantage for *B. cepacia* (Whitby et al. 2006; McClean and Callaghan 2009).

In addition to the processes of attachment and invasion, Bcc produces a range of virulence factors that enhance its pathogenicity in epithelial cells (Table 3). In most cases, synthesis of these factors is controlled by a quorum-sensing (QS) system. A QS system is a mechanism for regulating gene expression that allows bacteria to monitor their own population density. The QS system in the members of the *B. cepacia* complex is very well conserved and has been involved in the regulation of expression of extracellular proteins and siderophores and also with the regulation of motility, biofilm formation, plasmid transfer and antibiotic resistance (Huber et al. 2001; Conway *et al.* 2002; Aguilar et al. 2003). In such a system, it involves the production of autoinducer signaling molecules, which are normally *N*-acyl homoserine lactones (AHLs) in Gram-negative bacteria, and a transcriptional regulator. As mentioned above, all species in Bcc have been recovered from CF patients (Mahenthiralingam et al. 2002) which means all members of the *B. cepacia* complex may share pathogenic potential. But the most prevalent ones are *B. cenocepacia* and *B. multivorans*. *B. cenocepacia* H111, which was isolated from a CF patient, employs a QS system, encoded by *cep* genes, to control the

Table 3 Potential virulence determinants of *B. cepacia* complex

Class	Factors
Extracellular enzymes	Proteases Lipases Chitinases Collagenase Polygalacturonase Phospholipase C
Siderophores	Salicylic acid Pyochelin Omibactin Malleobactin Cepabactin Cepaciachelin
Toxins	Toxoflavin Tropolone Rhizobitoxine Rhizoxin Bongkrek acid Rhizonin
Antifungal and other antimicrobials	Pyrolnitrin Xylocandin complex Quinoline Derivatives Glidobactins CF661 2-Hydroxymethyl-chroman-4-one Altericidins Cepacins A and B Cepaciamides A and B Hydrogen Cyanide Phenazines Volatile Compounds

expression of virulence factors as well as the formation of biofilms (Huber et al. 2001). It has also been shown that ornibactin biosynthesis is influenced by QS. Mutations in the *cepR* or *cepI* genes, encoding a LuxR/LuxI type quorum sensing regulatory system, result in an approximately 65% increase in ornibactin biosynthesis in *B. cenocepacia*, but exert no effect on salicylate or pyochelin production (Lewenza et al. 1999; Lewenza and Sokol 2001; Malott et al. 2005).

The pathogenicity of these bacteria is believed to be involved a number of potential or contributing virulence factors. In order to identify a potential drug target, a gene of interest or gene product must be essential for survival of the pathogen while presenting little or no conservation in humans and it should be conserved in the various strains of the pathogen (Sousa et al. 2010). In this aspect, the pyrimidine biosynthetic pathway is ideal for the potential therapeutic targets. This pathway is not only the essential and conserved for almost all organisms, but also has significant differences between prokaryotes and eukaryotes.

The Pyrimidine Biosynthetic Pathway

Nucleotides participate in nearly all biological processes. Purines and pyrimidines are the activated precursors of nucleic acids. They can be universal energy sources and are involved in signal transduction pathways. A sufficient supply of nucleotides is vital for most life. Previous study has shown that pathogens require nucleotide biosynthesis to establish a successful infection (McFarland and Stocker 1987). Biosynthesis of pyrimidines is critical for the growth of bacteria in human serum (Samant

et al. 2008). Thus, nucleotide biosynthetic pathways are extremely important as interference points for therapeutic agents.

The pyrimidine nucleotide biosynthetic pathway provides the building blocks namely UTP and CTP for ribonucleic acid (RNA), and dCTP and dTTP for deoxyribonucleic acid (DNA). This pathway falls into two classes; de novo pathways and salvage pathways.

De novo Synthesis of UTP and CTP

In de novo pathways, the nucleotide bases are assembled from simpler compounds and a free base is converted to a nucleotide, UMP (Figure 4). The end product of this pathway, UMP (uridine- 5'-monophosphate), is synthesized in six steps catalyzed by conserved enzymes in all three domains of life even though structure and the regulation of the enzymes differ from one to another. UMP is the precursor for all the pyrimidine nucleotides. UTP is formed by phosphorylation of UMP, and CTP is synthesized by the amination of UTP. This pathway has been most extensively studied in *E. coli* and *Salmonella typhimurium* (O'Donovan and Neuhard 1970; Grogan and Gunsalus 1993), and is the same as found in *P. aeruginosa*. This pathway is a series of nine reactions, which lead to the formation of uridine-5-triphosphate (UTP) and cytidine-5-triphosphate (CTP).

Carbamoylphosphate synthetase (CPSase, EC 6.3.5.5.), encoded by *carAB* operon, is an allosteric enzyme that catalyzes the synthesis of carbamoylphosphate from bicarbonate and glutamine at the expense of two molecules of ATP (Anderson and Meister 1965).

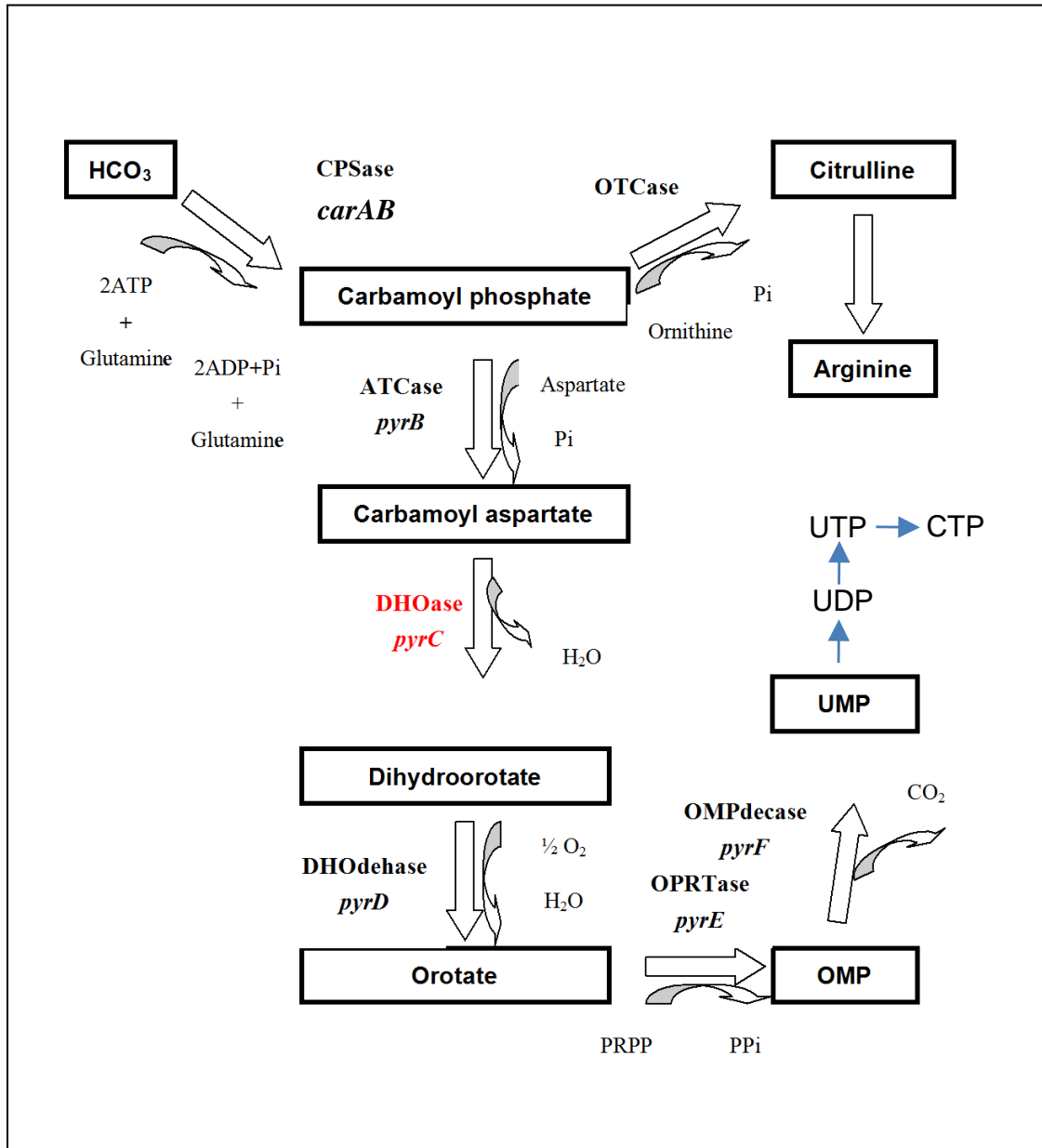


Fig. 4 Pyrimidine biosynthetic pathway.

Aspartate carbamoyltransferase (ATCase, EC 2.1.3.2), encoded by *pyrBI* in *E. coli*, catalyzes the first unique step of pyrimidine biosynthesis whereby the condensation of carbamoyl phosphate and L-aspartate forms N-carbamoyl-L-aspartate and releases inorganic phosphate (Pi) (Pardee and Yates 1956; Gerhart and Pardee 1962).

Dihydroorotase (DHOase, EC 3.5.2.3.), encoded by *pyrC*, catalyzes the cyclization of N-carbamoyl-L-aspartate (CAA), the product of the ATCase reaction, to L-dihydroorotate (DHO) (Washabaugh and Collins 1986). The reaction is readily reversible and pH-dependent (Christopherson and Jones 1979); (Porter et al. 2004). The biosynthetic direction (cyclization of L-CA-asp to L-DHO) is favored at lower pH, while the degradative rate (L-DHO to L-CA-asp) is maximal at alkaline pH. DHOase is a metallo-enzyme and has been reported to contain one tightly bound essential zinc ion per subunit in addition to two weakly bound structural zinc ions per subunit which are not essential for activity. Comparison of the amino acid sequences of DHOase from various species reveals that two conserved histidine-containing regions are likely to be involved in active-site zinc binding.

Dihydroorotate dehydrogenase (DHOdehase, EC 1.3.3.1), encoded by *pyrD*, is the only membrane bound enzyme in this pathway. This enzyme catalyzes the redox reaction in de novo UMP biosynthesis in which dihydroorotate is oxidized to orotate (Karibian and Couchoud 1974; Larsen and Jensen 1985).

Orotate phosphoribosyl transferase (OPRTase, EC 2.2.4.10), encoded by *pyrE*, produces the first nucleotide, orotidine-5'-monophosphate (OMP) (Lieberman and Kornberg 1954). OMP and PP_i are produced from orotate and PRPP in a Mg²⁺ -

dependent reaction.

OMP decarboxylase (OMPdecase, EC 4.1.1.23), encoded by *pyrF*, catalyzes the final reaction of de novo pyrimidine nucleotide biosynthesis (Scapin et al. 1993). OMP is decarboxylated to yield UMP, the precursor compound for all other pyrimidine nucleotides.

Uridine monophosphate kinase (UMP kinase, EC 2.7.4.4), encoded by *pyrH*, catalyzes the next step in pyrimidine synthesis which is the phosphorylation of UMP to UDP.

Nucleoside diphosphate kinase (NDK, EC2.7.4.6) catalyzes the phosphorylation of UDP to UTP using ATP (Ginther and Ingraham 1974).

Cytidine triphosphate synthetase (CTP synthetase, EC 6.3.4.2) is encoded by *pyrG*. In the last step in pyrimidine ribonucleotide biosynthesis, CTP synthetase catalyzes the formation of CTP from UTP, ATP, and glutamine (Long and Koshland 1978; Anderson 1983). This step is also stimulated by GTP (Levitzki and Koshland 1972).

To provide the cells with a balanced supply of rNTPs and dNTPs for RNA and DNA synthesis, the pathway is regulated at the transcriptional or translational level. In *E. coli*, the pathway is regulated through allosteric enzymes at five strategic points:

(i) In the first reaction of the pathway, CPSase is feedback-regulated in accordance with its metabolic role. If the supply of carbamoylphosphate becomes limiting for arginine synthesis, ornithine and inosine-5'-monophosphate (IMP) accumulates and antagonize the inhibition by UMP. In the presence of excess arginine, ornithine is not produced, and the enzyme is controlled solely by UMP. The

physiological importance of this control is illustrated by the observation that mutations rendering CPSase hypersensitive to inhibition by UMP induce a uracil-sensitivity phenotype.

(ii) ATCase catalyzes the second step, but is the first committed step of the pathway. It is inhibited by CTP (Gerhart and Pardee 1962; Gerhart and Pardee 1964) and activated by ATP (Wild et al. 1981). It is also regulated by UMP, which inhibits enzyme activity by increasing its apparent K_m for the carbamoyl phosphate substrate.

(iii) UMP kinase is one of the regulation points in the pyrimidine pathway and is allosterically regulated by the positive regulator GTP and a negative regulator UTP (O'Donovan and Gerhart 1972; Serino and Maliga 1997).

(iv) CTP synthetase, encoded by *pyrG*, catalyzes the amination of UTP to CTP, and is inhibited by CTP and activated by UTP (Long and Pardee 1967; Long and Koshland 1978).

(v) The conversion of dCTP to dTTP.

In addition, the pathway is controlled at the enzyme synthesis level by attenuation (Hoover et al. 1983; Turnbough et al. 1983). The genes *pyrBI* and *pyrE* that encode ATCase and OPRTase, respectively, have upstream leader sequences that allow attenuation control (Navre and Schachman 1983).

In *Pseudomonas*, the regulation is brought about by purine and pyrimidine nucleotide effectors (Chu and West 1990). CPSase enzyme activity is inhibited by UMP and activated by ornithine and N-acetylorithine (Abdelal et al. 1983). The *P. aeruginosa* ATCase, encoded by *pyrBC'*, is inhibited by ATP and UTP. CTP was also an

inhibitor but not to the same extent as ATP and UTP (Isaac and Holloway 1968; Condon *et al.* 1976; Schurr *et al.* 1995). A regulatory protein PyrR was identified that regulates the expression of downstream pyrimidine biosynthetic genes *pyrD*, *pyrE*, and *pyrF* and the expression of the *pyrR* gene (Patel 2000). The ATCase of *P. putida* was reported to be inhibited by pyrophosphate, ATP, UTP and CTP (Condon *et al.* 1976).

The Salvage Pathway

Pyrimidine bases or nucleosides, released by the degradation of mRNA, can be salvaged and recycled in the salvage pathway. This pathway economizes intracellular energy expenses. In prototrophs, scavenged bases and nucleosides are restored to the nucleotide level such as UMP, CTP, or ATP. These nucleotides increase feedback inhibition at the committed steps in the biosynthetic pathway while decreasing expression of the *pyr* genes. Thus, the salvage pathways share the RNA synthesis with the de novo pathway while providing all the necessary pyrimidine requirements to pyrimidine auxotrophs (O'Donovan and Shanley 1999).

The other importance of the salvage pathway is making the pentose portions of nucleosides as well as the free amino group of cytosine available for carbon, energy and nitrogen sources of bacteria. Accumulation of breakdown products of mRNA can be toxic to the cell and therefore are removed very quickly (Womack and O'Donovan 1978). The salvage pathway has been studied in more than 40 different wild type bacteria and their mutants (Beck 1995). Figure 5 and Figure 6 shows the pyrimidine salvage pathways of *P. aeruginosa* and *B. cepacia* which varies from organism to organism. Whereas the

biosynthetic pathway of pyrimidine ribonucleotides is virtually the same for all organisms, the salvage pathway differs among some species making it valuable as a potential taxonomic marker. While the biosynthetic pathway is present in all but a few bacteria that are obligate intracellular parasites (Zientz et al. 2004), some aspect of the salvage pathway is present in every bacterium so far studied (Turnbough and Switzer 2008).

Classification of Bacterial Aspartate Transcarbamoylase

In bacteria, the pyrimidine biosynthetic pathway is primarily regulated at the ATCase reaction. ATCase has been intensively studied over the last 40 years as a model of allosteric enzyme (Herve 1981; Lipscomb 1994). The molecular mass and kinetic properties of bacterial ATCases have been used to categorize ATCase into three classes that follow phylogenetic lines (Bethell and Jones 1969).

All ATCases are composed of a basic subunit - the product of gene *pyrB* - which assembles in catalytic homotrimers. The PyrB polypeptide itself is composed of two structural domains which respectively bind the substrates carbamoylphosphate (N-half) and aspartate (C-half). Prokaryotic ATCases correspond to different classes of quaternary structures according to the mode of association of the catalytic PyrB subunit with other polypeptides: either the PyrI regulatory subunit (class B) or a dihydroorotase (class A), which may be active (PyrC, subclass A1) or inactive (PyrC', subclass A2). Class C is made uniquely of trimers of PyrB (Table 4).

The best studied ATCase is that of *E. coli* and its properties have been reviewed extensively

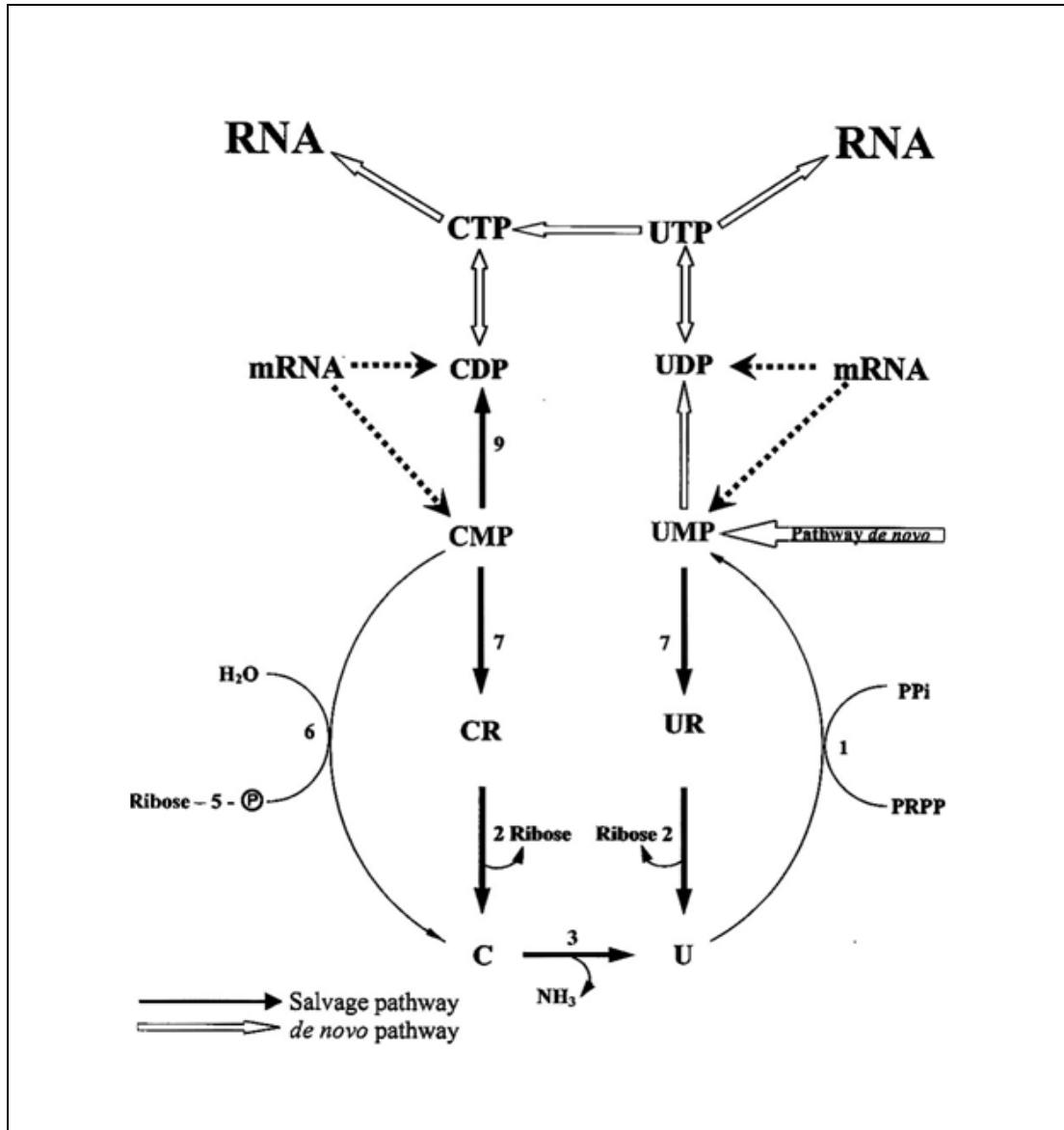


Fig. 5 Salvage pathway of *P. aeruginosa*. (Beck and O'Donovan 2008)

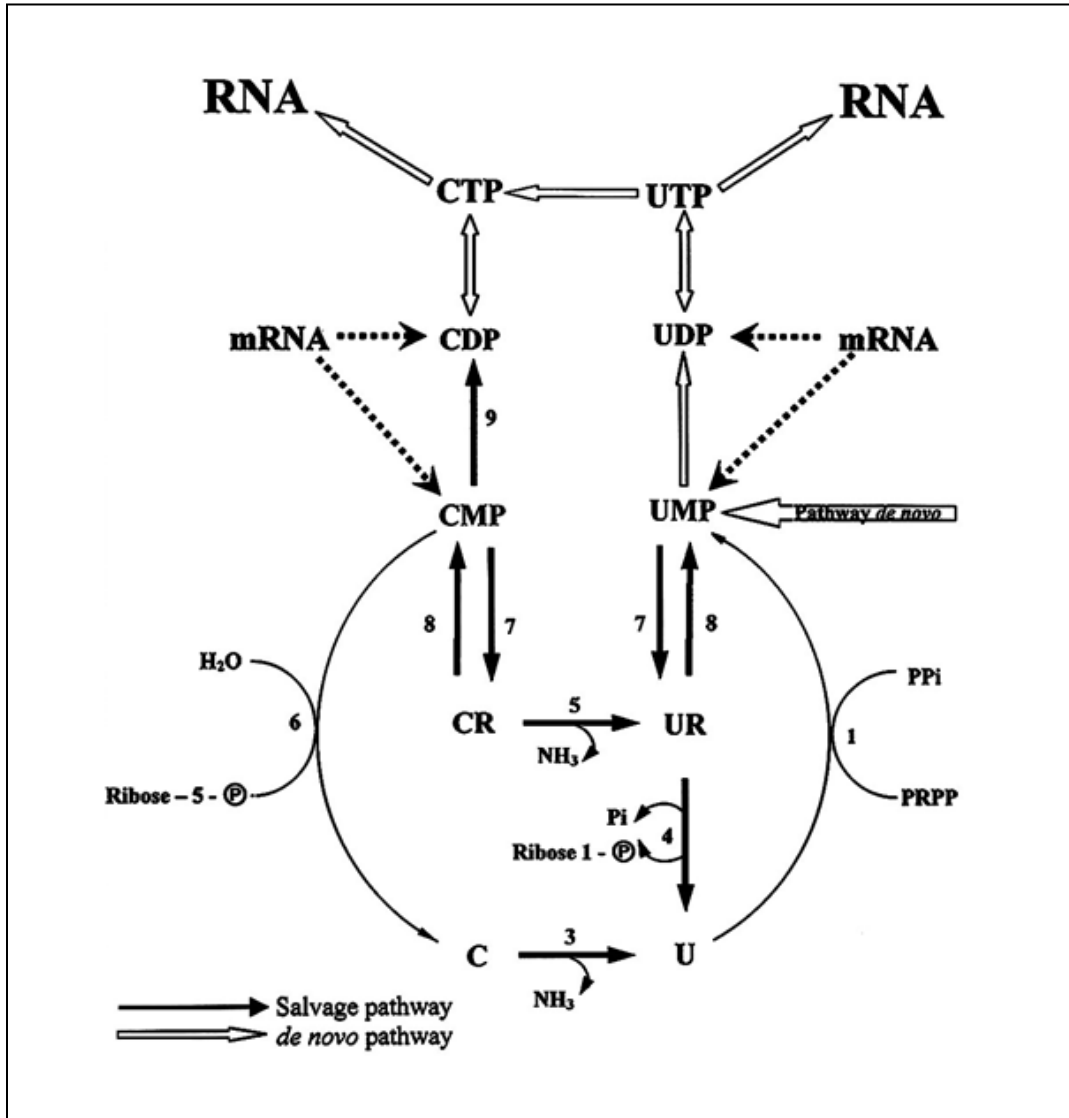
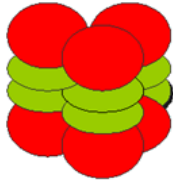
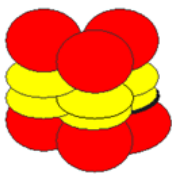
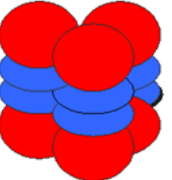
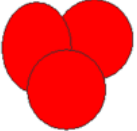









Fig. 6 Salvage pathway of *B. cepacia*. (Beck and O'Donovan 2008)

Table 4 Classes of bacterial ATCases.

Classes	Class A1	Class A2	Class B	Class C
Structure				
Subunit Structure	<p>PyrB catalytic 34 kDa </p> <p>PyrC active 45 kDa </p>	<p>PyrB catalytic 34 kDa </p> <p>PyrC' inactive 45 kDa </p>	<p>PyrB catalytic 34 kDa </p> <p>PyrI regulatory 17 kDa </p>	<p>PyrB catalytic 34 kDa </p> <p>active as trimer No holoenzyme</p>
Organism	<i>Streptomyces griseus</i> <i>S. coelicolor</i> <i>Mycobacterium smegmatis</i> <i>Thermus aquaticus</i>	<i>Pseudomonas putida</i> <i>P. aeruginosa</i> <i>Burkholderia cepacia</i>	<i>E. coli</i> <i>Salmonella typhimurium</i> <i>Neisseria meningitidis</i> <i>Pyrococcus abyssi</i>	<i>Bacillus subtilis</i> <i>B. caldolydicus</i> <i>Streptococcus pyogenes</i>
Size of Holoenzyme	450 kDa	480 kDa	310 kDa	No holoenzyme Trimer only 100 kDa

(Herve 1981) (Lipscomb 1994). ATCase of *E. coli* is classified as a class B ATCase. This enzyme consists of two trimers of *pyrB* encoded catalytic polypeptides (34 kDa each) united by three dimers of *pyrI*-encoded regulatory polypeptides (17 kDa each) containing the binding sites for the nucleotide effectors. The ATCase of *E. coli* is activated by ATP and inhibited by CTP and UTP (Wild et al. 1989). The dodecameric holoenzyme has a 2(c3): 3(r2) quaternary structure with a molecular mass of about 300 kDa, and exhibits sigmoidal substrate saturation kinetics for both aspartate (Gerhart and Pardee 1962) and carbamoylphosphate (Bethell and Jones 1969). Class C ATCases are the smallest in size and contains catalytic trimers (34 kDa each) only (c3) (Brabson and Switzer 1975). This 100 kDa enzyme is not regulated by allosteric effectors and exhibit typical Michaelis-Menten Kinetics for both substrates. A representative within this class of ATCases is the *Bacillus subtilis* enzyme, but several Gram negative bacteria also contain this size enzyme (Linscott 1996).

The largest ATCases are those that belong to Class A and have been most studied in the genus *Pseudomonas*. The ATCase of *P. fluorescens* (Bergh and Evans 1993), *P. putida* (Condon et al. 1976; Schurr et al. 1995), *P. aeruginosa* (Vickrey et al. 2002), *P. syringe* (Shepherdson and McPhail 1993) have all been extensively studied. ATCases in this class have a molecular mass ranging from 450 to 500 kDa, exhibit hyperbolic substrate saturation curves, and are inhibited by the nucleotide effectors ATP, CTP, and UTP. Purified *P. fluorescens* ATCase exists as a trimer with a 34 kDa catalytic chain in association with a 45 kDa polypeptide, which is arranged in a dodecamer. Both the active site for ATCase and the nucleotide effector binding sites were found to be located on the 34 kDa chain encoded by *pyrB* (Bergh and Evans 1993).

The 45 kDa chain, encoded by *pyrC'* produces an inactive DHOase-like

polypeptide. This inactive *pyrC* has been designated *pyrC'* because it has significant sequence homology to DHOase from other organisms, but has no DHOase activity. In *P. putida* and *P. aeruginosa*, *pyrB* overlaps a *pyrC'* gene encoding a nonfunctional DHOase, which is required for the assembly of the functional dodecameric ATCase (Schurr et al. 1995). Therefore, *Pseudomonas* ATCases are active only as dodecameric holoenzyme comprised of six *pyrB*-encoded polypeptides associated with six *pyrC'*-encoded polypeptide chains which give 480 kDa molecular mass. This holoenzyme does not have DHOase activity, but must be present for the holoenzyme to be active.

In the case of the ATCase of *Streptomyces griseus*, hyperbolic curves were obtained for ATCase activity when velocity-substrate plots for aspartate and carbamoyl phosphate were made. The ATCase enzyme was inhibited by ATP, CTP, UTP and GTP. This is typical of Class A ATCase found in other organisms. This led Hughes *et al.* to suggest a subtyping of the Class A ATCases (A₁ and A₂) (Hughes et al. 1999). Two other organisms, namely *Deinococcus radiophilus* and *Thermus aquaticus* also show this ATCase/DHOase activity in their holoenzyme structure. Many more organisms may also possess this unique complex.

Interaction between ATCases and DHOases

The evolution of the ATCase holoenzyme may have been influenced by the nature of the DHOase interacting with the ATCase. DHOase may be active or inactive, can be fused or overlapped to CPSase and ATCase activity, and affect the expression and construction of functional holoenzyme structure.

Eukaryotic ATCases are of different types. In lower eukaryotes the CPSase and ATCase activities are fused in a single polypeptide chain containing an inactive DHOase. In animals, *pyrB*- encoding ATCase is fused to the genes for CPSases and DHOase in a multifunctional unit encoding the so-called CAD protein (Coleman et al. 1977; Davidson et al. 1993). In plants, ATCase is similar to the prokaryotic class C except that the enzyme is sensitive to allosteric effectors (Khan et al. 1999). In fungi, a CAD-like protein occurs where the DHOase is not catalytically active, similar to prokaryotic subclass A2 (Souciet et al. 1989).

Whether a DHOase-like protein is catalytically active or not can be related to the presence or absence of four catalytically critical histidine residues in its amino acid sequence.

Holm and Sander (Holm and Sander 1997) proposed that DHOase belongs to a superfamily of amidohydrolases that catalyze a diverse series of hydrolytic reactions. Extensive phylogenetic analysis of the amino acid sequences of DHOase from 82 organisms reveals that the enzyme can be divided into two major groups (Fields et al. 1999).

Type I DHOases are the more ancient form of the enzyme with a subunit mass of ~ 45kDa and are found in all domains of life. They include the DHOase domain of mammalian CAD and monofunctional DHOases found in Gram-positive bacteria, including *Bacillus*, *Lactobacillus* and *Streptococcus*. Type II DHOases are smaller (~ 38 kDa compared with ~45 kDa for the type I DHOases) monofunctional enzymes that are found predominantly in Gram-negative bacteria (e.g. *Escherichia coli*) and considered

a more recent evolutionary development. The two DHOase families share only 20 % sequence identity.

Freund & Jarry (Freund and Jarry 1987) and Faure *et al.* (Faure et al. 1989) suggested that the fused DHOases may have independently evolved as descendants of a long spacer region separating the CPSase and ATCase domains in a common ancestral gene. Low sequence homology between two DHOase families is different enough to support convergent evolution.

However, there is the possibility that gene duplication is involved in the evolution of DHOase. During evolution, there may have arisen a duplication of a monofunctional DHOase gene, subsequently one copy may have been translocated and inserted into the spacer region and reactivated at some point. This led to extinction of the monofunctional DHOase. If this explanation is correct, all the DHOases are descendants of a common ancestor and the sequence differences between the two families are due to their divergent evolution (Simmer et al. 1989).

In pseudomonads, six active *pyrB* ATCase catalytic chains are coupled with six *pyrC'* polypeptides; in eukaryotes, the first three enzymes in pyrimidine pathway (CPSase, ATCase, and DHOase) reside in the single polypeptide, CAD. There is the possibility that dodecameric structure in pseudomonades may be a vestige of the eukaryotic CAD complex or more likely its progenitor (Schurr et al. 1995).

The completion of the *P. aeruginosa* genome sequence revealed that there are three *pyrC* genes, *pyrC'* which is inactive but necessary for structure of ATCase holoenzyme, and the other two *pyrC* and *pyrC2* encoding active DHOases. In an earlier

study from our lab, Brichta knocked out both individual *pyrC* genes to create double mutant which was the first block in DHOase synthesis for *P. aeruginosa*. DHOase mutants from *P. aeruginosa* showed it to be severely impaired in its ability to produce virulence factors and were defective for motility (Brichta 2003). The *P. putida* DHOase mutant also failed to produce the siderophore (Maksimova et al. 1993).

Moreover, since the genome of the genus *Burkholderia* consists of two to four chromosomes, the *pyrC* gene locus in the chromosome is varied. *B. mallei* and *B. pseudomallei* have two different *pyrCs* in chromosome 1 while *B. cenocepacia* has two different *pyrCs* in chromosomes 1 and 2. Study of the ATCase-DHOase interaction, especially in organism having multiple chromosomes, will give us valuable information in evolutionary history.

Unique ATCase in *B. cepacia* 25416

In earlier studies from our lab, the aspartate transcarbamoylase *pyrBC* complex was purified from *Burkholderia cepacia* 25416. Unlike other pseudomonads, in the course of the purification, four different ATCase activities appeared as two dodecameric holoenzymes of 550 kDa and 510 kDa, which is the longest PyrB polypeptide to date and as two trimeric ATCases of 140 kDa and 120 kDa which are more like class C ATCases (Kim 2004). Unlike class C ATCase, these trimers are regulated by nucleotide effectors. Both the holoenzymes and trimers were regulated by nucleotide effectors. The 140 kDa trimer consists of 3x47 kDa while the 120 kDa trimer consists of 3x40 kDa. The 40 kDa PyrB polypeptide arose by specific cleavage of the 47 kDa polypeptide between Ser 74

and Val 75 (Kim 2004). To verify the makeup of the *pyrBC* holoenzyme complex, *B. cepacia* dihydroorotase (DHOase) was cloned and purified and active dimeric subunits of 90 kDa were observed.

B. cepacia ATCase had been previously classified as a Class A2, *pyrBC*' dodecamer like the *Pseudomonas* ATCases but the result of this study requires reclassification of *B. cepacia* ATCase. Here we present the first evidence that the ATCase of *B. cepacia* occurs in an active ATCase/DHOase complex encoded from *pyrBC* genes. Accordingly we propose a new class of ATCase named class D. In order to determine more about the roles of DHOase in *B. cepacia*, *pyrC* gene was knocked out.

This study will help us understand the structure and regulation of ATCase holoenzyme with DHOase, and this could prove useful to future studies examining its biological control and its taxonomic assignment. Moreover, this research demonstrates the possibility of a potential drug target for *B. cepacia*.

CHAPTER 2

MATERIALS AND METHODS

Bacterial Strains and Plasmids

The bacterial strains used in this study are listed in Table 5. The plasmids used and constructed in this study are also listed in Table 5.

Media and Growth Conditions

E. coli strains were grown in Luria-Bertani (LB) enriched medium or in *E. coli* minimal medium (Ecm) as indicated by Miller, 1992. Ecm was supplemented with the addition of arginine, uracil or both at a concentration of 50 µg/mL as needed. To prepare 1 L Ecm, 10.5 g K₂HPO₄, 4.5 g KH₂PO₄, 0.5 g Na₃-citrate, and 1.0 g (NH₄)₂SO₄ were dissolved in 984 mL distilled, deionized water (dd-H₂O). After autoclaving, sterile solutions of 10 mL 20% glucose (w/v) (0.2 % final), 1 mL 1 M MgSO₄ (1 mM final) and 5 mL 0.337 % thiamine (w/v) (0.0015 % final) were added to the Ecm. *B. cepacia* and *P. aeruginosa* were cultivated in Luria-Bertani (LB) enriched medium or *Pseudomonas* minimal medium (Psm) (Ornston and Stanier 1966) as needed. Metals 44 and concentrated base were prepared in advance to make Psm. Metals 44 consisted of 2.5 g EDTA, 10.95 g ZnSO₄ • 7H₂O, 5.0 g FeSO₄ • 7H₂O, 1.54 g MnSO₄ • H₂O, 0.392 g CuSO₄ • 5 H₂O, 0.251 g CuSO₄(anhydrous), 0.25 g Co(NO₃)₂ 6H₂O, and 0.177 g Na₂B₄O₇ • 10 H₂O (Borax) in dd-H₂O for a final volume of 1 L.

Table 5 List of strains and plasmids

Strain or Plasmid	Genotype or relevant property	Source or reference
Strain		
<i>B. cepacia</i>		
<i>B. cepacia</i> 25416	Wild type	ATCC
<i>B. cepacia</i> SKB1	<i>B. cepacia pyrB</i> ⁻	This study
<i>P. aeruginosa</i>		
PAO1	<i>P. aeruginosa</i> wild type	ATCC
<i>E. coli</i>		
BL21	<i>E. coli</i> B, F ⁻ , <i>ompT</i> , <i>hsdS</i> , <i>gal</i> , <i>dcm</i> and used for GST	Amersham
DH5α	<i>recA1</i> , <i>hsdR17</i> , <i>endA1 supE44</i> , <i>relA1</i> , <i>gyrA96</i> , Δ(<i>argF-lacZYA</i>)U169	BRL, 1986
MA1008	<i>lacZ43(Fs) λ⁻ pyrC68 relA1 thi-1</i>	Beckwith <i>et al</i> , 1962
Plasmids		
pUC18	pMB1 origin, high copy <i>E. coli</i> shuttle vector, Amp ^r	Bio-rad
pHKεBC	pUC18 with 1.4 kb insert of gene containing <i>B. cepacia pyrC</i>	This study
pHKBC	pUC18 with 1.1 kb insert of <i>B. cepacia pyrC</i>	This study
pMAL-c2e	Maltose gene fusion vector, <i>tac</i> promoter, <i>lac I^q</i> , Amp ^r	New England Biolab
pMHKBC	pMAL-c2e with 1.1 kb insert of <i>B. cepacia pyrC</i>	This study
pEX18Gm	GmR <i>oriT sacB</i> ⁺ gene replacement vector with multiple cloning site	Hoang <i>et al</i> , 1998
pEXHKBC	pEX18Gm with 1.1 kb insert of <i>B. cepacia pyrC</i>	This study
pEXHKBCX	pEX18Gm with insert of <i>B. cepacia pyrC</i> ⁻	This study
pGEX2T	GST gene fusion vector, <i>tac</i> promoter, <i>lac I^q</i> , Amp ^r	Amersham
pSK2T	pGEX2T with 1.29 kb insert of <i>B. cepacia pyrB</i>	Kim 2004

Table 6 PCR primers used in this study

Primer	Sequence (5' – 3')	Relevant property	Restriction site
BurkC-F	AAAGGTACCTTCAAGCATATCACCGAGCC	Left primer used to amplify <i>B. cepacia pyrC</i> containing gene for cloning into pUC18 (1400 bp)	<i>KpnI</i>
BurkC-R	AAAAAGCTTTGCAGATTGTGGCGGCACG	Right primer used to amplify <i>B. cepacia pyrC</i> containing gene for cloning into pUC18 (1400 bp)	<i>HindIII</i>
BCpyrC-F	CGGGGTACCATGACTGCCTCGAACGCT	Left primer used to amplify <i>B. cepacia pyrC</i> gene for cloning into pUC18 (1065 bp)	<i>KpnI</i>
BCpyrC-R	CCCAAGCTTTCACGCCAGTTTCCAGCC	Right primer used to amplify <i>B. cepacia pyrC</i> gene for cloning into pUC18 (1065 bp)	<i>HindIII</i>
SBBCpyrC-F	TTCGAACCGCTGATGACGCTTTCGAACCGCTGATGACGCT	Left primer used to synthesize the probe to detect <i>B. cepacia pyrC</i> in Southern blot analysis	N/A
SBBCpyrC-R	GCCTGAAGGTCGTGTTTCGAATTCGAACACGACCTTCAGGC	Right primer used to synthesize the probe to detect <i>B. cepacia pyrC</i> in Southern blot analysis	N/A

Primers were purchased from Biosynthesis, Lewisville, TX

Concentrated base consisted of 14.6 g of KOH, 20 g nitriloacetic acid, 28.9 g MgSO₄ anhydrous, 6.67 g CaCl₂•7H₂O, 18.5 g (NH₄⁺)₆Mo₇O₂₄ • 7H₂O, 0.198 g FeSO₄•7H₂O, and 100 mL Metals 44 in dd-H₂O for a final volume of 1 L. 1 L Psmm was prepared with 25 mL 0.5 M Na₂HPO₄, 25 mL 0.5 M 1 KH₂PO₄, 10 mL 10 % (NH₄)₂SO₄, and 10 mL concentrated base with dd-H₂O. The pH was then adjusted to 6.8 with HCl. 0.2 % glucose was added to the medium as the carbon and energy source after autoclaving. *Pseudomonas* Isolation Agar (PIA) from Difco was prepared as directed by the company and used as a selective medium for transconjugation in the Bi-parental mating experiment.

Isolation of Chromosomal DNA from Bacteria

Bacterial chromosomal DNA was extracted using the Wizard® Genomic DNA Purification Kit from Promega Corporation. A culture of *B. cepacia* was grown in 5 mL of *Pseudomonas* minimal medium supplemented with 0.2 % glucose overnight. A 1% inoculum was used to initiate growth. 1 mL of the overnight culture was transferred to a 1.5 mL microcentrifuge tube and collected by centrifugation at 13,000-16,000 × g for 2 min (Eppendorf Microcentrifuge Model 5430, Hauppauge, NY). After the supernatant was removed, 600 μL of Nuclei Lysis Solution was added and the pellet was resuspended by pipetting the cells. The lysed cells were incubated at 80°C for 5 min and then cooled to room temperature. 3 μL of RNase Solution was added to the cell lysate and the tube was inverted 2–5 times to mix. The cell lysate was incubated at 37°C for 15-60 min and cooled to room temperature. 200 μL of Protein Precipitation Solution was added to the RNase-treated cell lysate. The cell lysate was vortexed vigorously at high speed for 20 s to mix the Protein Precipitation

Solution with the cell lysate and then incubated on ice for 5 min. After centrifugation, the supernatant containing the DNA was transferred to a clean 1.5 mL microcentrifuge tube containing 600 μ L of room temperature isopropanol. The centrifuge tube was gently mixed by inversion until the thread-like strands of DNA formed a visible mass. After centrifugation at 13,000-16,000 \times g for 2 min, the supernatant was discarded. 600 μ L of room temperature 70 % ethanol was added and the tube was gently inverted several times to wash the DNA pellet. After a further centrifugation, ethanol was carefully aspirated and the tube was drained on clean absorbent paper and air-dried for 10-15 min. 100 μ L of DNA Rehydration Solution was added to the tube and incubated at 65°C for 1 h to hydrate the DNA. The tube was tapped periodically to mix the solution. The isolated DNA was stored at 2 - 8°C until further use. The purity and quantity of DNA was determined by absorbance at 280 nm and 260 nm respectively in as Shimadzu 500 UV spectrophotometer. A DNA concentration of 2 μ g/ μ L was recovered using the above preparation.

Isolation of Plasmid DNA from Bacteria

Plasmid DNA of transformed bacteria was extracted using Wizard® Plus SV Minipreps DNA Purification kit from Promega Cooperation. 1-2 mL overnight cell culture of transformed *E. coli* bacterial cell culture was harvested by centrifugation for 5 min at 10,000 \times g in a tabletop centrifuge. The supernatant was poured off and 250 μ L of Cell Resuspension Solution was added. The cell pellet was completely resuspended by pipetting. Then 250 μ L of Cell Lysis Solution was added and the centrifuge tube was inverted four times. 10 μ L of Alkaline Protease Solution was added and mixed by inverting the tube four times then incubated for 5 min at room

temperature. 350 μL of Neutralization Solution was added to the cell lysate and immediately mixed by inverting the tube four times. After centrifugation at 13,000-16,000 $\times g$ for 10 min, the cleared lysate was transferred to the prepared Spin Column by decanting. After centrifugation for 1 min at room temperature, the Spin Column was removed from the tube and the flow-through was discarded from the Collection Tube. The Spin Column was reinserted into the Collection Tube and 750 μL of Column Wash Solution, previously diluted with 95 % ethanol, was added to the Spin Column. Following centrifugation at maximum speed for 1 min at room temperature, the Spin Column was removed from the tube and the flow-through was discarded. The Spin Column was reinserted into the Collection Tube, and 250 μL of Column Wash Solution was added. After centrifugation at maximum speed for 2 min at room temperature, the Spin Column was transferred to a new, sterile 1.5 mL microcentrifuge tube. The plasmid DNA was eluted by adding 100 μL of Nuclease-Free Water to the Spin Column. The tube was then centrifuged at maximum speed for 1 min at room temperature. The flow-through plasmid DNA was stored at -20°C until further use.

Elution of DNA from an Agarose Gel

The DNA of interest in an agarose gel was isolated using an Agarose Gel extraction kit from Roche Applied Science. Following gel electrophoresis, the slice of agarose containing the DNA band was excised by using clean razor blade and transferred to weigh 1.5 mL microcentrifuge tubes. 300 μL of the Agarose Solubilization buffer per 100 mg of agarose gel was added, and then incubated for 10 min at 56 - 60°C and vortexed every 2 - 3 min. During the incubation time, the silica

suspension from the kit was resuspended thoroughly by vortex until a homogeneous suspension was obtained. After the agarose gel was completely solubilized, 10 μL of the silica suspension was added to the sample. The mixture was incubated for 5 min with continuous mixing in a rocker, and then centrifuged for 30 s at maximal speed, the supernatant was then discarded. 500 μL of Nucleic Acid Binding Buffer was added to the matrix containing the DNA on a vortex mixer, and then centrifuged at 13,000-16,000 $\times g$ for 30 s and the supernatant was discarded as before. The pellet was washed with 500 μL Washing Buffer by centrifugation and the supernatant was discarded as before. The washing step was repeated twice more and all of the liquid was removed with a pipette. The tube was then inverted on an adsorbent tissue and dried at room temperature for 30 min. The matrix color turned bright white when dried. The DNA was eluted with 20 μL of dd- H_2O . Then tube was centrifuged at 14,000 $\times g$ for 2 min and the supernatant, which contained the eluted DNA, was transferred to a clean centrifuge tube and stored at $-20\text{ }^\circ\text{C}$ until use.

The purity and the concentration of extracted DNA were checked by their absorbance at A_{260} and A_{280} .

Polymerase Chain Reaction (PCR)

To amplify potential genes of interest, the PCR reaction cycle was performed in a Programmable Thermal Controller from MJ. Research, Inc.

The PCR reaction contained 2 μL of template DNA (1 μg), 1 μL of forward and reverse primer (0.02 nmol each), 2 μL of 10 mM dNTP, 5 μL of 10 X Pfu polymerase buffer mixed in a 0.2 mL thermal PCR tube. 1 U of Pfu polymerase was added last. The final volume to 50 μL was adjusted by the amount of dd- H_2O . The

template DNA was denatured at 95°C for 5 min and the reaction entered 30 cycles of 5 min of denaturation at 95°C, 30 s of annealing at 5°C below that of the lower melting point primer, and 90 s of polymerization at 72°C. After completion of 30 cycles, the reaction had 10 min more extension of polymerization at 75°C to complete the reaction, and then was stopped at 4°C. The amplified DNA was stored in -20°C until use. Before cloning, the DNAs were cleaned using the Agarose Gel extraction kit from Roche Applied Science.

Competent Cell Preparation

For the transformation of constructed plasmid into *E. coli*, cells were made chemically competent by CaCl₂ by the Mandel and Higa method with slight modification (Mandel and Higa 1970). 50 mL of LB in a 200 mL flask were inoculated with 500 µL of an overnight starter culture of *E. coli*. This was incubated at 37°C with shaking at 250 rpm for 3-4 h until the culture reached an A₆₀₀ of 0.5. The culture was aseptically transferred to a 50 mL polypropylene conical tube and placed on ice for 30 min, and then centrifuged at 1300 x g for 20 min at 4°C. The supernatant was removed and the pellet was resuspended with 20 mL of ice-cold 0.1 M CaCl₂ solution and incubated on ice for 30 min. This mixture was centrifuged at 1300 x g for 10 min. The supernatant was aseptically removed and the pellet was resuspended with 20 mL ice-cold 0.1 M CaCl₂ solution again and centrifuged at 1300 x g for 10 min. The supernatant was removed and the pellet was gently resuspended in 812 µL of ice cold 0.1 M CaCl₂. The mixture was left on ice and incubated in the refrigerator at 4°C overnight. The next morning, 188 µL of sterile 80 % glycerol was aseptically added and the suspension was gently mixed and then dispensed as 0.1 mL aliquots

into pre-chilled 1.5 mL Eppendorf® tubes. The competent cells were stored at -80°C.

Transformation Procedures

The 100 µL prepared competent cells were removed from the -80°C and allowed to thaw on ice. When thawed, plasmid DNA was added, usually between 40-500 ng (not more than 1 µg) in a volume of 3 – 10 µL. To maximize the efficiency of transformation, the plasmid DNA was added to the competent cells immediately after the cells were thawed. The plasmid DNA/cell mixture was kept on ice for 20 min then heat-shocked by incubation in a 42°C water bath for 30 s, then cold-shocked on ice for 2 min. Next, 500 µL of room temperature LB was added to each transformation tube and the cells were incubated at 37°C for 1 h in the shaker. Finally, 50 µL of incubated cells were collected by centrifugation and plated on to selective medium with appropriate antibiotics. If minimal medium plates were used, cells were washed with the same minimal medium broth prior to plating, in order to avoid carry-over of the rich nutrients of the LB medium.

Preparation of Cell Extract for Enzymatic Assay

Cell extracts of *P. aeruginosa*, *E. coli*, and *B. cepacia* were prepared from 50 mL cultured cells. Cells ($OD_{600} = 0.8$ to 1.0) were harvested by centrifugation at $13,000-16,000 \times g$ for 20 min at 4°C. After removal of supernatant, 1 mL of ATCase breaking buffer (50 mM Tris-HCl, pH 8.0, 2 mM β-mercaptoethanol (BME), 20 µM ZnSO₄, and 20 % glycerol) was added and the cells were resuspended by vortex. The resuspended cells were broken by ultrasonic disruption using a Branson cell disruptor200 for 1 min on ice, followed by 1 min of rest on ice, this was repeated

three times. The disrupted cell suspension was transferred into 1.5 mL centrifuge tubes and centrifuged at 13,000-16,000 × g for 20 min. The supernatant was transferred to previously prepared dialysis tubing and dialyzed for 30 min at 4°C in a 1 L dialysis buffer consisting of 50 mM Tris-HCl (pH 8.0), 2 mM BME, and 20 μM ZnSO₄, with stirring. The dialysis buffer was then replaced by 1 L fresh dialysis buffer and dialyzed overnight at 4°C with stirring. Dialysis tubing was prepared in the method of Sambrook *et al.* (Sambrook 1989). The recommended dialysis buffer volume of 300 times the total cell extract volume was used. Each dialyzed cell extract was then transferred to a new centrifuge tube and stored at 4°C for further use.

Cloning of the *B. cepacia pyrC* Gene

Bioinformatics Study to Obtain the pyrC Gene Sequence

To study the assembly and the kinetics of *B. cepacia* DHOase and ATCase holoenzyme, the *pyrC* gene was cloned. Since the sequence of *B. cepacia pyrC* was not available, the already identified *pyrC* genes of other *Burkholderia* species such as *B. mallei*, *B. pseudomallei*, and *B. fungorum* were obtained from the NCBI database. The gene alignment was performed using the GENE DOC computer program and the conserved sequence upstream and downstream of the *pyrC* gene was available.

Cloning of the Gene Containing B. cepacia pyrC into pUC18 Plasmid

The chromosomal DNA of *B. cepacia* was purified as previously described. The primers used in PCR were designed based on the gene alignment derived from bioinformatics. To the end of the forward primer (BurkC-F), a *KpnI* site was added, and at the end of reverse primer (BurkC-R), a *HindIII* site was added (Table 6). The

PCR reaction for the DNA containing *B. cepacia pyrC* gene was performed as described earlier using a 63°C of annealing temperature. The 1.4 kb amplified DNA was cleaned and isolated by agarose gel using Agarose Gel extraction kit from Roche Applied Science. This PCR product and the pUC18 plasmid (Figure 7) were cut using *KpnI* and *HindIII* restriction enzymes and run on a 1 % agarose gel. The DNA was cleaned and purified by the above mentioned protocol. The gene containing the *pyrC* gene of *B. cepacia* was then ligated to the pUC18 plasmid at a molar ratio of 3 to 1. The transformation was performed as described earlier and the resulting ampicillin (Amp) resistant plasmid, pHKeBC18, 4.1 kb in size, was obtained.

Sequencing was performed by Lonestar Laboratory in Houston, Texas. The sequence was analyzed using PC-gene software and homology was evaluated by the on-line NCBI-BLAST resource.

Cloning of B.cepacia pyrC into pUC18 plasmid

The primers of PCR were designed based on the gene sequence acquired from the results of cloning the gene containing the *B.cepacia pyrC*. To the end of forward primer (BCpyrC-F), a *KpnI* site was added, and to the end of reverse primer (BCpyrC-R), a *HindIII* site was added (Table 6). The cloning step was similar to the previous one. PCR reaction of *B. cepacia pyrC* was performed as described earlier at 53°C annealing temperature. After digesting the PCR product (1.1 kb) and the pUC18 plasmid containing *KpnI* and *HindIII* sites, the cleaned and purified DNA was ligated and transformed on LB agar plate supplemented with 100 µg/mL of Amp. The resulting plasmid pHKBpC18 was then sequenced by Lonestar Laboratory in Houston, Texas.

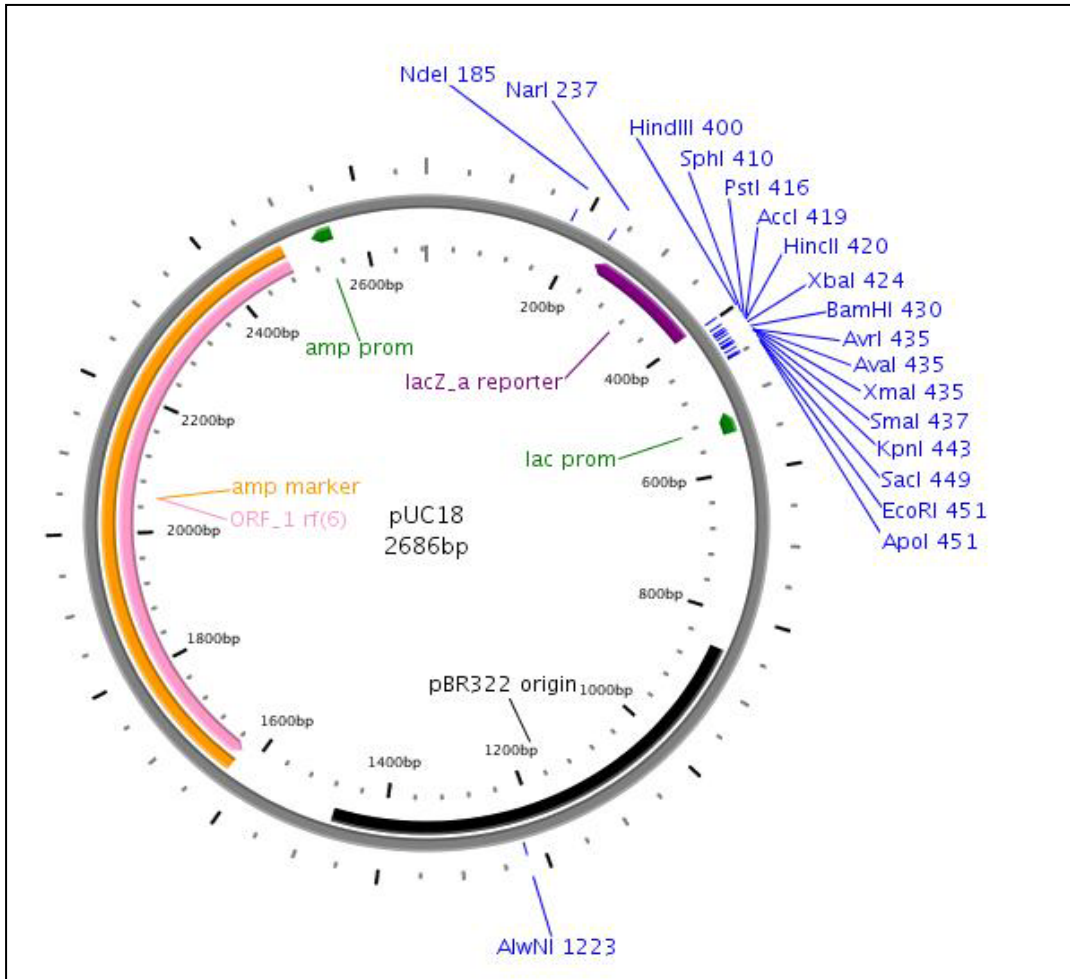


Fig. 7 Map of pUC18 plasmid. Figure is drawn by PlasMapper version 2.0.

The sequence was analyzed using PC-gene software and homology was searched through the on-line NCBI-BLAST resource. From this sequencing result, the *pyrC* gene of *B. cepacia* was identified and reported to NCBI (GenBank: EU718731.1).

Complementation Test of *pyrC* Gene in MA1008 Cell

To check the expression of *pyrC* gene, the complementation test was performed with DHOase deficient *E. coli* MA1008l. Chemically competent MA1008 cells were made as described earlier. pHKBpC18 plasmid was transformed into MA1008 cell by heat shock. The transformants were plated on LB plate containing Amp (100 µg/mL) and incubated at 37°C overnight. Colonies were patched on to a LB plate containing 100 µg/mL of Amp and incubated at 37°C overnight. Colonies on the plate were patched onto an Ecmm plate containing 0.2 % glucose and 50 µg/mL of uracil, and onto an Ecmm plate containing 0.2 % glucose without uracil. Colonies that grew on Ecmm plates without uracil were selected because these cells survived onto Ecmm without uracil by the expression of *B. cepacia pyrC* gene through complementation. This MA1008 cell designated as MA1008pHKBpC18 was inoculated into 50 mL Ecmm broth and incubated at 37 °C and the cell extracts were prepared as before. The expression of DHOase was confirmed by the DHOase conventional activity assay.

Purification of DHOase Enzyme by the pMAL Protein Fusion and Purification System

Purification of DHOase was carried out by the pMAL protein fusion and

purification system from New England Biolab. Inc. The pMAL vectors (Figure 8) provided a method for expressing and purifying a protein produced from a cloned gene or open reading frame. The cloned gene is inserted downstream from the *maltE* gene of *E. coli*, which encodes maltose-binding protein (MBP), resulting in the expression of an MBP fusion protein. The MBP in these vectors has been engineered for tight binding to amylose.

The method uses the strong “tac” promoter and the *maltE* translation initiation signals resulting in high-level expression of the cloned sequences, and a one-step purification of the fusion protein using MBP’s affinity for maltose. The vectors carry the *lac*^{lq} gene, which codes for the Lac repressor. This keeps expression from Ptac low in the absence of IPTG induction. The pMAL-5 vectors also contain the sequence coding for the recognition site of a specific protease such as enterokinase, located just 5’ to the polylinker insertion sites. This allows MBP to be cleaved from the protein of interest after purification.

Subcloning of B. cepacia pyrC Gene into the pMAL-c2e Plasmid

The first digestion of pHKBpC18 plasmid by *KpnI* and *HindIII* enzyme was purified by gel electrophoresis; results revealed a 1.1 kb size of the *pyrC* gene. The pMAL-c2e plasmid was also restricted by *KpnI* and *HindIII* enzyme and purified by gel electrophoresis. 1.1 kb of the *pyrC* gene was then ligated to the pMAL-c2e. 20 ng of this plasmid was transformed into a protease deficient *E. coli* BL21 host cell. In the pMAL Protein Fusion and Purification System, *E. coli* BL21 is the recommended host cell strain. The transformant *E. coli* BL21 was selected on LB plate with Amp (100 µg/mL) and cultivated overnight in LB broth with Amp (100 µg/mL). The *B. cepacia pyrC* subcloned pMAL-c2e transformant was confirmed by restriction

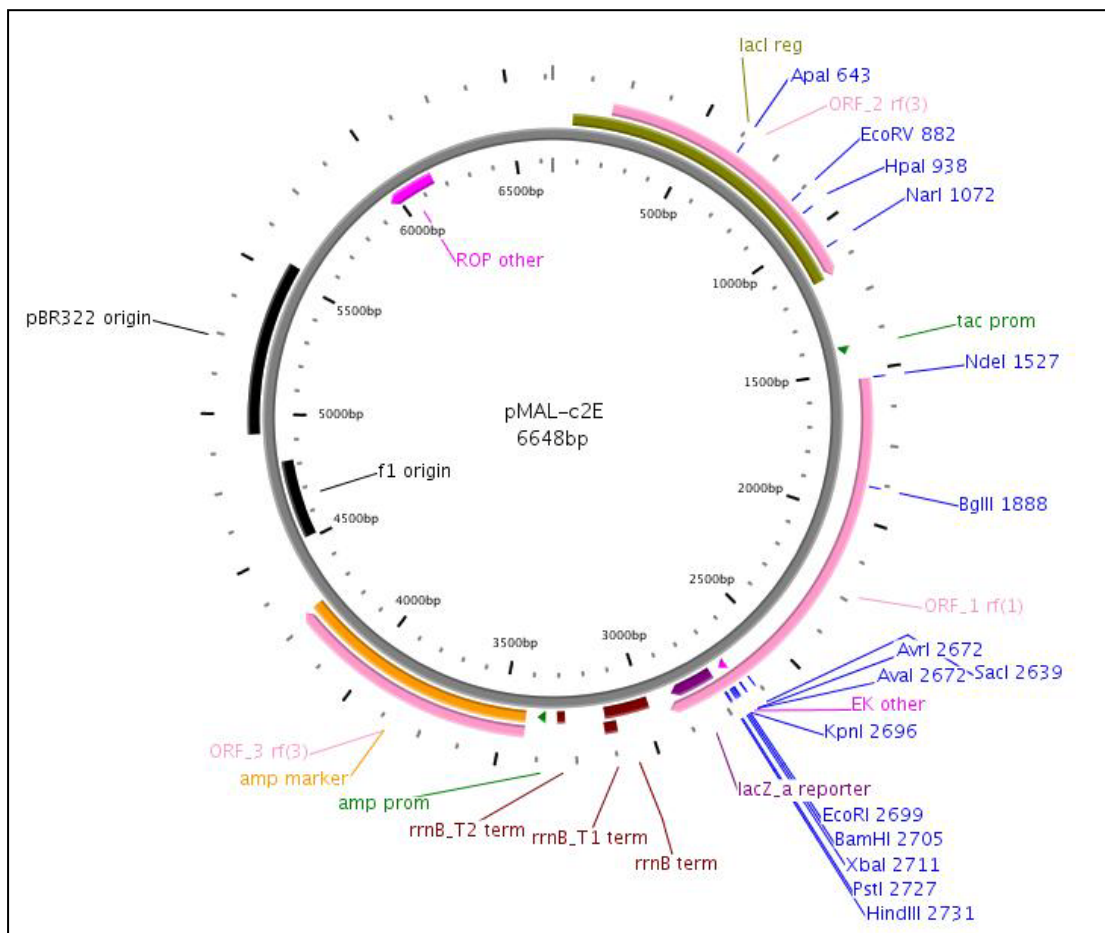


Fig. 8 Map of pMAL-c2E plasmid. Figure is drawn by PlasMapper version 2.0.

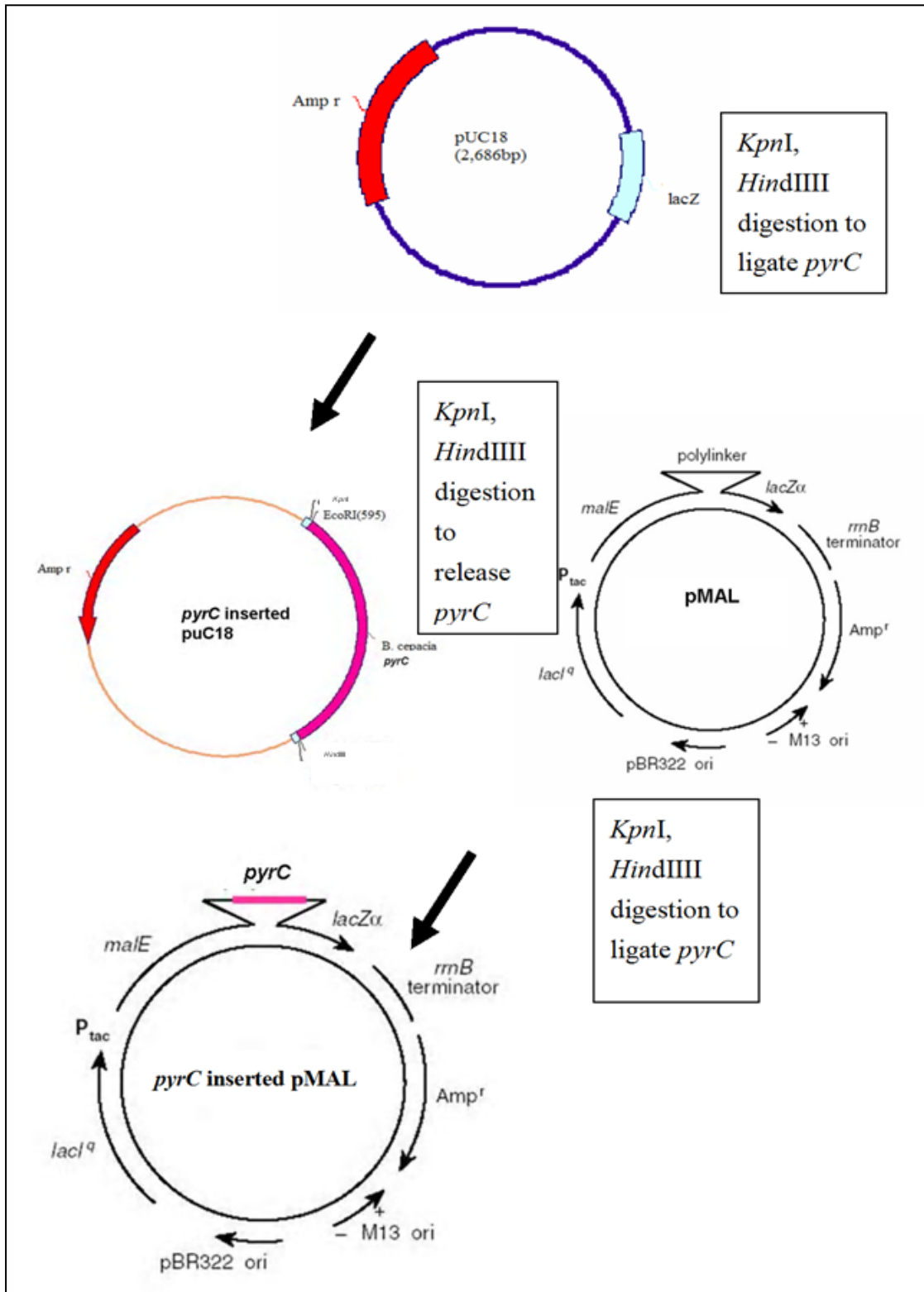


Fig. 9 Schematic diagram of the construction of pMAL-*B. cepacia pyrC* fusion plasmid.

digestion with *KpnI* and *HindIII* enzymes and sequencing. The overall schematic diagram to construct the pMAL-*B.cepacia pyrC* fusion plasmid is given in Figure 9.

Purification of DHOase Enzyme

Purification of DHOase was performed as indicated by the protocol provided by the manufacturer for MBP fusion proteins with slight modifications (Figure 10). A 200 μ L of selected *E. coli* BL21 were inoculated in 20 mL LB broth containing Amp (100 μ g/mL) and cultivated overnight. The next day, this overnight culture was transferred into 2 L LB broth with Amp (100 μ g/mL) and incubated at 37°C shaker for 4 h until the culture reached the OD₆₀₀ of about 0.8. In order to induce the overexpression, 0.5 mM (final concentration) of isopropyl- β -D-thiogalactoside (IPTG) was added and the cells were incubated for 3 h on a 37°C shaker. The cells were then harvested using a 500 mL centrifugal bucket at 6,000 x g for 15 min in 4°C. After removing the supernatant, the pellet was resuspended with 50 mL cold PBS buffer, pH 7.3. To prevent excessive viscosity, 37.5 μ g/mL (final concentration) of DNase was added to the resuspension solution. The cells were then broken by means of a French pressure cell at 2000 psi. and then transferred into a clean 50 mL centrifuge tube and the cell debris was removed by centrifugation at 15,000 x g for 30 min. The clear supernatant was transferred to a 50 mL conical tube and used for protein purification.

The amylose column was washed with 1X PBS buffer. A 1.33 mL of bead slurry (1 mL bed volume) was transferred to a 15 mL conical tube. This bead slurry was centrifuged at 1,750 x g for 5 min in 4°C. After removing the supernatant, the beads were washed with 10 mL ice cold 1X PBS and centrifuged as described above. This step was repeated twice and the beads were then transferred to a 50 mL conical

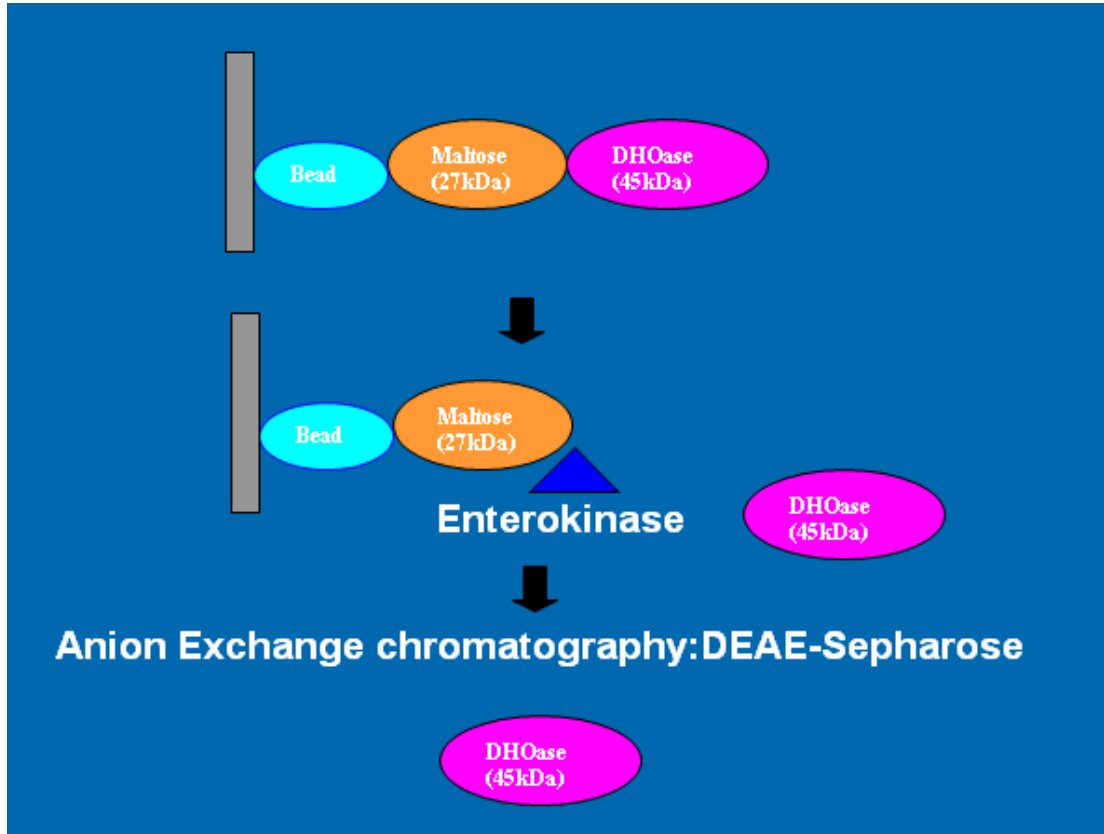


Fig. 10 Schematic diagram of DHOase purification from the pMAL-fusion protein purification system.

tube. The prepared cell lysate was transferred to the washed beads and incubated with a rocker at room temperature for 1 h, then centrifuged at the same condition as above. The beads were then washed with 10 mL of 1X PBS gently and centrifuged at the same condition as above. This step was repeated 3 times.

Then fusion proteins were eluted by 50 U enterokinase. 50 μ L of enterokinase (50U) solution was mixed with 950 μ L of cold 1X PBS buffer and added to the beads. This mixture was incubated in a rocker for 20 min at room temperature and centrifuged as described above. The supernatant was carefully transferred to a new tube and labeled as “Elute 1”. This step was repeated once and the eluted protein was labeled as “Elute 2”. After elution, all proteins were immediately stored in 12 % glycerol at -80°C .

Purification of DHOase Enzyme by Anion Exchange Column Chromatography

To further purify the partially purified DHOase by pMAL protein fusion and purification system, 1 mL of eluted DHOase was loaded onto a 1 mL DEAE Sepharose column (Pharmacia) and washed three times with 1 mL of PBS buffer. Then, the DHOase was eluted using linear gradient from 0 mM NaCl to 1000 mM NaCl with 1 mL collections three times for each gradient. The eluted DHOase was pooled together and dialyzed by 300X volume of 1X PBS buffer at 4°C overnight, then stored at -80°C with glycerol.

The purity of purified DHOase was checked by 10 % Sodium dodecyl sulfate polyacrylamide gel electrophoresis. The protein concentration of DHOase was determined by Bradford assay using Bovine serum albumin (BSA) as the standard.

Sodium Dodecyl Sulfate Polyacrylamide Gel Electrophoresis (SDS-PAGE)

SDS-PAGE is a method used to separate proteins according to their size. Since

different proteins with similar molecular weights may migrate differently due to their differences in secondary, tertiary or quaternary structure, SDS, an anionic detergent, is used in SDS-PAGE to reduce proteins to their primary (linearized) structure and coat them with uniform negative charges. A 10 % SDS polyacrylamide separating gel with a 4 % stacking gel was used to analyze the samples.

The apparatus used to conduct the electrophoresis was the Mini-Protean II™ chamber (Bio-Rad). The gel was prepared by first pouring a 10 % separating gel, which contained 1.67 mL of Solution A (30 % w/v acrylamide and 0.8 % w/v bis-acrylamide in dd-H₂O), 1.25 mL of Buffer B (1.5 M Tris-HCl, pH 8.8, 0.4 % w/v SDS in dd-H₂O), 2.08 mL of dd-H₂O, and 50 µL of 10 % ammonium persulfate. The gel began to polymerize with the addition of 5 µL of N, N, N' N' - tetramethylethylenediamine (TEMED). The mixture was gently inverted and poured into the assembled apparatus using a Pasteur pipet. A space of 2 cm was left at the top to pour the stacking gel. The gel was overlaid with *n* - butanol to prevent oxidation. The gel was allowed to polymerize for approximately 20 min after which the stacking gel was prepared. The stacking gel contained 0.27 mL of Solution A, 0.4 mL of buffer C (0.5 M Tris, pH 6.8, 0.4 % w/v SDS), 0.92 mL dd-H₂O, ammonium persulfate (0.01 g), and 5 µL of TEMED.

A 10 well comb was inserted and the gel was allowed to polymerize for 15 min. The gel was then placed into the apparatus and the tank was filled with denaturing gel running buffer (25 mM Tris, 192 mM glycine and 0.1 % SDS w/v, pH 8.3). The sample was mixed at a ratio of 4:1 with the gel loading dye (60 mM Tris-HCl, pH 6.8, 25 % glycerol v/v, 2 % SDS w/v, 14.4 mM β-mercaptoethanol, 0.1 % Bromophenol Blue) in a sterile microcentrifuge tube. The samples and the standards

were boiled for 5 min and cooled on ice. The samples and the pre-stained low range SDS standards were loaded onto the gel and electrophoresed for 90 min at 100 volts. The proteins were stained with Coomassie Blue staining solution (45 % methanol v/v, 10 % acetic acid v/v, 0.1 % Coomassie Brilliant Blue R-250 w/v in dd-H₂O) for 10 min with gentle rocking. The gel was destained with a solution of 10 % methanol v/v and 10 % glacial acetic acid v/v in dd-H₂O for 3 h.

DHOase Activity Assay

DHOase activity was measured with the modified color development procedure using the reverse assay of Beckwith *et al.* (Beckwith *et al.* 1962).

The reaction mixture contained in a total volume of 100 μ L 1 mM EDTA, 100 mM Tris/HCl buffer pH 8.6, 2 mM L-dihydroorotic acid (DHO) dissolved in 0.1 M phosphate buffer, 1 μ L purified DHOase or 10 μ L cell extract and sterile dd-H₂O. A control tube was prepared to obtain a blank reading (without cell extract) and the background (without DHO). All ingredients except dihydroorotate (DHO) were preincubated at 30°C for 2 min. Following the addition of dihydroorotate, the reaction mixture was incubated for 10 min at 30°C. Stop color mix was added and incubated at 65°C for 1 h. The stop reaction buffer was made by two parts of 5 mg /mL antipyrine in 50 % sulfuric acid (v/v) mixed with one part of 8 mg/mL of 2, 3-butanedione monoxime in 5 % acetic acid (v/v).

After the tubes were cooled in the dark for a brief period of time, the reverse reaction of carbamoylaspartate (CAA) from DHO was measured at 450 nm in a kinetic microplate reader from Molecular Devices.

Enzyme Kinetics of DHOase of *B. cepacia*

The purified DHOases were assayed for DHOase activity by measuring the amount of CAA produced by conversion from dihydroorotate (DHO) produced at 20 min at 37°C. DHOase assay was performed to determine the V_{max} , and K_M . The assay was conducted at pH 9.5 in a microtiter plate as indicated in DHOase assay.

DHO was varied from a final concentration of 0.5 mM to 6 mM. The total volume of the assay was 200 μ L. A blank control containing all ingredients excluding the enzyme was used. This reading was then subtracted from the final reading for the experimental reaction. The assay reaction plate was preincubated at 37°C for 2 to 3 min. The reaction was initiated with the addition of DHO. At 20 min, the reaction was stopped with the addition of 100 μ L of stop mix (2 parts antipyrine (5 mg/mL) in 50 % sulfuric acid and 1 part monoxime (8 mg/mL) in 5 % acetic acid). After the addition of the stop mix, clear tape was applied to the top of the wells to prevent the evaporation of the reaction mixture.

The color was developed at 60°C in a waterbath. The assay was read at 450 nm in a kinetic microplate reader from Molecular Devices. Velocity-substrate curves were generated by plotting the specific activity of the enzyme (μ mol CAA/min/ μ g of protein). The μ mol produced was calculated by generating a CAA standard curve.

Purification of ATCase of *B. cepacia* by GST Gene Fusion System

Purification of ATCase was carried out by the glutathione S-transferase (GST) gene fusion system from GE Life Sciences. The GST gene fusion system is an integrated system for the expression, purification and detection of fusion proteins produced in *E. coli*. The pGEX2T plasmid vector (4.8kb) (Fig 11) is designed for

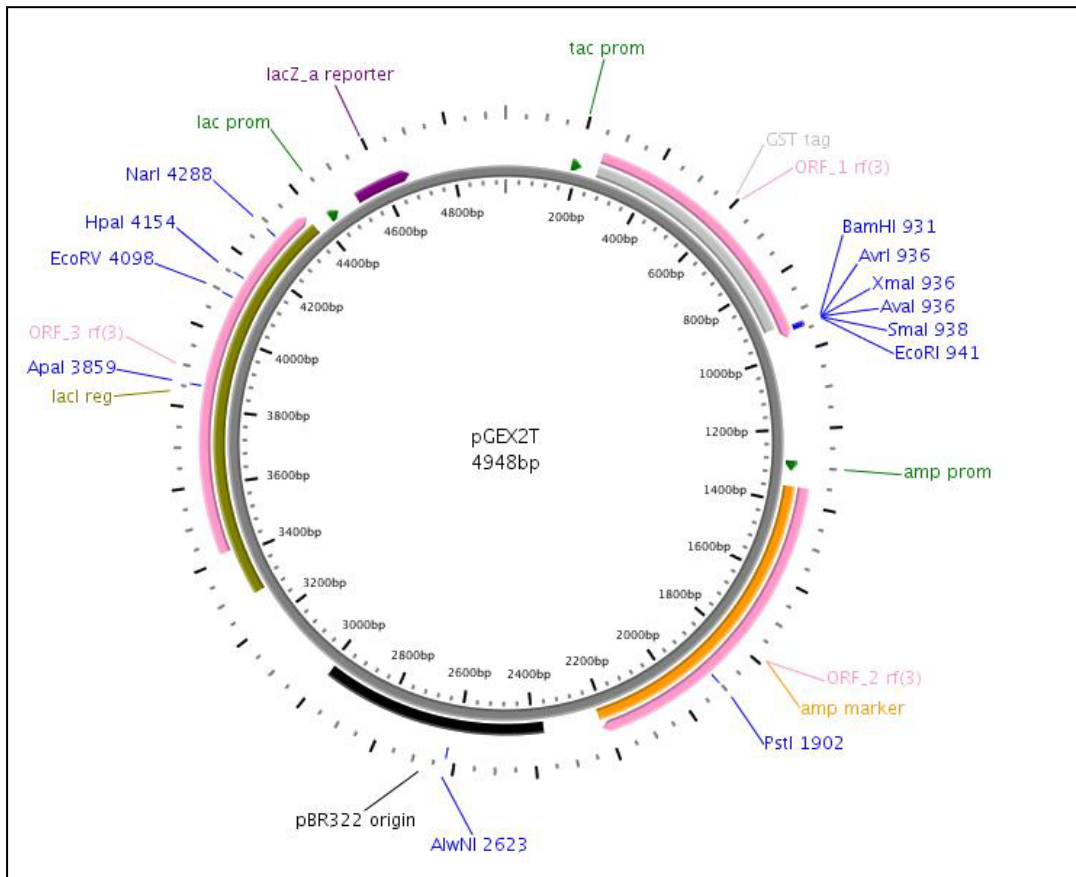


Fig. 11 Map of pGEX2T plasmid. Figure is drawn by PlasMapper version 2.0.

inducible, high level intracellular expression of genes as fusions with *Schistosoma japonicum* GST in this system. Fusion proteins are easily purified from bacterial lysates by affinity chromatography using Glutathione Sepharose 4B. Cleavage of the desired protein from GST is achieved using site-specific protease whose recognition sequence is located immediately upstream from the multiple cloning site on the pGEX plasmid.

The plasmid pSK2T was previously constructed in this lab (Kim 2004). The ATCase purification steps in GST Gene Fusion system are similar as those in the pMAL protein fusion and purification system. 2 L of BL21 containing pSK2T plasmid in LB broth with Amp (100 µg/mL) were incubated at 37°C shaker for 4 h until the culture reached the OD₆₀₀ of about 0.8. 0.5 mM (final concentration) of isopropyl-β-D-thiogalactoside (IPTG) was added and the cells were incubated for 3 h further on a 37°C shaker. Then, the cells were harvested using a 500 mL centrifugal bucket at 6,000 x g for 15 min in 4°C. After removing the supernatant, the cell pellet was resuspended with 50 mL cold PBS buffer, pH 7.3, and 37.5 µg/mL (final concentration) of DNase and 0.1 % (final concentration) Triton X-100 were added to the resuspension solution. Then cells were broken by means of a French pressure cell at 2000 psi. 1 mM of phenylmethylsulfonyl fluoride (PMSF) was added to the broken cell mixture and stirred gently at 4°C overnight. The cell debris was removed by centrifugation at 15,000 x g for 30 min. The clear supernatant was then transferred to a 50 mL conical tube and used for protein purification. The purification was performed as instructed by the manufacturer with slight modifications. The dialyzed fusion proteins were transferred to the new 15 mL conical tube and 50 U of thrombin

were added to cut the fusion portion of the GST and ATCase. This tube was incubated at room temperature in a rocker for 2 to 16 h. The next day, thrombin-cut protein was stored in 12 % glycerol at -80°C until being used.

To further purify the partially purified ATCase, anion exchange chromatography was performed using DEAE Sepharose column (Pharmacia). Eluted ATCase was dialyzed by 300X volume of 1X PBS buffer at 4 °C overnight and washed three times with 1 mL of PBS buiffer each time. The purity of purified ATCase was checked using 10 % sodium dodecyl sulfate polyacrylamide gel electrophoresis. The protein concentration of ATCase was determined by Bradford assay using BSA as the standard.

Aspartate Transcarbamoylase (ATCase) Assay

ATCase activity was measured by quantifying the amount of carbamoylaspartate (CAA) produced in 20 min at 30°C. This was accomplished using the method of Gerhart and Pardee (Gerhart and Pardee 1962), with modifications, by using the color development procedure of Prescott and Jones (Prescott and Jones 1969).

This assay was performed using a microtiter plate. The assay mixture contained the following in a 100 µL reaction volume: 4 µL of Tri-buffer pH 9.5 (51mM diethanolamine, 51 mM N-ethylmorpholine, and 100 mM MES, with an adjusted pH to 9.5 (Ellis and Morrison 1992), 10 mM potassium aspartate (pH 9.5), 2 mM dilithium carbamoylphosphate and cell extract or purified enzyme, usually 3 to 10 µL. The final volume was adjusted to 100 µL with dd-H₂O. Assay wells containing all components, except for carbamoylphosphate, were prepared in advance

and pre-incubated at 30°C for 5 min. The reaction was initiated by the addition of carbamoylphosphate and incubated at 30°C for 30 min. Then the reaction was stopped by the addition of 100 µL of stop reaction buffer (Prescott and Jones 1969). The microtiter plate was run in a 65°C heating block under fluorescent light for 1 h. The plates were taped shut to prevent loss of volume due to evaporation. The stop reaction buffer was made by two parts of 5 mg /mL antipyrine in 50 % sulfuric acid (v/v) mixed with one part of 8 mg/mL of 2, 3-butanedione monoxime in 5 % acetic acid (v/v). This mixture has to be made just prior to use and kept on ice. Then the micro titer plate was allowed to cool in the dark for 10 to 15 min and the assay was read at A₄₅₀ by the Kinetic Micro Plate reader from Molecular Device Company.

The amount of CAA produced was determined using a CAA standard curve. The standard curve was prepared using the same buffering system and known concentrations of CAA ranging from 0 to 1.0 mM.

Non-denaturing Polyacrylamide Aspartate Transcarbamoylase Activity Gels

A nondenaturing polyacrylamide gel with 4 % stacking gel and an 8 % separating gel was used. The gel was prepared by first pouring the separation gel, which contained 1.33 mL of the stock solution of acrylamide (30 % w/v acrylamide and 1 % w/v bis-acrylamide in dd-H₂O), 1.25 mL of Buffer B (1.5 M Tris-HCl, pH 8.8), and 2.41 mL of dd-H₂O. Ammonium persulfate (0.01g) was added to the mixture. The gel was polymerized with the addition of 5 µl of N, N, N' N' - tetramethylethylenediamine (TEMED). The mixture was gently inverted and poured into the assembled Bio-Rad mini protein II apparatus. A space of 2 cm was left at the top to pour the stacking gel. The gel was overlaid with *N*- butanol to exclude oxygen,

which inhibits the polymerization. The *N*-butanol also helped to flatten the top of separating gel. This set was allowed to polymerize for approximately 30 min after which the stacking gel was prepared. The stacking gel contained 0.27 mL of acrylamide, 0.4 mL of buffer C (0.5 M Tris, pH 6.8) and 0.92 mL dd-H₂O, ammonium persulfate (0.01g) and 5 μ L of TEMED. A 10 well comb was inserted and the gel was allowed to polymerize. 20 μ L of sample was mixed with 5 μ L of 5X loading buffer (312.5 mM Tris, 50 % v/v glycerol, and 0.05 % w/v bromophenol blue in dd-H₂O). The samples were loaded onto the gel. The chamber was filled with gel running buffer (25 mM Tris, 192 mM glycine in dd-H₂O) and electrophoresis was performed with 100volts for 1 h 40 min at room temperature.

Activity Stain of the ATCase in Non-denaturing Polyacrylamide Gels

The gels were stained specifically for ATCase activity by the method described by Bothwell (Bothwell and Schachman 1974) as modified by Kedzie (Kedzie 1987). The principle of this method is demonstrated when ATCase catalyses the reaction between carbamoylphosphate and aspartate to produce carbamoylaspartate, an inorganic phosphate is generated. This phosphate group reacts with lead nitrate to form a white precipitate. A modified version of the above method by Kedzie (1987) was performed.

The gels were placed in 250 mL of cold histidine buffer (50mM, pH 7.0) for 10 min. Then freshly made 5 mL of 1 M aspartate and 10 mL of 0.1 M carbamoylphosphate were added; the gels were incubated at room temperature for 5 min on a rocking shaker. The reactants were removed by rinsing the gel in 100-200 mL of cold dd-H₂O for three times. Lead nitrate, at a concentration of 3 mM, was

added to another 250 mL of histidine buffer, pH 7.0, which was then poured onto the gel. After 10 min, the lead nitrate was removed by 3 washes in cold dd-H₂O. ATCase activity was observed at the site of lead phosphate precipitation. The gel was left overnight at 4 °C to increase the visibility of the bands, and then stained with 3 % sodium sulfide for 3 min and washed three times with dd-H₂O to convert the white lead nitrate to black lead sulfide. The gels were soaked in 10 % glycerol and dried for preservation.

Enzyme Kinetics of ATCase of *B. cepacia*

The purified ATCases were assayed for ATCase activity by measuring the amount of carbamoylaspartate (CAA) produced at 20 min at 37°C. The method utilized was the color reaction described by Prescott and Jones, 1969. ATCase assays were performed to determine the V_{max}, and K_M. A tribuffer system (0.05 M MES, 0.1 M diethanolamine, and 0.051 M N-ethymorpholine) was used. The assay was conducted at pH 9.5 in a microtiter plate as indicated in ATCase assay. Aspartate was varied from a final concentration of 0.5 mM to 6 mM and carbamoylphosphate was kept at a concentration of 5 mM. The total volume of the assay was 200 µL.

The reaction was initiated with the addition of carbamoylphosphate. The assay was read at 450 nm by a kinetic microplate reader from Molecular Devices. Velocity-substrate curves were generated by plotting the specific activity of the enzyme (µmol CAA/min/µg of protein). The µmol produced was calculated by generating a CAA standard curve.

Refolding of ATCase Holoenzyme

To investigate the structure of ATCase holoenzyme of *B. cepacia*, the purified DHOase from *B. cepacia* was refolded with the previously purified ATCase from *B. cepacia* (Kim 2004) using the method provided by New England Biolabs. Inc. Kim reported that there are two active trimeric forms of ATCase in *B. cepacia*, the normal *B. cepacia* ATCase polypeptide (consists of 47 kDa PyrB subunits) and truncated PyrB subunit *B. cepacia* ATCase (consists of 40 kDa PyrB subunits) (Kim 2004).

As a pilot experiment, 10 μ L of purified DHOase from *B. cepacia* was mixed with previously purified ATCase, and incubated at 37°C for 1 h. The practical refolding method provided by New England Biolab. was performed with slight modification. First, equal molar amounts of purified ATCase and DHOase (10 μ L each) were mixed with guanidine hydrochloride to give a final concentration of 6 M. Then mixture was transferred to a dialysis tube, and dialyzed against 300 volumes ATCase Buffer, 2 times: once for 4 h and once overnight. Following collection from the dialysis tube, the reconstructed ATCase holoenzyme was stored at -80°C. The refolded ATCase holoenzyme was run on nondenaturing polyacrylamide gels for ATCase activity staining to investigate the refolding of cleaved and non cleaved ATCase with DHOase.

Construction of a *pyrC* Knockout in *B. cepacia*

The *pyrC* knockout was constructed by deletion of 300 bp of *pyrC* gene cloned into the pUC18 plasmid. The 300 bp from *pyrC* gene of *B.cepacia* was deleted by the *Bst*B1 restriction enzyme. The interrupted *pyrC* gene was subcloned into pEX18-Gm plasmid (Figure 12) using *Kpn* I and *Hind* III restriction enzymes. This subcloned pEX18 plasmid was transformed into *E.coli* SM10 for conjugation. Recombination of

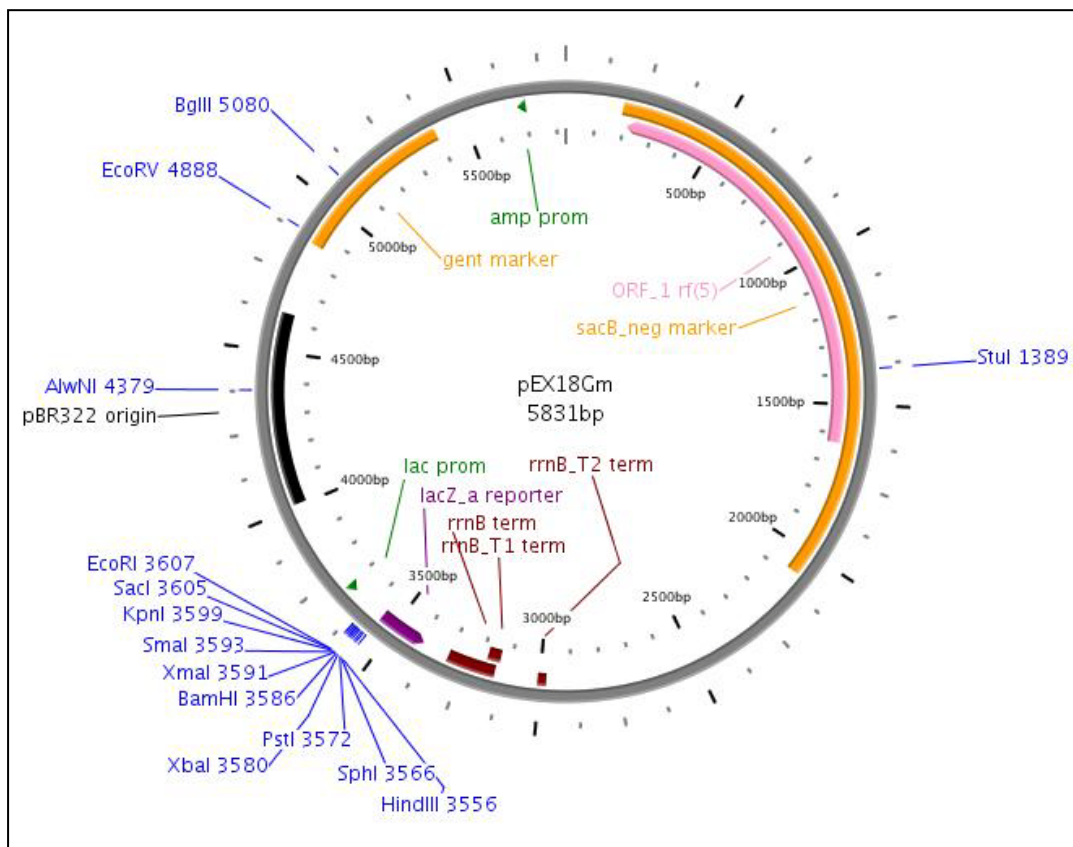


Fig. 12 Map of pEX18Gm plasmid. Figure is drawn by PlasMapper version 2.0.

the *pyrC* gene from *B. cepacia* with the interrupted *pyrC* gene was achieved by the biparental mating method (Van Haute et al. 1983). The wild-type *B. cepacia* was grown in LB broth at 42°C with shaking to mid-log phase ($OD_{600} = 0.5$). *E. coli* SM10 transformed with *pyrC* interrupted pEX18-Gm was grown in LB broth at 37°C with shaking to mid-log phase ($OD_{600} = 0.5$). The *B. cepacia* and SM10 cultures were combined in microcentrifuge tubes in the ratio of 20: 1. The mixed cultures were collected by centrifugation at 14,000 x g in a Sorvall® microcentrifuge for 1 min. The supernatant was discarded and the cells were resuspended in 30 µL LB broth. The suspension was transferred onto an LB plate in one location and allowed to mate overnight at 37°C. The mating growth was then scraped off of the agar and suspended in 1 mL of PBS. Dilutions were made and 50 µL of 10^{-6} through 10^{-8} dilution samples were plated onto PIA with gentamicin (Gm) 15 µg/mL. The plates were incubated at 37°C for 12 h. *E. coli* SM10 was selected on PIA with Gm 15 µg/mL in order to collect any surviving *B. cepacia* colonies containing *B. cepacia pyrC* interrupted pEX18-Gm incorporated into the genome by a single recombination. These colonies were then picked and touched to two patch plates: 1) PIA with Gm 15 µg/mL and 2) PIA with 10 % sucrose, and allowed to incubate at 37°C for 12 h.

Colonies that grew on both plates were picked and grown in LB with Gm 15 µg/mL an additional 12 h at 37°C with shaking to allow time for a second recombination. The cells were collected by centrifugation and plated onto PIA with Gm 15 µg/mL. Colonies were picked with sterile toothpicks, touched to two patch plates: 1) PIA with Gm 15 µg/mL and 2) PIA with 10 % sucrose, and allowed to incubate at 37°C for 12 h. Colonies that grew on 1) but not on 2) were then moved onto two more patch plates: 3) Psmm and 4) Psmm with 50 µg per mL uracil. The

colonies that grew on 4) but not on 3) contained the new *B. cepacia pyrC* mutant. To confirm the construction of *pyrC* knockout *B. cepacia*, PCR, sequencing and Southern blot analysis were performed.

Southern Blot

A Southern blot was performed using the procedure described by Sambrook *et al.* (Sambrook 1989) with slight modifications. This allows us to determine the molecular weight of a restriction fragment, to measure relative amounts in different samples and to locate a particular sequence of DNA within a complex mixture. DNA (genomic or other source) is digested with a restriction enzyme and separated by gel electrophoresis and transferred from an agarose gel onto a membrane which is then incubated with a probe of single-stranded DNA. This probe will form base pairs with its complementary DNA sequence and bind to form a double-stranded DNA molecule. The probe is labeled before hybridization either radioactively or enzymatically.

Restriction of Chromosomal DNA with Restriction Enzyme

The chromosomal DNAs of wild-type *B. cepacia* and *pyrC* knockout *B. cepacia* were prepared as described earlier. 20 μL (10 μg) of each chromosomal DNA was restricted overnight at 37°C by 3 μL of *EcoRI* and 3 μL 10X NEB buffer (1 M Tris-HCl, 500 mM NaCl, 1M MgCl₂, and 0.25 % Triton X-100) in the final reaction volume of 30 μL after adjusting with dd-H₂O. Other restriction enzymes were used with the same reaction conditions.

Separation of Restricted DNA by Agarose Gel Electrophoresis

The restricted DNA was run on 1 % agarose. The gel was initially

electrophoresed at 65 volts for 30 min to move the DNA out of the wells, then at 25 volts for 20 h, and then again at 100 volts for 30 min to sharpen up the bands for better size separation.. Once electrophoresed, a picture was taken to document the ladder location.

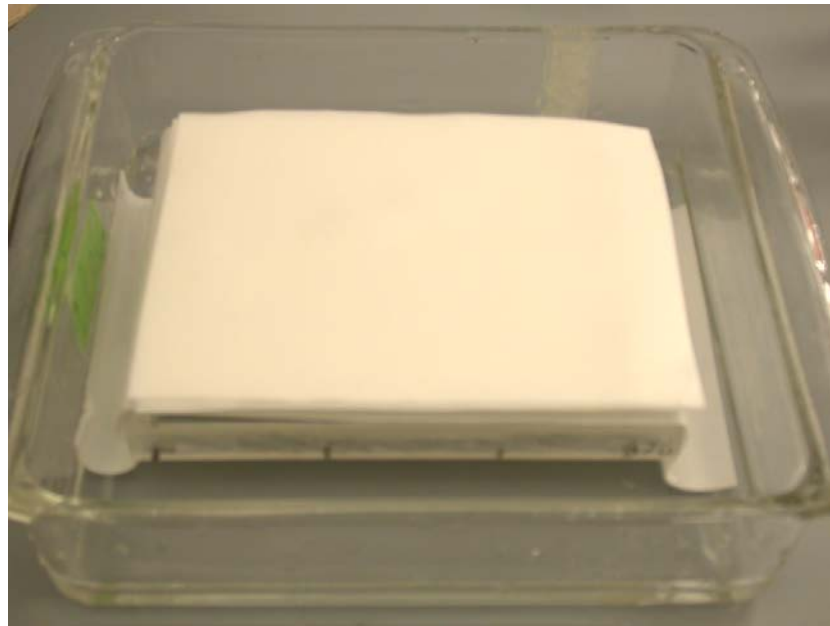
DNA Blotting

A series of washes were performed on the gel. The gel was washed with 100 mL of 1X denaturation solution (1.5 M NaCl, 0.5 N NaOH) for 15 min with gentle rocking twice. Then the gel was washed with 100 mL of 1X neutralization solution (1 M Tris, pH 7.4, 1.5 M NaCl) for 30 min with gentle rocking three times. For the DNA blotting, a Nalgene® positively charged nylon membrane was used. The membrane was always handled with sterile forceps to avoid foreign DNA contamination, and all paper described was handled with gloved hands. A gel stand wrapped with Whatman® paper was set into a baking dish and transfer solution (5X SSC) was poured into the dish to halfway fill up the gel stand and paper.

The DNA denatured and neutralized gel was trimmed and notched on one corner for orientation recognition and placed wells down (DNA up) onto the stand wrapped with Whatman® paper soaked in transfer solution. The membrane was thoroughly wetted with sterile dd-H₂O, placed onto the gel and marked with a permanent marker in one corner to indicate the non-DNA side, and the well location on the membrane. On top of the membrane, 3 pieces of Whatman® paper, a stack of paper towels, and a glass plate weight were used as a wick system to pull the transfer solution up through the gel and into the membrane (Figure 13).

The transfer was allowed to proceed for 24 h with periodic exchange of wet paper towels for dry ones, and replenishment of transfer solution. The membrane was

(A)



(B)



Fig. 13 Transferring DNA from gel to nitrocellulose membrane.

A. Stacking the membrane on gel. B. Completion of stacking nitrocellulose membrane and paper towels on gel.

removed from the gel, and placed DNA side up onto a piece of Whatman® paper wet with 10X SSC. The DNA was then fixed to the membrane using ultra violet radiation in a UVP CL-1000 ultraviolet crosslinker. The membrane was exposed for 40 s at $1500 \times 100 \mu\text{J}/\text{cm}^2$ and then allowed to air dry on a dry paper towel. The membrane was sandwiched in Whatman® paper, wrapped in aluminum foil and stored at 4°C until ready for hybridization with the probe.

Probe Creation and Hybridization

The probe creation and hybridization was achieved using the Roche® DIG High Prime DNA Labeling and Detection Starter Kit II. The probe was labeling as random primed labeling method.

10 ng-3 μg template DNA was added to a reaction vial. The DNA was denatured by heating the sample in a boiling water bath for 10 min and then the sample was quickly chilled in an ice/water bath. 4 μL mixed DIG-High Prime was added to the denatured sample and centrifuged briefly. The sample was incubated for at least 1 h at 37°C. The reaction was finished by adding 2 μL 0.2 M EDTA (pH 8.0) to the sample, and heating the sample to 65° C for 10 min.

For hybridization, an appropriate volume of DIG Easy Hyb (10 mL/100 cm^2 filter) was preheated to hybridization temperature (37 - 42°C). Then the filter was prehybridized for 30 min with gentle agitation in an appropriate container. The DIG-labeled DNA probe (about 25 ng/mL DIG Easy Hyb) was denatured by boiling for 5 min and rapidly cooling in ice/water. Then, the denatured DIG-labeled DNA probe was added to pre-heated DIG Easy Hyb (3.5 mL/100 cm^2 membrane) and mixed well. The prehybridization solution was poured off and the probe/hybridization mixture was added to the membrane, and then incubated overnight with gentle agitation.

Visualization

Visualization was achieved as indicated in the manual provided by the manufacturer without modification. After hybridization and stringency washes, the membrane was rinsed briefly for 1-5 min in washing buffer. The membrane was treated in series of incubations: 30 min in 100 mL Blocking solution, 30 min in 20 mL Antibody solution, washed 2×15 min in 100 mL washing buffer, and equilibrated 2-5 min in 20 mL Detection buffer.

Growth Study

A growth curve was performed for the wild type and mutant strain in minimal and rich media. Growth curves of *pyrC* and wild-type *B. cepacia* were initiated by first inoculating a 5 mL starter culture of the appropriate medium and incubated overnight. This overnight culture (15 – 20 h) was used to inoculate 50 mL of medium in a 125 mL Erlenmeyer flask. The bacteria were diluted 1:1000 (0.5 mL inocula for a 50 mL culture) and the OD₆₀₀ was measured and recorded for time point zero. The cultures were incubated at 37°C with shaking at 250 rpm. At the indicated time point, 1 mL of each culture was aseptically removed and the OD₅₉₅ recorded.

Virulence Tests

Motility Tests

The ability of *B. cepacia* to be an opportunistic pathogen by producing virulence factors is entitled by adherence factor. Swimming and swarming motilities were tested on *B. cepacia* wild type and *pyrC* knockout mutant strain. Swimming motility is the assay to test the ability of motility provided by flagella, while

swarming and twitching motilities are the assays to test the type IV pili.

Twitching Assay

Twitching agar (Rashid *et al.* 2000) used to detect the twitching motility contained 25 g Difco® Luria-Bertani (LB) Miller broth and 10 g of Difco bacto agar (1 %) per one liter. After sterilization, uracil 40 µg/mL concentration was supplemented. Colonies were picked from the overnight culture with a sterile toothpick and moved to the corresponding Twitching plates. The plates were incubated at 37°C for 24 h. Pictures were taken to document the resulting characteristics.

Swarming Assay

Swarming agar (Rashid and Kornberg 2000) used to detect swarming motility contained 0.5 % (w/v) Difco Bacto Agar, 0.8 % Difco® nutrient broth, and 0.5 % glucose supplemented with uracil 40 µg/ mL concentration. Test organisms were streaked onto LB plates and incubated overnight at 37°C. Colonies were picked from the overnight culture with a sterile toothpick and touched to the corresponding swarm plates. The plates were incubated at 37°C for 24 h. Pictures were taken to document the resulting characteristics.

Swimming Assay

Swim agar plates (Rashid and Kornberg 2000) used to detect swimming motility contained tryptone broth (1% tryptone, 0.5% NaCl), and 0.3% (w/v) agarose supplemented with uracil 40 µg/ml concentration. Test organisms were streaked onto LB plates and incubated overnight at 37°C. Colonies were picked from the overnight culture with a sterile toothpick and touched to the corresponding swim plates. The

plates were incubated at 30°C for 24 hours. Pictures were taken to document the resulting characteristics.

Biofilm Assay

Microtiter Plate Biofilm Assay

This experimental system, whose most common format is often referred to as the 96-well plate assay, is a simple high-throughput method used to monitor microbial attachment to an abiotic surface (MacKenzie et al. 1994; Pratt and Kolter 1999).

Cells are grown in microtiter dishes for 24h and 48h then the wells are washed to remove planktonic bacteria. Cells remaining adhered to the wells are subsequently stained with a dye that allows visualization of the attachment pattern. A modified method was used in this research. To reduce the complexity of complexity of extracellular components and to avoid uracil in LB medium, *Pseudomonas* minimal media (Psmm) were used.

First, 5 µl of overnight cultured cells were added into the one set of sterile microtiter plates filled with 100 µl of the Psmm without uracil per well. To check the uracil effect on the biofilm formation, uracil 40 µg/mL concentration was added in the other sets. Four wells were used for wild type and mutant, and were incubated overnight 37°C with a cover. The next day, planktonic bacteria were removed from each microtiter dish by briskly shaking the dish out over the waste tray. To wash the wells, plate was submerged into water tray and liquid was vigorously shaken out over the waste tray. Each well was stained with 125 µl of 0.1 % crystal violet solution for 10 min at room temperature. The crystal violet solution from the microtiter dish was removed by shaking each microtiter dish out over the waste tray. The microtiter dish was washed successively in each of the next two water trays and shaken out as much

excess liquid as possible was removed after each wash and was then inverted on paper towels to remove any additional liquid. After being air dried, 200 μL of 95 % ethanol was added to each stained well.

Plates were covered and incubated at room temperature for 15 min to allow the dye to solubilize. The contents of each well were briefly mixed by pipetting, and then 125 μL of the crystal violet/ethanol solution was transferred from each well to a separate well in an optically clear flat-bottom 96-well plate. The optical density (OD) of each of these 125 μL samples was measured at a wavelength of 500 to 600 nm.

Air-liquid Interface Coverslip Assay

Often, a great deal can be learned about the biofilm formation behavior of a particular bacterium simply by observing the early stages of this process, including attachment and early microcolony formation. The air-liquid interface (ALI) assay provides a simple system for microscopic analysis of biofilm formation over a time range of ~ 4 to 48 h (Caiazza and O'Toole 2004).

A 24-well plate is placed at an angle of 30° to 50° relative to horizontal, and stationary-phase cultures are diluted and slowly applied to these wells such that the upper edge of each culture aliquot is positioned at the center of a well's bottom. The bacteria of interest are allowed to grow in this manner for an appropriate length of time, and then the wells are rinsed gently and viewed by phase-contrast microscopy.

First, each bacterium of interest was inoculated and grown to stationary phase in a 5 mL Psmm medium. Then, the stationary-phase (or other appropriate) cultures was diluted 1:100 in Psmm not supplemented with uracil and 1 mL of diluted culture was transferred into a well in a flat-bottom multiwell plate. A coverslip was inserted into each well so that it was held at a 90° angle relative to the bottom of the well (i.e.,

perpendicular to the bottom of the well) so that the meniscus of the medium was at the center of the coverslip. Then, plate was covered and incubated at 37°C for 24 h. Each coverslip was removed from its well and nonadherent cells were rinsed off by dipping in sterile Psmm. Bacteria on the coverslip were stained by submerging coverslips in 0.1 % crystal violet for 10 min. After rinsed off excess dye by dipping each coverslip in two successive water baths, coverslip was air dried. The bacteria on each coverslip were visualized by microscopy. To check the uracil effect on the biofilm formation, uracil 40 µg/mL concentration was added in the other set and performed exactly the same way.

CHAPTER 3

RESULTS

Cloning of the *B. cepacia pyrC* Gene

To clone the *pyrC* gene of *B. cepacia*, the *pyrC* genes of *Burkholderia* spp. were aligned by using Genedoc® software due to unavailable *B. cepacia pyrC* gene information. The *pyrC* genes of *B. fungorum*, *B. mallei*, and *B. pseudomallei* showed variance at the 5' and 3' regions (Figure 14). From the gene alignment, the conserved sequences 130 bp upstream from the start codon and 700 bp downstream from the stop codon were identified and used to develop primers (BurkC-F and BurkC-R) (Table 6) for PCR reaction in the cloning procedure (Figure 15). The PCR reaction using these primers yielded a product with a size of 1.4 kbp (Figure 16). This PCR product was inserted into the pUC18 plasmid (Figure 17) and the cloned plasmid was confirmed by restriction digestion (Figure 18). This cloned plasmid was named pHKeBC plasmid. Lane 1 shows 1 kb DNA ladder and lane 2 and 3 identifies the cloned plasmid digested with *KpnI* and *HindIII*. Lane 4 shows undigested cloned plasmid. The sequence of the cloned gene was aligned with the genes of *B. fungorum*, *B. mallei*, and *B. pseudomallei* again to achieve the sequence of *B. cepacia pyrC* gene. As a result, 1,065 bp of *B. cepacia pyrC* gene was identified. Based on this identified gene, primers were designed (BCpyrC-F and BCpyrC-R) (Table 6). After being amplified (Figure 19), 1,065 bp *B. cepacia pyrC* gene was inserted into the pUC18 plasmid (Figure 20), and the cloned plasmid was confirmed by restriction digestion (Figure 21). This cloned plasmid was named as pHKBC plasmid.

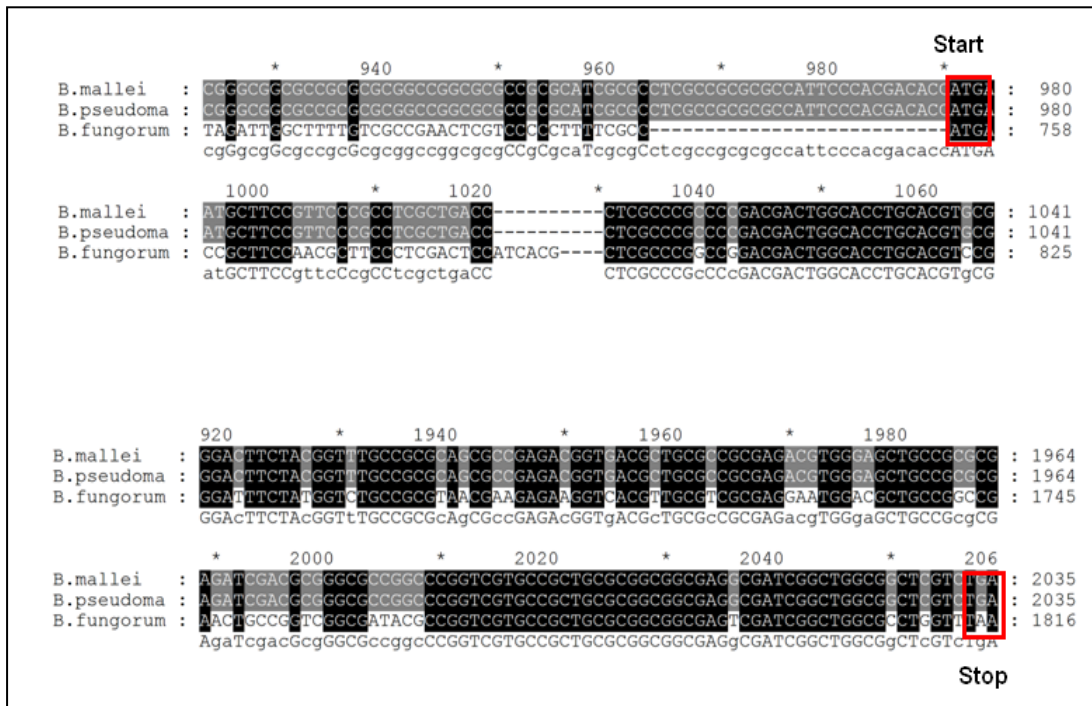


Fig. 14 DNA sequence alignment of PyrC from *Burkholderia* spp.

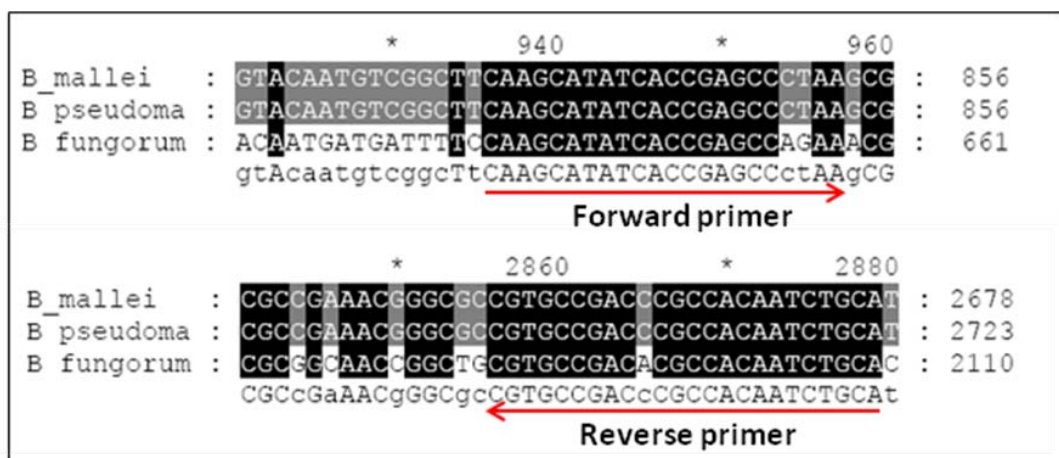


Fig. 15 Design of forward and reverse primers to amplify gene containing *B. cepacia pyrC* gene.

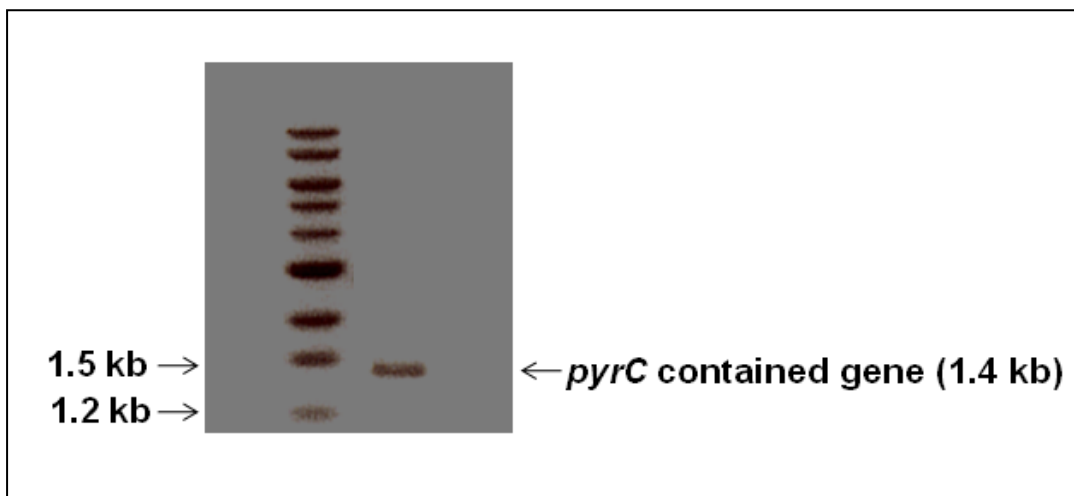


Fig. 16 PCR reaction to amplify *B. cepacia* *pyrC*-contained gene.

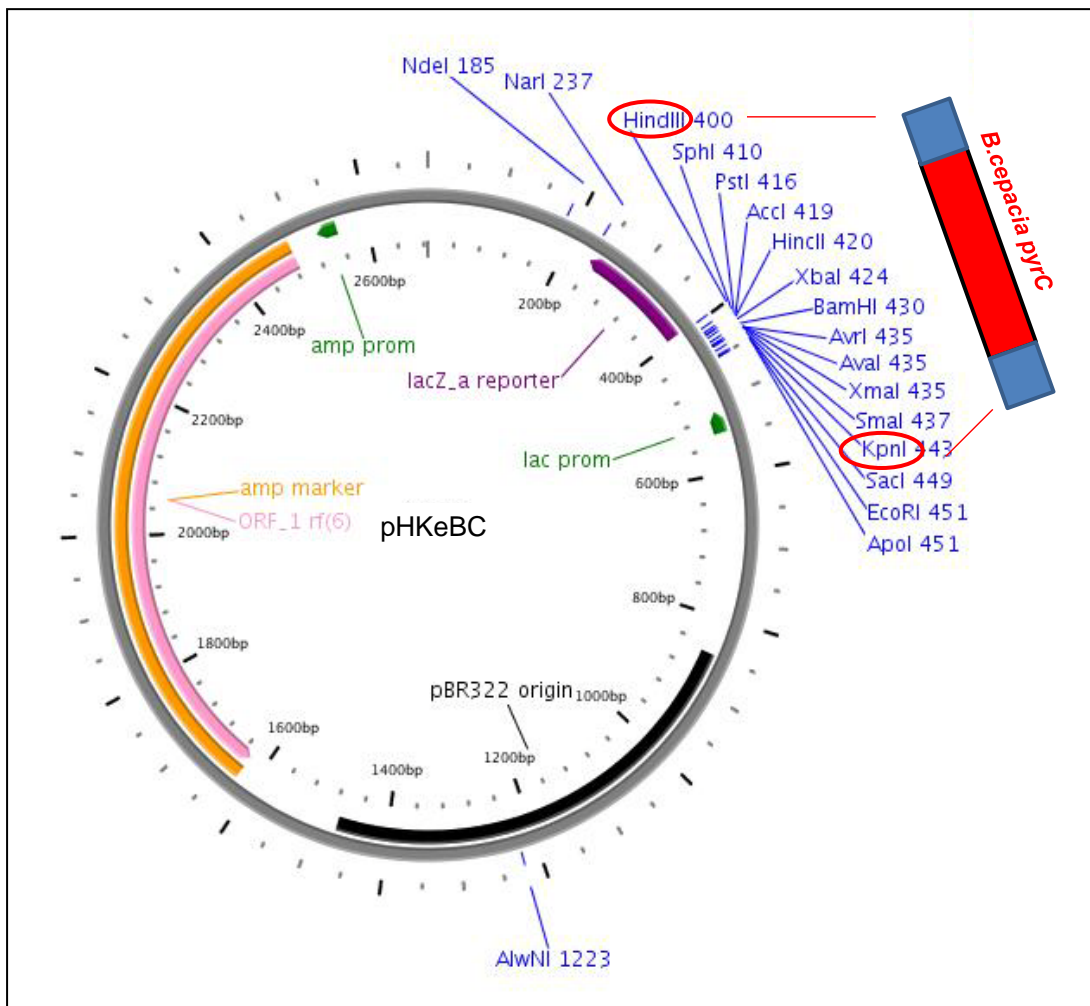


Fig. 17 Schematic diagram of construction of pHKeBC plasmid from inserting gene containing *B. cepacia pyrC* gene into pUC18 plasmid. Figure is drawn by PlasMapper version 2.0.

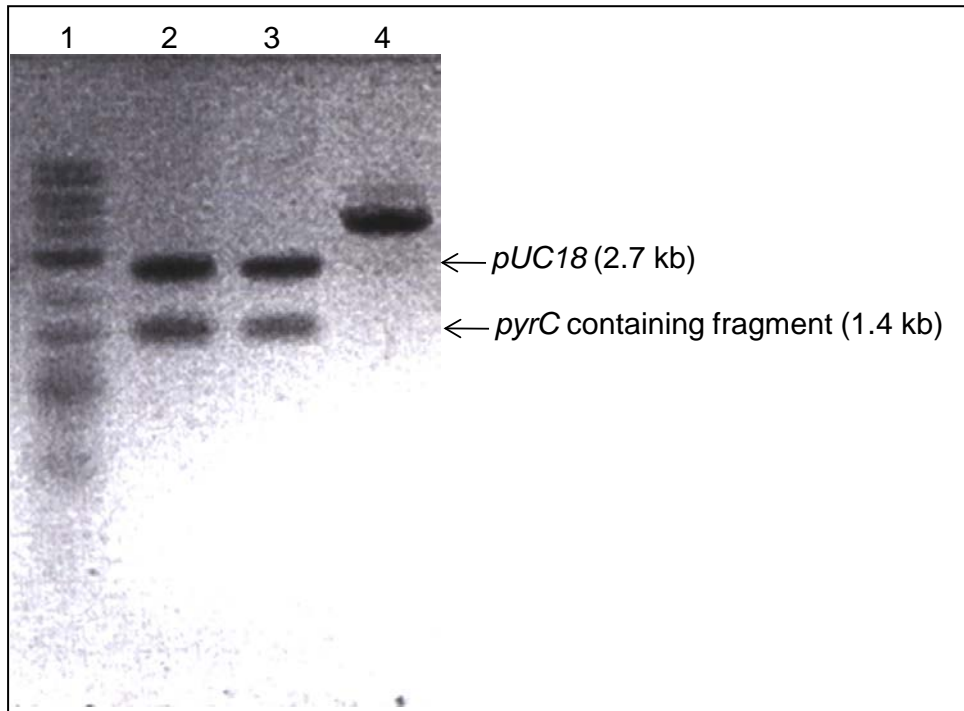


Fig. 18 Restriction digestion of pHKeBC plasmid. pHKeBC plasmid was digested with *KpnI* and *HindIII* enzyme and run on a 1.5 % agarose gel. Lane 1: 1 kb ladder, lane 2, 3: cloned pHKeBC plasmid.

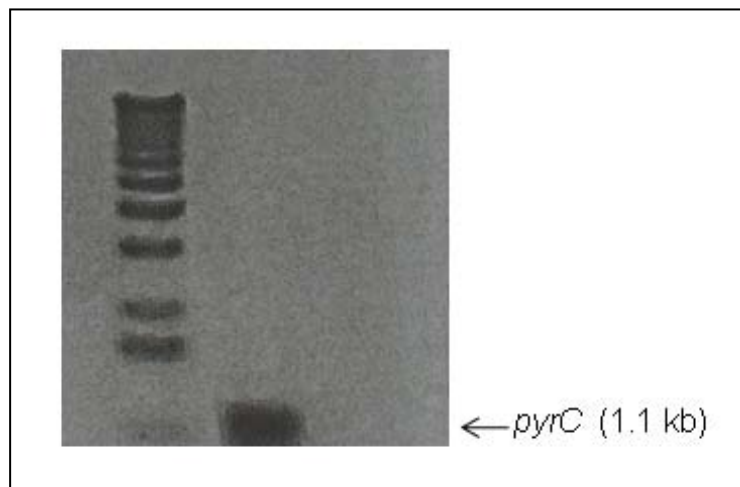


Fig. 19 PCR reaction to amplify *B. cepacia pyrC* gene.

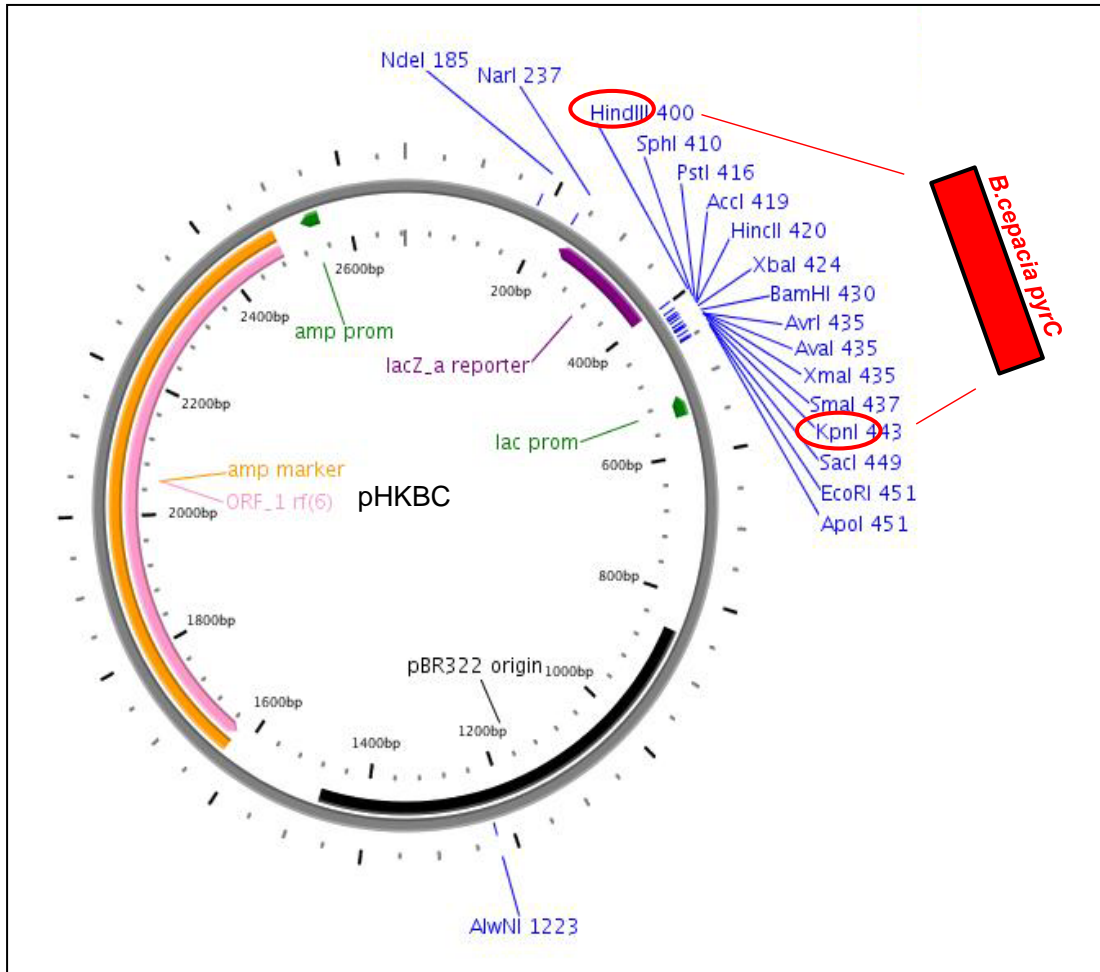


Fig. 20 Schematic diagram of construction of pHKeBC plasmid from inserting *B. cepacia pyrC* gene into pUC18 plasmid. Figure is drawn by PlasMapper version 2.0.

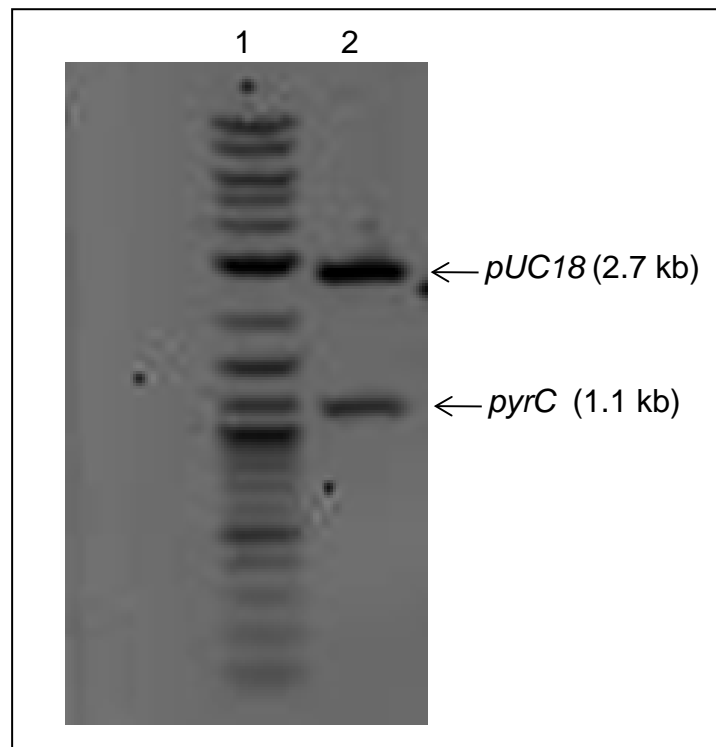


Fig. 21 Restriction digestion of pHKBC plasmid. pHKBC plasmid was digested with *Kpn*I and *Hind*III enzyme and run on a 1.5 % agarose gel. Lane 1: 1 kb ladder, lane 2: cloned pHKBC plasmid.

Lane 1 shows 1 kb DNA ladder and lane 2 represents the cloned plasmid digested with *KpnI* and *HindIII* (Figure 21). The sequenced 1,065 bp *B. cepacia pyrC* gene (Figure 22) was reported and registered in NCBI data base (Figure 23). The protein-protein blast was also performed using 1,065 bp *B. cepacia pyrC* gene (Figure 24). The protein sequence of *B. cepacia* DHOase was homologous to other *Burkholderia* spp. (>99 %), and gave 98 % homology to *Bordetella pertussis* and >93 % to *Pseudomonas aeruginosa*. These results demonstrate the conserved protein sequences of DHOase from *Burkholderia* spp. even with slight variation in the nucleotides sequences.

Complementation Test Using DHOase Deficient *E.coli* MA1008

In the complementation test using DHOase deficient *E. coli* MA1008, *E. coli* containing *B. cepacia pyrC* gene grew in *E. coli* minimal medium without uracil while the control DHOase deficient *E. coli* MA1008 was not able to survive (Figure 25 top panel A and B). In addition to that, *E. coli* containing *B. cepacia pyrC* gene showed DHOase activity of 35 nmol/min/mg (Figure 25 bottom panel A and B). From these results, the cloned *B. cepacia pyrC* gene expressed active DHOase and complemented the *E. coli pyrC* auxotroph.

Purification of DHOase Enzyme by the pMAL Protein Fusion and Purification System

The DHOase from *B. cepacia* ATCC25416 was purified by the pMAL protein fusion and purification system. After being digested from the cloned plasmid, 1,065 bp *B. cepacia pyrC* gene was re-inserted into the pMAL plasmid (Figure 26), and the

```
ATGACTGCCTCGAACGCTTCCTCCCCGGCGACGCTCTCGCTCGCCCGT
CCCGACGACTGGCACCTGCACCTGCGAGACGGCGACATGCTGGCCGC
CGTGCTGCCGCACACCGCGCGCCAGTTTCGGCCGCGCGATCGTCATGC
CGAACCTGAAGCCCGCCGGTGACGACCACCGCGCAGGCGCAGGCCTAT
CGCGAGCGCATCCTCGCCGCGCTGCCGGCCGGGATGACGTTTGAACC
GCTGATGACGCTGTACCTGACCGACAACATGCCGCCCGACGAGATCC
GCCGCGCGCGCGAAAGCGGCTTCGTGCACGGCGTGAAGCTGTATCCG
GCCGGTGCACGACGACGAATTCGACCAACGGTGTACCCGATCTCGCGAA
ATGCGCGAAGACGCTCGAGGCGATGCAGGAAACCGGCATGCCGCTGC
TCGTGCACGGCGAGGTGACCGACGCATCGATCGACCTGTTGACCCGC
GAGAAGGTCTTCATCGACCGCGTGATGACGCCGCTGCGCCGCGATTT
CCCGGGCCTGAAGGTCGTGTTTGAACACATCACGACGAAGGACGCG
GCCGACTACGTGCGCGACGCCGATGCGGCGCCCGGCCTGCTCGGCGC
GACGATCACCGCGCATCACCTGCTGTACAACCGCAATGCGCTGTTCTG
CGGCGGGATTGCCCCGATTACTACTGCCTGCCGGTGCTGAAGCGCG
AGACGCATCGCGTCGCGCTGGTGCAGGCCGCGACGTGCGGCAACCCG
CGCTTCTTCCTCGGAACCGACAGCGCGCCGCATGNGCGCGACGCGAA
GGAAACCGCGTGCGGCTGCGCGGGTTGCTATACGGCGCTGCATGCGC
TCGAACTGTATGCGGAAGCGTTCGACCAACCGGTGCGCTCGACAAG
CTGGAAGGTTTCGCGAGCTTCTTCGGCGCCGATTTCTACGGGCTGCCG
CGCAGCGCCGAGACGGTCACGCTGCGTCGCGAGGCGTGGGAGTTGC
CGCGCGAGATCTTCGCGGGCGATACGCCGTCGTGCCGCTGCGCGGC
GGCGAGACGATCGGCTGGAACTGGCGTGA
```

Fig. 22 Identified sequence of *B. cepacia pyrC* gene.

GenBank: EU718731.1

Features		Sequence	
LOCUS	EU718731	1065 bp	DNA linear BCT 10-JUN-2008
DEFINITION	Burkholderia cepacia strain 25416 dihydroorotase (pyrC) gene, complete cds.		
ACCESSION	EU718731		
VERSION	EU718731.1 GI:189409345		
KEYWORDS	.		
SOURCE	Burkholderia cepacia		
ORGANISM	Burkholderia cepacia Bacteria; Proteobacteria; Betaproteobacteria; Burkholderiales; Burkholderiaceae; Burkholderia; Burkholderia cepacia complex.		
REFERENCE	1 (bases 1 to 1065)		
AUTHORS	Kim,H., Kim,S. and O'Donovan,G.A.		
TITLE	Purification and characterization of dihydroorotase (DHOase) of Burkholderia cepacia 25416 and construction of pyrC knockout mutant		
JOURNAL	Unpublished		
REFERENCE	2 (bases 1 to 1065)		
AUTHORS	Kim,H., Kim,S. and O'Donovan,G.A.		
TITLE	Direct Submission		
JOURNAL	Submitted (14-MAY-2008) Biological Sciences, University of North Texas, 1510 Chestnut St., Denton, TX 76203, USA		

Fig. 23 Deposit of identified *B. cepacia pyrC* gene. The sequence of *B. cepacia pyrC* gene was reported in NCBI data base (GenBank:EU718731.1).

Sequences producing significant alignments:				
Accession	Description	Max score	Total score	Query coverage
YP_368007.1	dihydroorotase [Burkholderia sp. 383]	716	716	100%
YP_001763942.1	dihydroorotase [Burkholderia cenocepacia MC0-3]	712	712	100%
YP_002232455.1	dihydroorotase [Burkholderia cenocepacia J2315]	712	712	100%
YP_620079.1	dihydroorotase [Burkholderia cenocepacia AU 1054] >ref YP_83432	710	710	100%
ZP_04946553.1	Dihydroorotase, homodimeric type [Burkholderia dolosa AU0158]	705	705	100%
YP_001580889.1	dihydroorotase [Burkholderia multivorans ATCC 17616] >ref YP_0C	688	688	100%
ZP_02378522.1	dihydroorotase [Burkholderia ubonensis Bu]	684	684	100%
YP_001807309.1	dihydroorotase [Burkholderia ambifaria MC40-6]	670	670	100%
ZP_02911250.1	dihydroorotase, homodimeric type [Burkholderia ambifaria MEX-5]	669	669	100%
ZP_02890634.1	dihydroorotase, homodimeric type [Burkholderia ambifaria IOP40-1	667	667	100%
YP_772463.1	dihydroorotase [Burkholderia ambifaria AMMD]	667	667	100%
YP_001118488.1	dihydroorotase [Burkholderia vietnamiensis G4]	659	659	100%
ZP_02356994.1	dihydroorotase [Burkholderia oklahomensis EO147] >ref ZP_02364	653	653	98%
ZP_02464737.1	dihydroorotase [Burkholderia thailandensis MSMB43]	647	647	98%
YP_441777.1	dihydroorotase [Burkholderia thailandensis E264] >ref ZP_0237346	646	646	98%
ZP_02491454.1	dihydroorotase [Burkholderia pseudomallei NCTC 13177]	645	645	98%
YP_334796.1	dihydroorotase [Burkholderia pseudomallei 1710b] >ref ZP_046094	644	644	98%
ZP_04819720.1	dihydroorotase, homodimeric type [Burkholderia mallei PRL-20]	644	644	98%
YP_109508.1	dihydroorotase [Burkholderia pseudomallei K96243] >ref YP_10397	644	644	98%
YP_001060393.1	dihydroorotase [Burkholderia pseudomallei 668]	643	643	98%
YP_002910464.1	Dihydroorotase, homodimeric type [Burkholderia glumae BGR1]	637	637	99%
YP_001858785.1	dihydroorotase, homodimeric type [Burkholderia phymatum STM81	629	629	99%
ZP_02412942.1	dihydroorotase [Burkholderia pseudomallei 14]	629	629	96%
YP_001896972.1	dihydroorotase [Burkholderia phytofirmans PsJN]	625	625	99%
ZP_06293854.1	dihydroorotase, homodimeric type [Burkholderia sp. CCGE1001]	623	623	99%
ZP_06845754.1	dihydroorotase, homodimeric type [Burkholderia sp. Ch1-1]	620	620	99%
YP_560383.1	dihydroorotase [Burkholderia xenovorans LB400]	620	620	99%

Fig. 24 Gene blast using NCBI data base. The amino acid sequence from *B. cenocepacia* *pyrC* gene was blasted against other strains using NCBI data base.

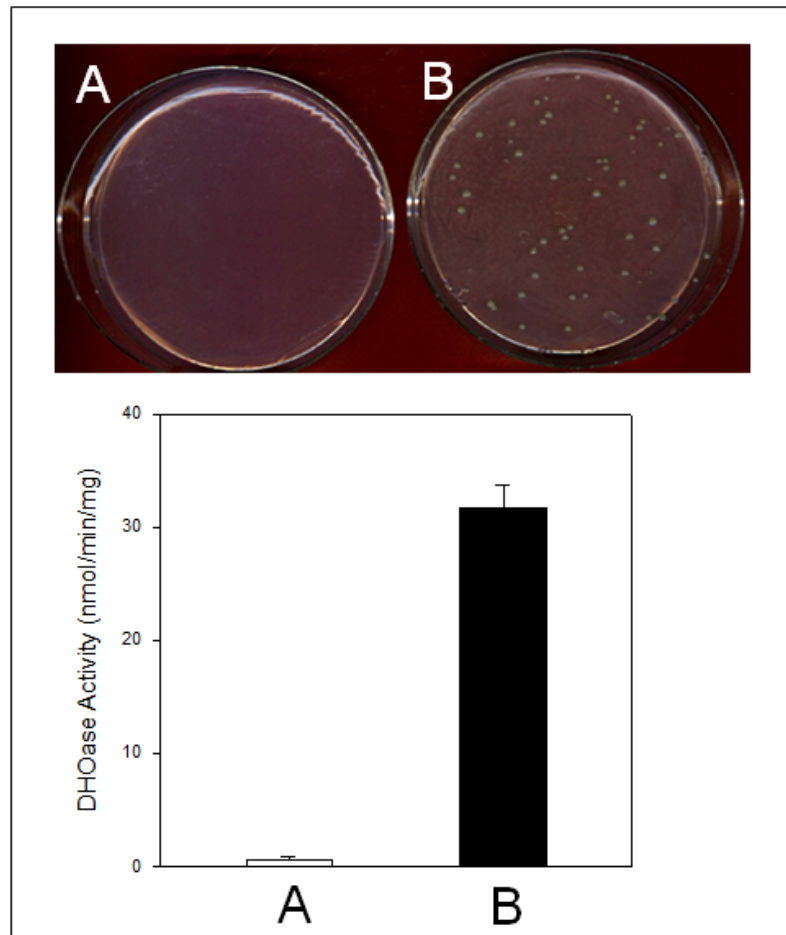


Fig. 25 Complementation test. Each of cloned *pyrC* genes from *B. cepacia* was transformed into the DHOase mutant *E. coli* MA1008 (Top panel). The cell extract of A. MA1008 (*pyrC*) and B. MA1008 (*B. cepacia pyrC*) was used for DHOase activity assay (Bottom panel) (T-test, $p < 0.001$).

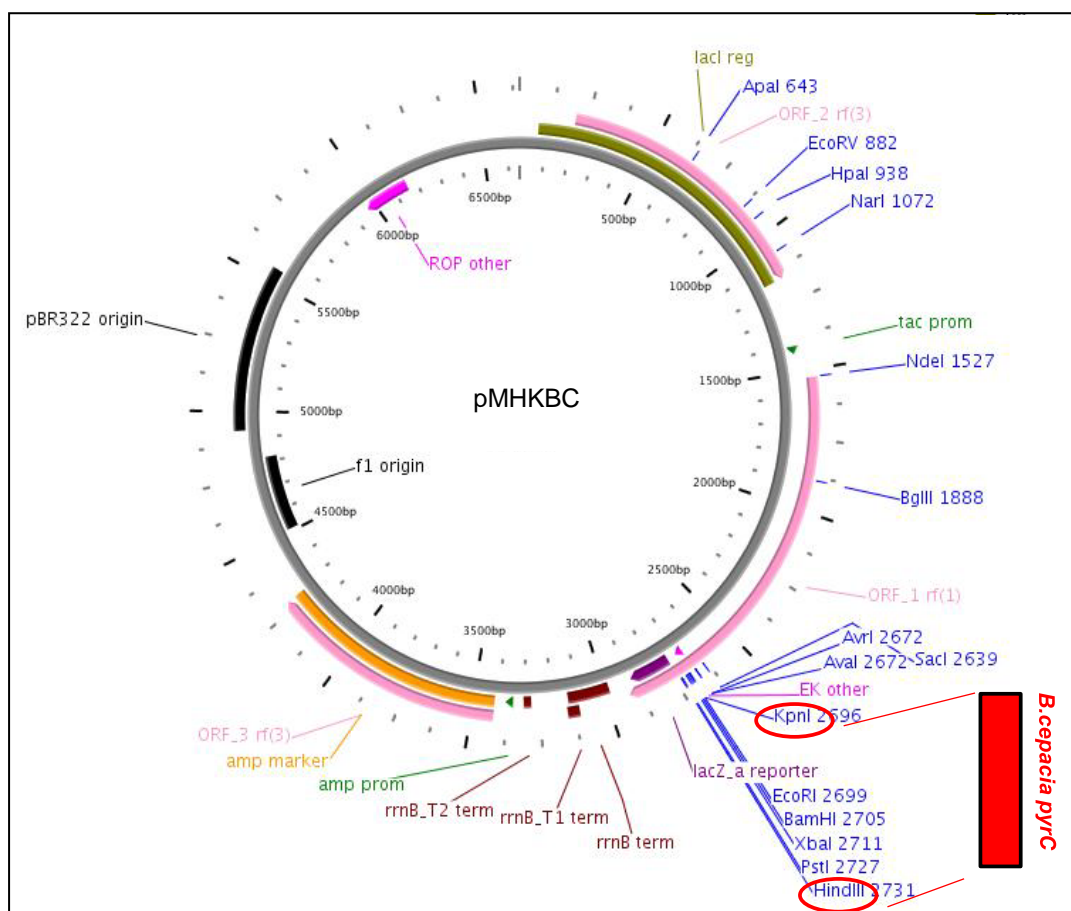


Fig. 26 Schematic diagram of construction of the pMHKBC plasmid from inserting *B. cepacia pyrC* gene into the pMAL-c2E plasmid. Figure is drawn by PlasMapper version 2.0.

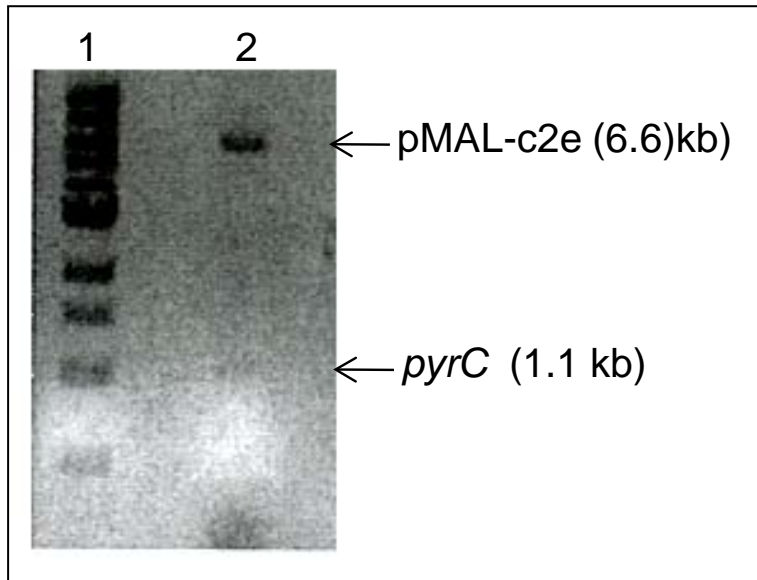


Fig. 27 Restriction digestion of the pMHKBC plasmid. pMHKBC plasmid was digested with *KpnI* and *HindIII* enzyme and run on a 1.5 % agarose gel. Lane 1: 1 kb ladder, lane 2: cloned pMHKBC plasmid.

cloned plasmid was confirmed by restriction digestion (Figure 27). This cloned plasmid was named pMHKBC plasmid. Lane 1 shows 1 kb DNA ladder and lane 2 represents the cloned plasmid digested with *KpnI* and *HindIII*. Based on the known sequence of the *pyrC* gene, the expected size of the subunit was 45 kDa. When the fusion proteins were cut by enterokinase, only the DHOase was cut from the fusion protein and collected. To check the efficiency of over expression and the size of the monomer of DHOases, purified DHOases were run on 10 % SDS-PAGE (Figure 28). The expected size of the fusion or overexpression protein was 87 kDa because the monomer size of DHOase was 45 kDa and the maltose binding protein (MBP) size was 42 kDa. The overexpressed 87 kDa fusion protein was seen in lane 1. The purified DHOase by enterokinase elution was reapplied on the amylose resin after dialysis. The flow-thru contained partially purified DHOase as seen in lane 2. The partially purified DHOase was applied on an anion exchange chromatography using DEAE Sepharose column. DHOases were eluted with 200 mM NaCl of linear gradient from 0 mM NaCl to 1000 mM NaCl. DHOase-containing fractions were collected and dialyzed, and run on a 10 % SDS-PAGE to check the purity of sample (Figure 29). Lane 1 shows the low range protein marker and lane 2 represents the highly purified DHOase. The final protein concentration was measured as 50 $\mu\text{g}/\mu\text{l}$ by the Bradford assay.

Enzyme Kinetics of DHOase of *B. cepacia*

To characterize the nature of purified DHOases, enzyme kinetic studies were performed to determine the K_M and V_M for the *B. cepacia* DHOase. The purified DHOases were assayed for DHOase activity by measuring the reverse reaction, the

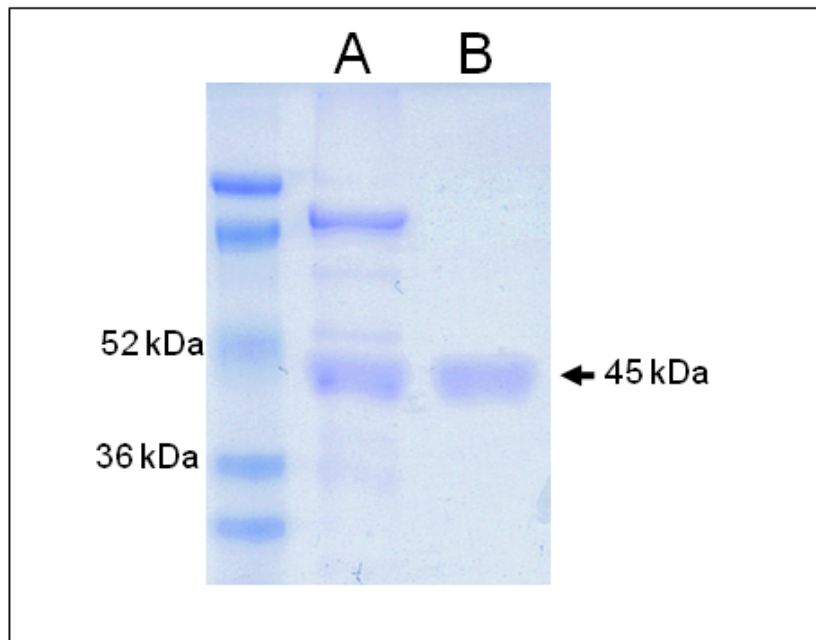


Fig. 28 Purification of *B. cepacia* DHOase using pMAL protein fusion and purification system. The purified DHOase was run on 10 % SDS-PAGE. A. Purified DHOase cut by 50 U enterokinase. B. Partially purified DHOase from flow thru of the second application on the beads.

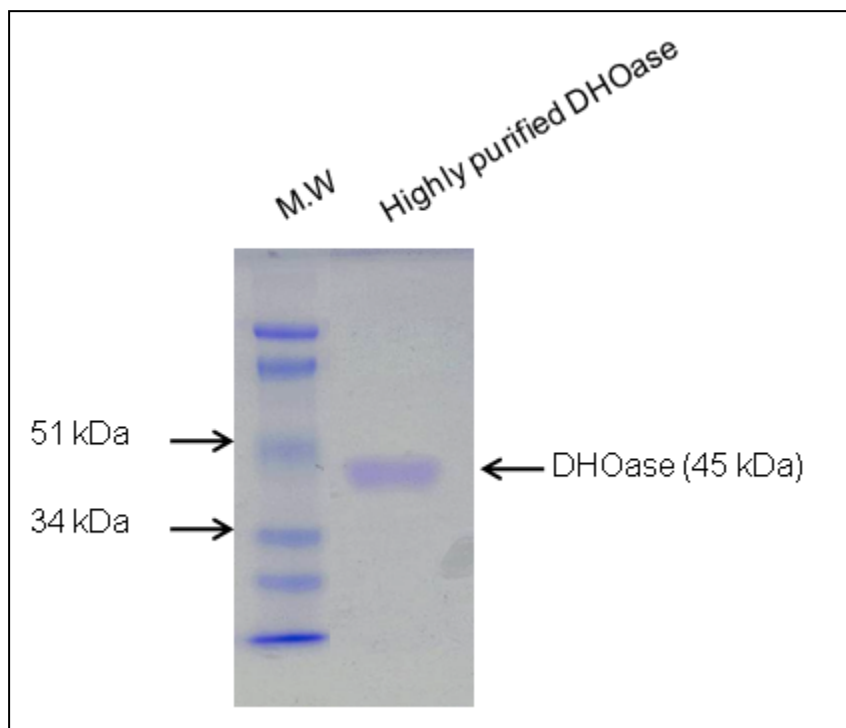


Fig. 29 Further purification of highly purified *B. cepacia* DHOase by anion exchange chromatography. The purified DHOase was run on 10 % SDS-PAGE.

amount of CAA produced from dihydroorotate at 37°C for 20 min using the colorimetric method for the assay of Beckwith *et al.* (Beckwith *et al.* 1962).

The assay was conducted in a microtiter plate and the absorbance was read at 466 nm in a kinetic microplate reader. To calculate the K_m and V_m value of purified *B. cepacia* DHOase, Michaelis-Menten kinetics (Figure 30A) and a Lineweaver-Burk plot were analyzed (Figure 30B). From this assay, purified dimeric 90 kDa (2X 45 kDa) *B. cepacia* DHOase revealed very strong activity without ATCase. K_M and V_M for dihydroorotase were calculated to be 0.87 mM and 32 mmol CAA/min/mg proteins, respectively. In addition, the purified *B. cepacia* DHOase also showed substrate inhibition by Michaelis-Menten kinetics which is similar to DHOase activity in other organism.

Purification of ATCase Enzyme by GST Gene Fusion System

The cloned ATCase from *B. cepacia* ATCC25416 was purified by the Glutathione S-Transferase Gene Fusion System as previously described by Kim (Figure 31) (Kim 2004). Kim proposed that trimers from the uncleaved 47 kDa and the cleaved 40 kDa ATCase subunits are present in the *B. cepacia* cell. 40 kDa ATCase has a cleavage between Ser74 and Val75 residues downstream from the initial f-Met start codon.

During the protein purification system, ATCases were cut out from the fusion protein by thrombin. In addition to the expected 47 kDa subunit, a 40 kDa polypeptide was also detected in the eluted samples (Figure 32A). Purified cleaved and uncleaved ATCases were run on anion exchange chromatography using DEAE Sepharose column. ATCases were eluted with 300 mM NaCl of linear gradient from 0 mM NaCl

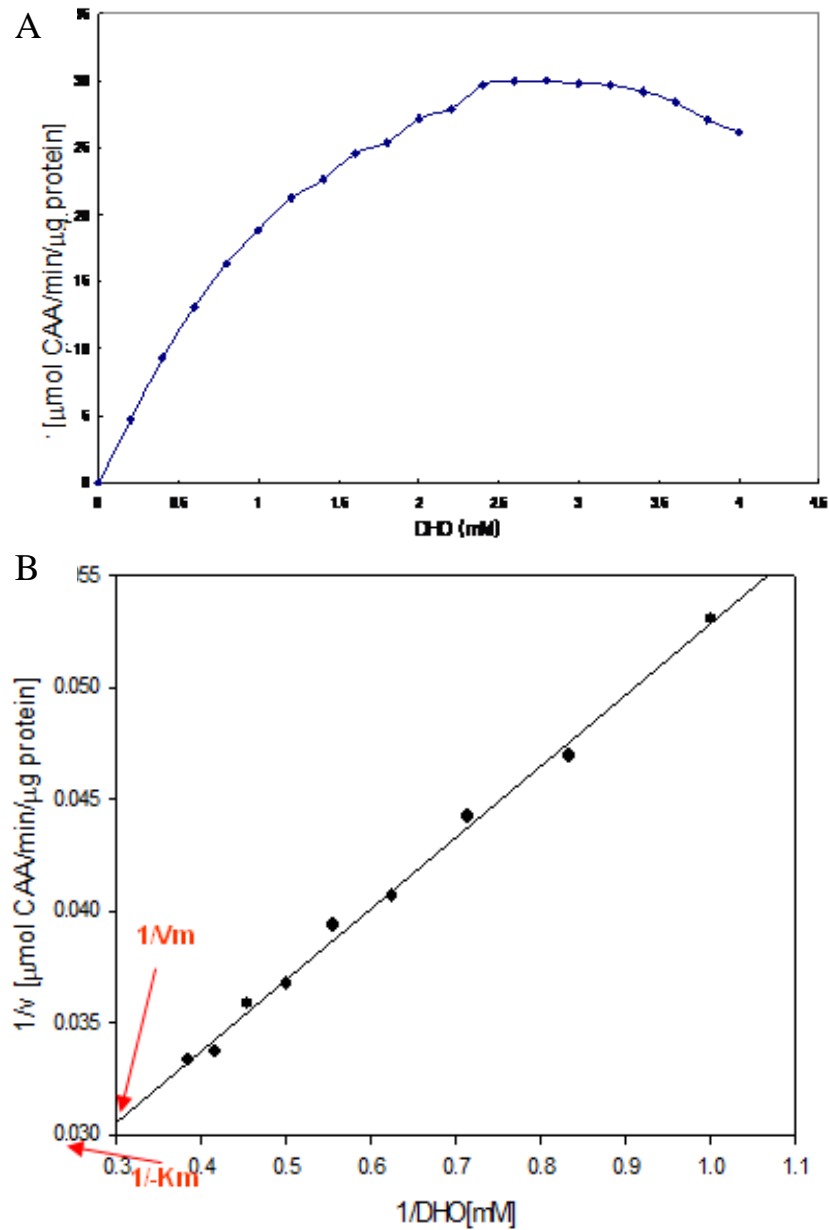


Fig. 30 Enzyme kinetics of purified *B. cepacia* DHOases. A. Michaelis-Menten kinetics. B. Lineweaver-Burk plot. K_m (0.64 mM) and V_m (32 μmol CAA/min/mg protein) value were calculated from the Lineweaver-Burk plot. The data represent the mean value of three experiments and the error bars were removed from graphs for clarity. The DHOase revealed substrate inhibition.

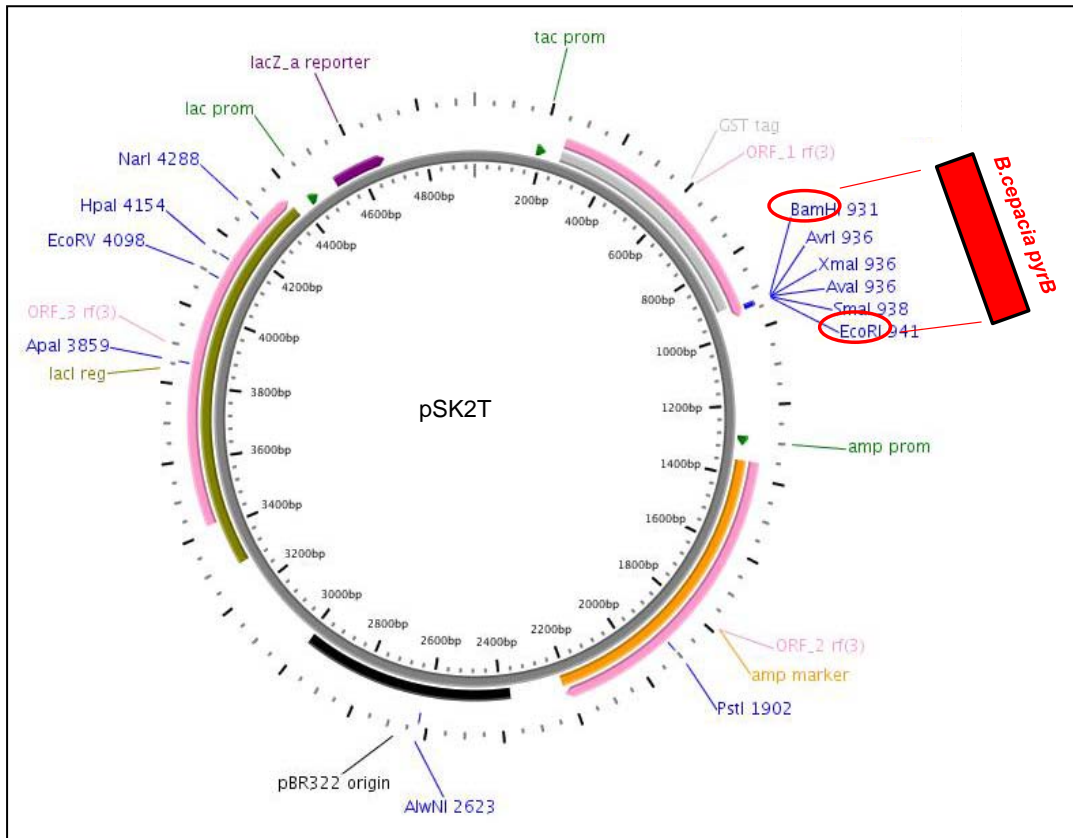


Fig. 31 Schematic diagram of construction of pSK2T plasmid from inserting *B. cepacia pyrB* gene into pGEX2T plasmid. Figure is drawn by PlasMapper version 2.0.

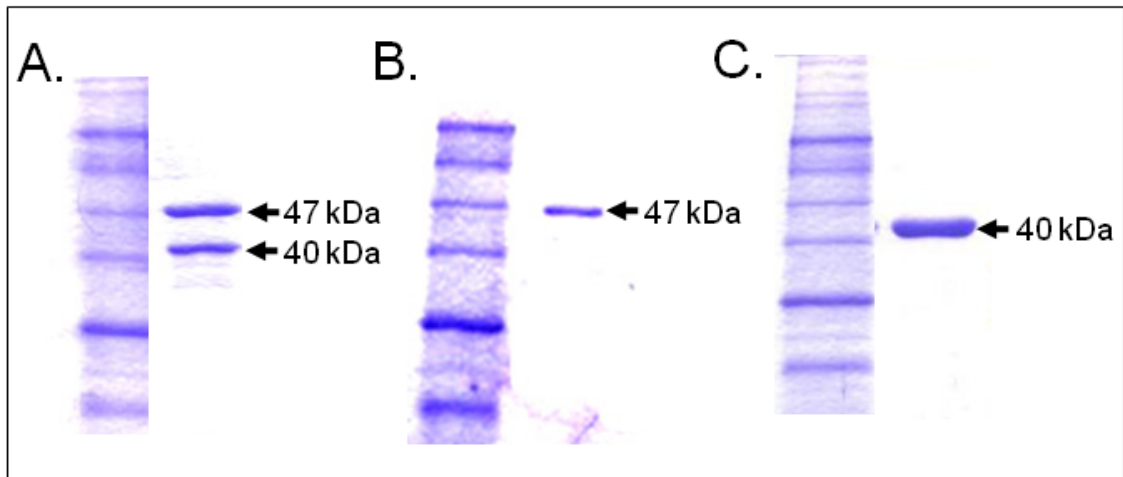


Fig. 32 Purification of *B. cepacia* ATCase using Glutathione S-transferase (GST) Gene Fusion System. The purified ATCases were run on 10 % SDS-PAGE. A. ATCase cut by 50 U thrombin. B, C. Separation of uncleaved (47 kDa) and cleaved (40 kDa) ATCase by anion exchange chromatography, respectively.

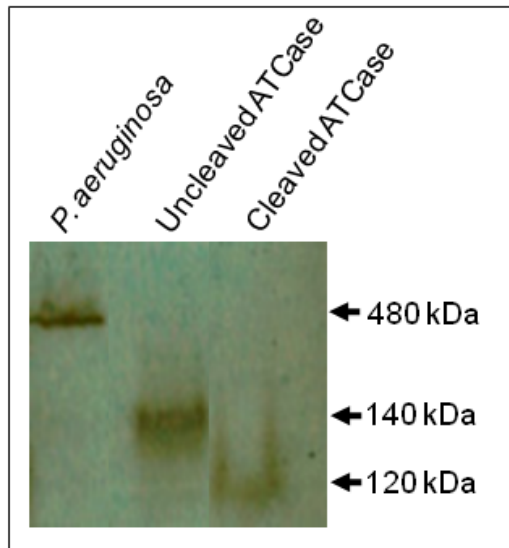


Fig. 33 ATCase activity gel assay. *in situ* detection of purified ATCase was performed by the procedure of Bothwell with the histidine buffer modification of Kedzie (1987).

to 1000 mM NaCl. The ATCase-containing fractions were detected by a 10 % SDS-PAGE. ATCase-containing fractions were collected and dialyzed, and run on a 10 % SDS-PAGE to check the purity of the sample (Figure 32B and 32C). This result was in accordance with those previously reported by Kim (2004).

Conventional ATCase Activity Gel Assay

To investigate the structural characteristic for ATCase activity, purified ATCase enzymes were run on a 6 % native gel and *in situ* detection of purified ATCase was performed by the procedure of Bothwell with the histidine buffer modification of Kedzie (Figure 33). Lane 1 shows the ATCase holoenzyme from *P. aeruginosa*. Lane 2 and 3 represents purified uncleaved and cleaved ATCase. This ATCase activity gel assay shows that uncleaved ATCase forms 140 kDa size of active trimer from 47 kDa monomer and cleaved ATCase forms 120 kDa size of active trimer from 40 kDa monomer.

Enzyme Kinetics of Purified ATCase Enzymes

To investigate the nature of purified ATCases, the ATCase assay was performed with uncleaved and cleaved ATCase (Figure 34). Both purified ATCases were assayed for ATCase activity by measuring the amount of CAA produced at 37°C for 20 min using the colorimetric method described by Prescott and Jones 1969. The assay was conducted in a microtiter plate and the absorbance was read at 450 nm in a kinetic microplate reader.

Both uncleaved and cleaved ATCases showed significant ATCase activity but the cleaved ATCase produced 37 % more ATCase activity than did the uncleaved

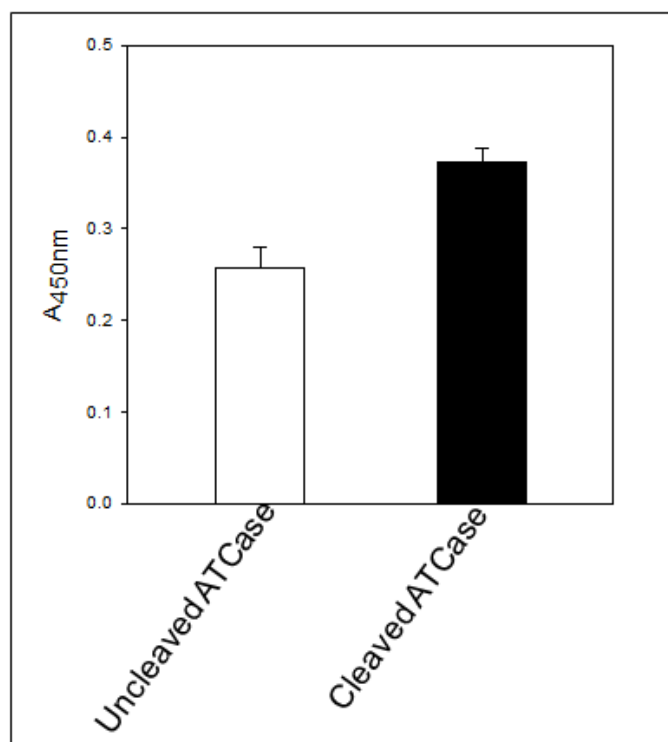


Fig. 34 ATCase activity assay using purified uncleaved and cleaved *B. cepacia* ATCase. The data represent the mean value of three experiments (T-test, $p=0.013$).

ATCase. From this result, it was shown that the cleaved ATCase had a higher affinity for aspartate than did the uncleaved ATCase. Both the uncleaved ATCase (47 kDa) and the cleaved ATCase (40 kDa) made active trimers.

Effectors Assay for Purified ATCase

To characterize the property of uncleaved and cleaved *B. cepacia* ATCases, the effectors assay was performed using ATP, UTP, GTP, and CTP (Figure 35). Based on pre-experiment results, 10 mM concentration was used as a final effector concentration to give saturation. The graph of Figure 35 shows the ATCase activities of uncleaved and cleaved ATCase under 10 mM of each effector. The percentage numbers in the table represent the relative inhibition degree by comparing the each ATCase activity with effectors with the ATCase activity without effectors.

From this result, it is clear that ATCase specific activities of both uncleaved and cleaved ATCase are decreased when the nucleotides were present. Moreover, cleaved ATCase revealed less inhibition than did the uncleaved ATCase. Specifically cleaved ATCase had about twenty times less inhibition under UTP effect than uncleaved ATCases'.

Refolding of ATCase Holoenzyme

To investigate the structure of ATCase holoenzyme of *B. cepacia*, the purified DHOase from *B. cepacia* was refolded with the purified ATCase from *B. cepacia* using thermal process method at 37°C (Figure 36) and the method provided by New England Biolab. From this result, both reconstituted ATCase holoenzyme from 140 kDa ATCase trimer with DHOase dimer and 120 kDa ATCase trimer with DHOase

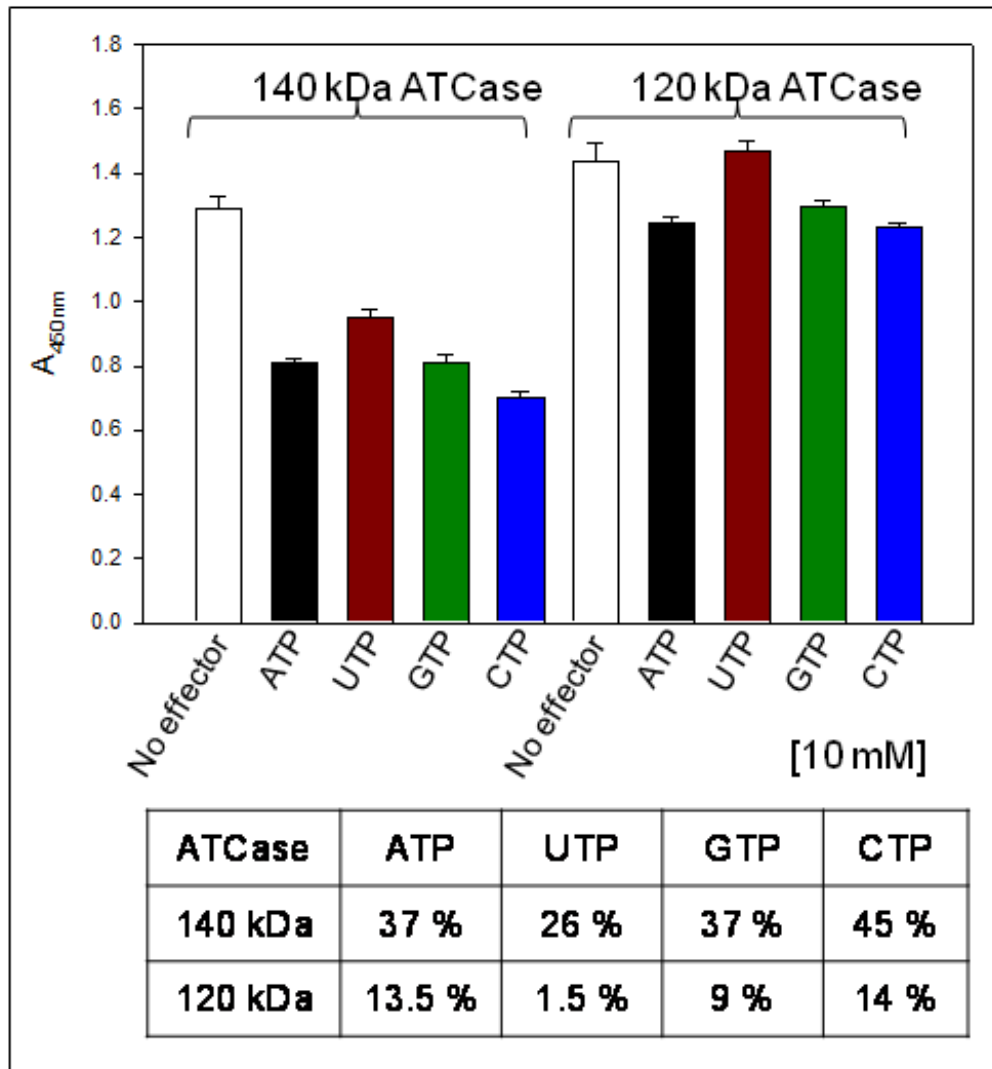


Fig. 35 Effector assay of purified ATCases. The purified ATCases, 140 kDa and 120 kDa, were assayed using effectors. Bottom table represents the relative inhibition percentage versus control (no effector). 120 kDa ATCase revealed less inhibition.

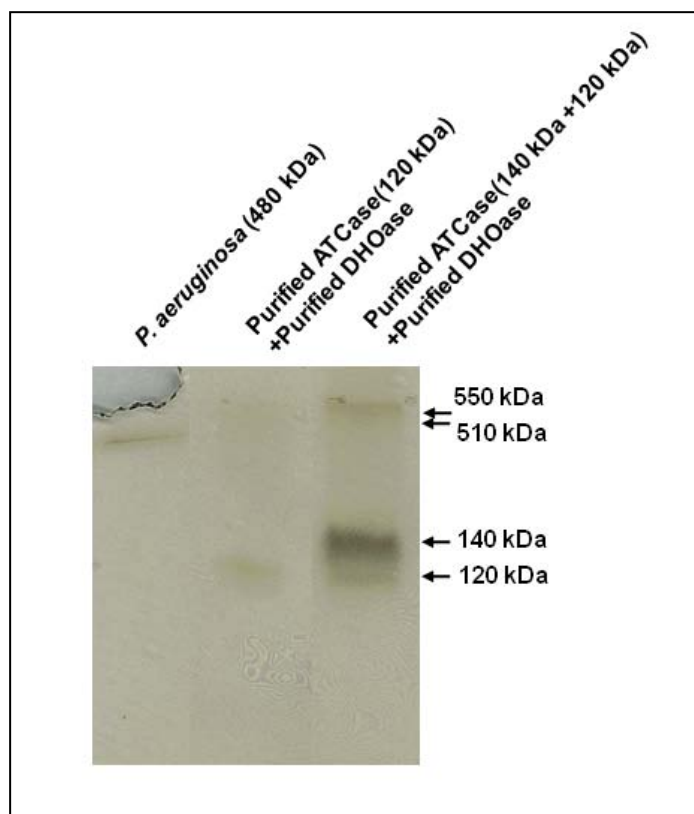


Fig. 36 Refolding of ATCase holoenzyme using purified *B. cepacia* ATCase and DHOase. Refolding was performed using procedure from New England Biolab. *In situ* detection of activity of refolded ATCase holoenzyme was performed by the procedure of Bothwell with the histidine buffer modification of Kedzie (1987).

dimer revealed the ATCase activity. Moreover, 120 kDa ATCase trimer with DHOase dimer showed better refolding affinity to each other than purified 140 kDa ATCase trimer with DHOase dimer.

However, the refolding method provided by New England Biolab did not produce active ATCase holoenzyme from any combination.

Construction of *pyrC* Knockout in *B. cepacia*

From previous research, it was likely that two DHOases are present in *B. cepacia*. To learn more about the *B. cepacia* ATCase, we constructed a *pyrC* knockout strain using the gene deletion method followed by bi parental mating. The *pyrC* gene from the cloned pUC18 plasmid was subcloned into pEX18Gm plasmid (Figure 37). The constructed pEXHKBC plasmid was digested with *KpnI* and *HindIII* enzyme and run on a 1.5 % agarose gel (Figure 38). Then, partial deletion of *B. cepacia pyrC* gene from pEXHKBC was achieved by *BstBI* enzyme digestion and sequential self-ligation (Figure 39). The constructed pEX18Gm-*pyrC*⁻ plasmid was selected by *BstBI* enzyme digestion (Figure 40), and named as pEXHKBCX plasmid. Lane 1 and lane 2 show the 1 kb ladder and constructed plasmid, respectively. The cloned pEX18Gm-*pyrC*⁻ plasmid was confirmed by sequencing.

After being transformed into the SM10 *E. coli* strain, this construction was then mated into wild type *B. cepacia* using bi-parental mating.

B. cepacia is naturally very resistant to a range of antibiotics. In the case of gentamicin, the Minimum Bactericidal Concentration (MBC) was 3 mg/mL (data not shown). The screenings successfully identified a colony whose single recombination phenotype was gentamicin resistant and sucrose sensitive, and whose double

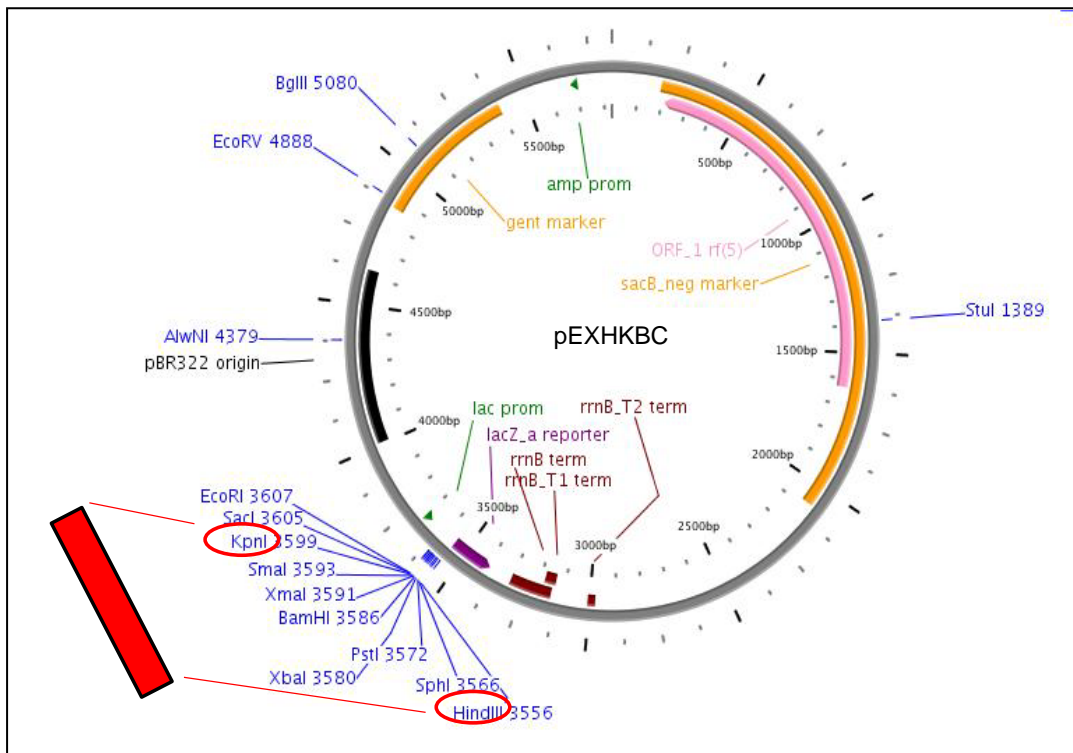


Fig. 37 Schematic diagram of construction of pEXHKBC plasmid from inserting *B. cepacia pyrC* gene into pEX18Gm plasmid. Figure is drawn by PlasMapper version 2.0.

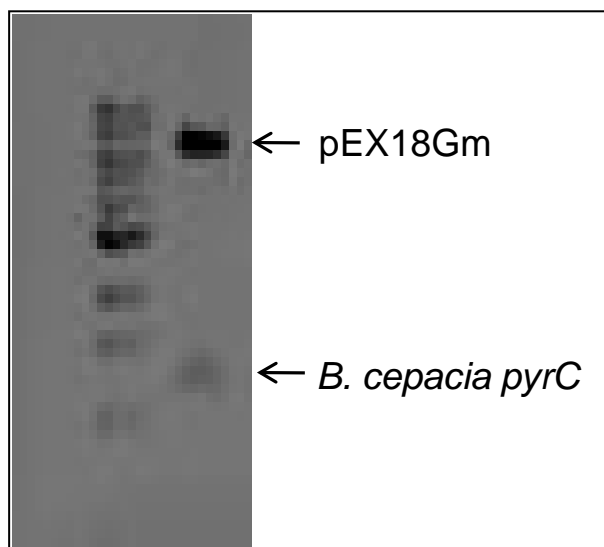


Fig. 38 Restriction digestion of pEXHKBC plasmid. pEXHKBC plasmid was digested with *KpnI* and *HindIII* enzyme and run on a 1.5 % agarose gel. Lane 1: 1 kb ladder, lane 2: cloned pEXHKBC.

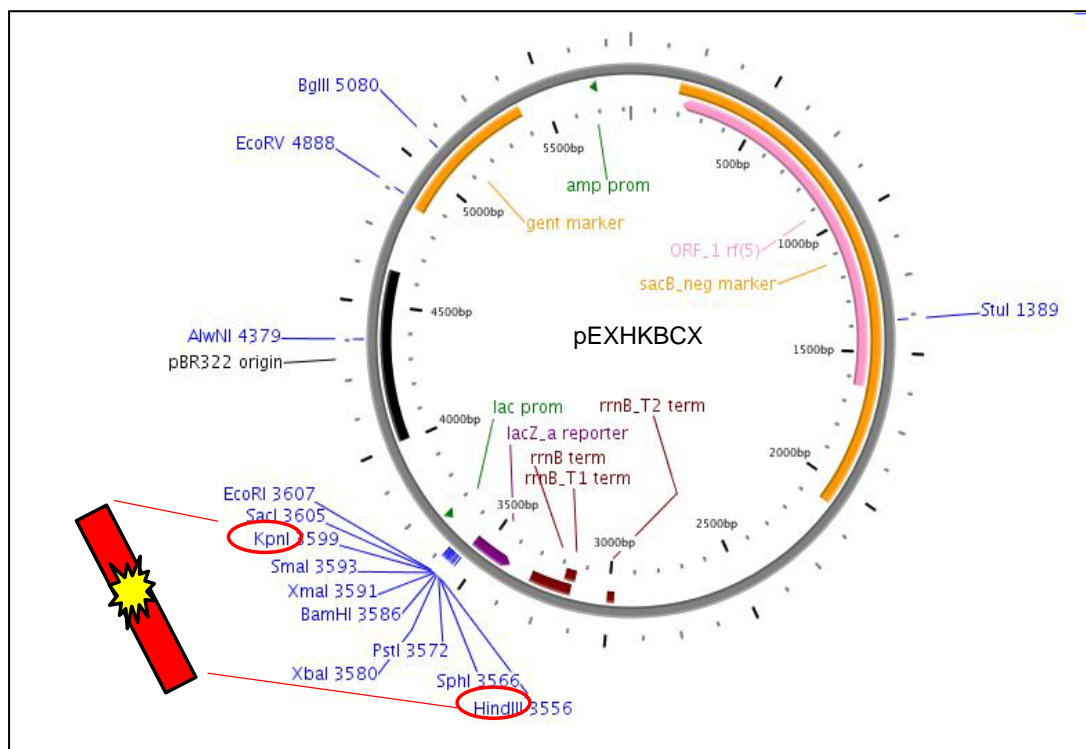


Fig. 39 Schematic diagram of construction of pEXHKBCX plasmid from inserting *B. cepacia pyrC* gene into the pEX18Gm plasmid. Figure is drawn by PlasMapper version 2.0.

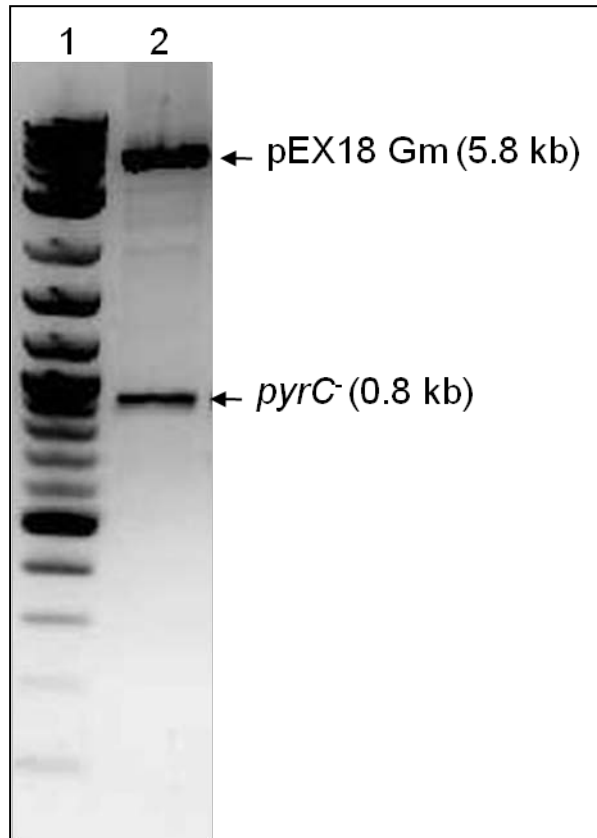


Fig. 40 Restriction digestion of pEXHKBCX plasmid. pEXHKBCX plasmid was digested with *KpnI* and *HindIII* enzyme and run on a 1.5 % agarose gel. Lane 1: 1 kb ladder, lane 2: cloned pEXHKBCX.

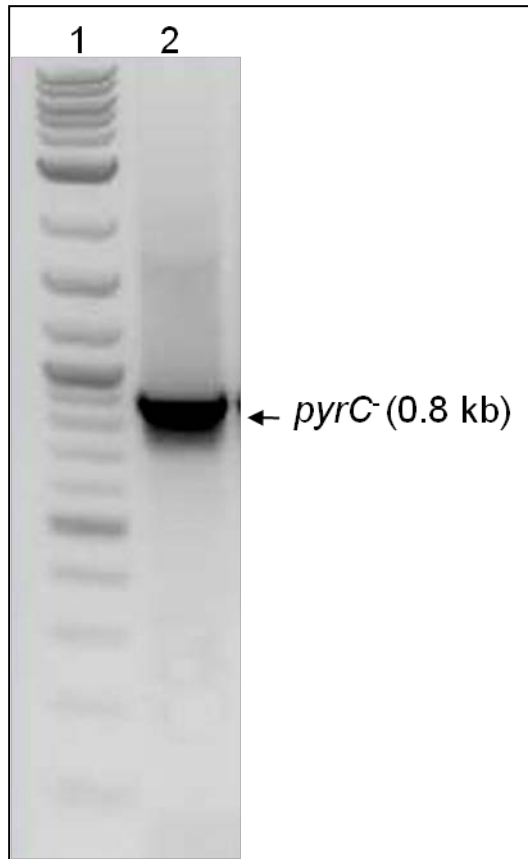


Fig. 41 PCR results to confirm the construction of *pyrC* knockout *B. cepacia* 25416. PCR was performed using BCpyrC-F and BCpyrC-R primers. The PCR product was run on a 1.5 % agarose gel.

recombination phenotype was gentamicin sensitive and sucrose resistant as described in Material and Methods. The resulting recombinant *B. cepacia* was screened by plating on Psmm containing supplemented with uracil. The *pyrC* knockout strains grew very slowly in minimal medium at 30°C but after fully growing then the growth rate was comparable to that of wild type *B. cepacia*. Moreover, this strain became prototrophic and grew in Psmm without uracil. Despite the deletion of *pyrC*, the strain grew without uracil suggesting that another *pyrC* was present as seen by Brichta for *P. aeruginosa* (Brichta 2003). Insertion of the *pyrC* allele into the appropriate site of the *B. cepacia* chromosome by homologous exchange was confirmed by PCR, the product has a 300 bp-less fragment than 1.1 kb size of *pyrC* gene from wild type (Figure 41). Additionally, the deleted portion at *pyrC* gene in mutant strain was confirmed by sequencing.

Southern Blot

To confirm the selected *pyrC* *B. cepacia*, Southern blot analysis was performed using high prime DNA labeling and a detection kit from Roche Applied Sciences. This kit uses non-radio labeling with digoxigenin-dUTP (DIG), and an alkali-labile detection method. To detect the deleted part of *pyrC* gene, the probe was designed to target 100 bp upstream and downstream of the deleted region resulting in a product size of 300 bp. PCR primers to produce probes were designed using Primer 3 software (SBBCpyrC-F and SBBCpyrC-R) (Table 6). To the PCR, DIG- Random primed DNA labeling was performed as described in the manual provided by vendor (Figure 42).

For Southern blot analysis to confirm the construction of *pyrC* knockout *B.*

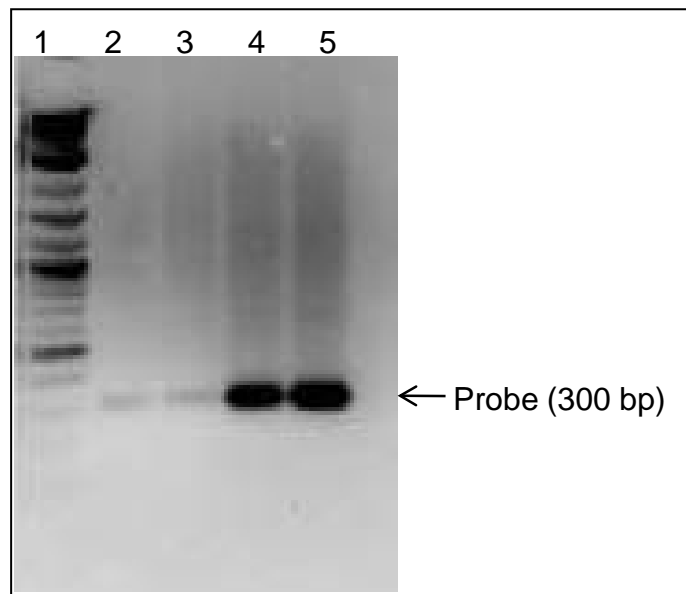


Fig. 42 PCR reaction to synthesize the probe used to detect the deleted part of *pyrC* gene for Southern blot analysis.

1. 2-log DNA marker, 2-5. Synthesized probes.

cepacia, the genomic DNA of wild-type *B. cepacia* and *pyrC* *B. cepacia* were digested by *EcoRI* and *BamHI* enzyme. *EcoRI* enzyme was chosen because it digests in the middle of the deleted 300 bp of *B. cepacia pyrC* gene used to construct the *pyrC* knockout mutant strain. *BamHI* enzyme was chosen because it digests upstream and downstream of the deleted 300 bp of *B. cepacia pyrC* gene to construct the *pyrC* knockout mutant strain. Restriction digestion with *EcoRI* and *BamHI* was performed on 10 µg of each genomic DNA overnight at 37°C. The digested each genomic DNA was loaded on a 1 % agarose gel and separated by electrophoresis. The results of the restriction digest performed on genomic DNA of wild- type *B. cepacia* and *pyrC* *B. cepacia* are shown in Figure 43. Digested genomic DNA was transferred onto 2 nitrocellulose membrane and hybridized with the constructed probe. The hybridized DNA and probe were visualized by BCIP/NPT substrates, and the result was photographed (Figure 44).

Lane A3 and lane A4 represent the digested genomic DNA of *B. cepacia* wild type and *pyrC* knockout mutant strain by *EcoRI*. *EcoRI* digested within the middle of the deleted *pyrC* gene. As seen on figure, *B. cepacia* wild type produced two fragments of 0.5 kb and 1.3 kb while *pyrC* knockout mutant strain produced one fragment of 1.5 kb. The anticipated kb size difference of 0.3 kb matched the size of the deleted portion of *pyrC*.

Lane B3 and lane B4 represent the digested genomic DNA of *B. cepacia* wild type and *pyrC* knockout mutant strain by *BamHI*. *BamHI* digested upstream and downstream of *pyrC* gene. As seen on Figure 44, *B. cepacia* wild type produced 1.5 kb fragment while *pyrC* knockout mutant strain produced 1.2 kb. From Southern blot analysis, the construction of *pyrC* knockout mutant strain was confirmed.

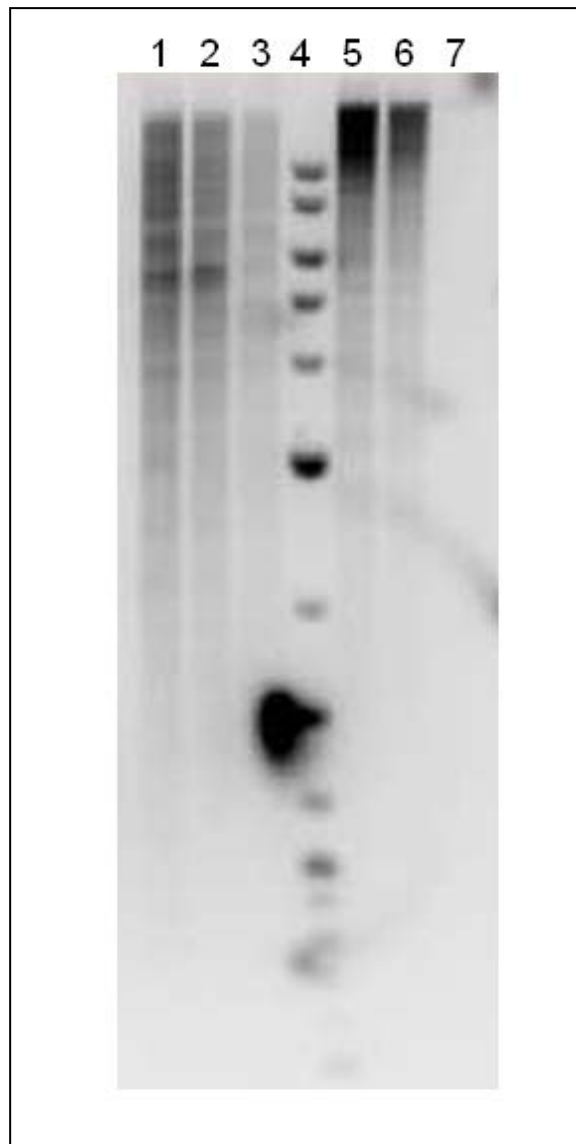


Fig. 43 Restriction digestion of genomic DNA of wild type and *pyrC* knockout *B. cepacia* with *EcoRI* and *BamHI* enzyme. 1. Wild type with *EcoRI*, 2. *pyrC*⁻ with *EcoRI*, 4. 2 log DNA marker, 5. Wild type with *BamHI*, and 6. *pyrC*⁻ with *BamHI*. Lane 1, 2, and 3 represent the genomic DNA of wild-type *B. cepacia* and two *pyrC*⁻ *B. cepacia* mutants digested by *EcoRI*. Lane 4 shows the 2-log DNA marker, and lane 5, 6, and 7 represent the genomic DNA of wild-type *B. cepacia* and two *pyrC*⁻ *B. cepacia* mutants digested by *BamHI*.

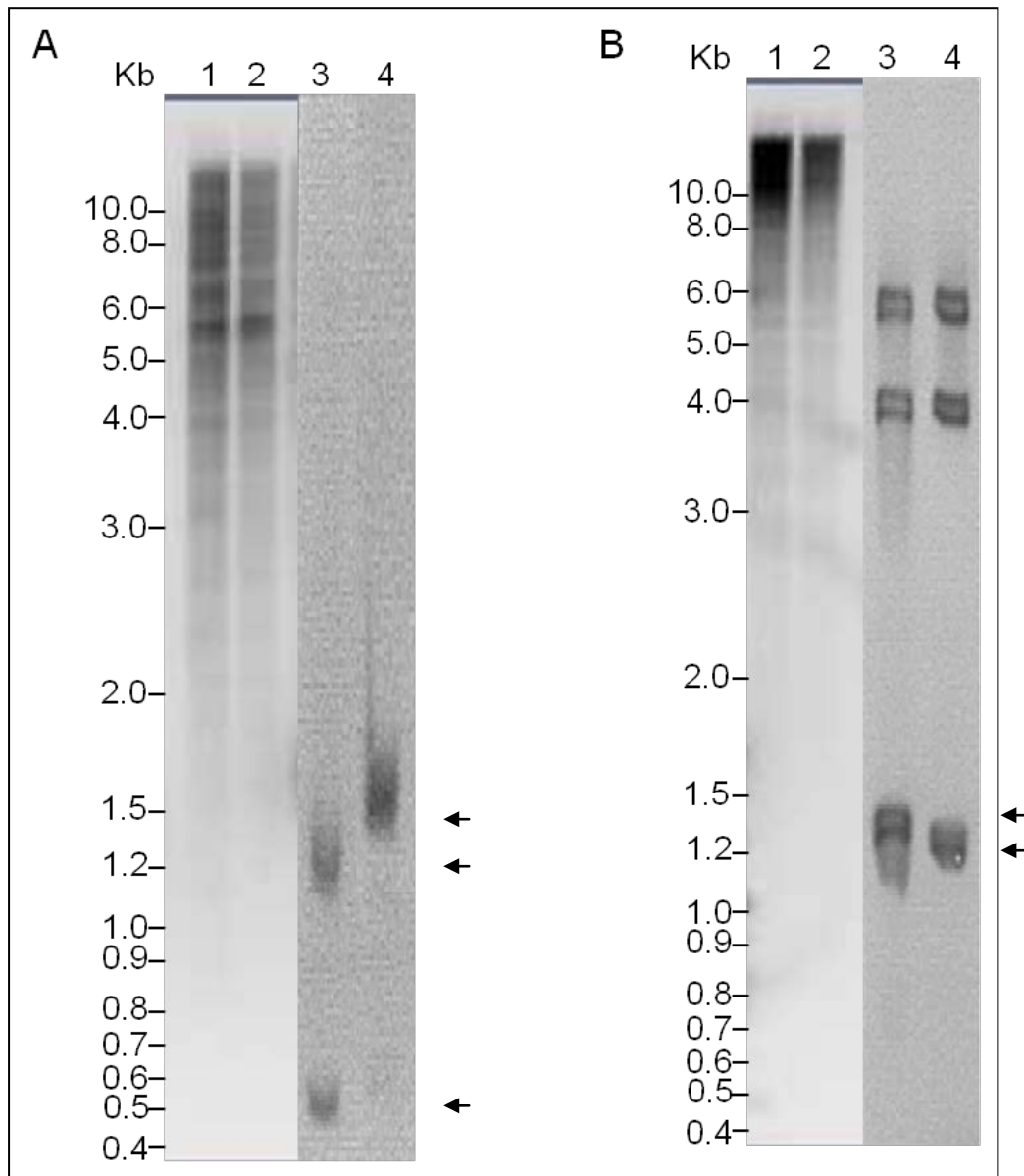


Fig. 44 DIG-dUTP Hybridized Southern blot of *B. cepacia* wild type and *pyrC* mutant. Genomic DNA of wild type and *pyrC* knockout *B. cepacia* was digested with *EcoRI* and *BamHI* enzyme. A. 1, 3. Wild type with *EcoRI*, 2, 4. *pyrC* with *EcoRI*. 3,4. Southern blot. B. 1, 3. Wild type with *BamHI*. 2, 4. *pyrC* with *BamHI*. 3, 4. Southern blot.

Growth Study

Growth curves were performed for the wild type and mutant strain in Psmm with and without supplying uracil as described in Materials and Methods. All the cultures were started at the similar optical density to maintain a consistent basal starting point (Figure 45). In this study, wild-type *B. cepacia* showed a lag in growth rate in Psmm supplemented with uracil. Exogenously supplied uracil might cause the cells to grow for a longer period of time. The *pyrC* *B. cepacia* mutant showed longer generation time in comparison to wild-type *B. cepacia* in Psmm with and without uracil.

Interestingly, *pyrC* *B. cepacia* mutant did not show any difference in growth rate in the presence or absence of exogenously added uracil. Therefore, this growth curve of wild type and the *pyrC* *B. cepacia* mutant provides a characteristic of the prototrophic life of *pyrC* *B. cepacia*. Once we discovered that the knockout mutation in *pyrC* did not produce pyrimidine auxotrophy we concluded that there must be two active *pyrCs* in *B. cepacia*. This explains the growth curve seen in Figure 45.

Virulence Tests

Twitching, swarming, and swimming motilities were tested on wild type and the *B. cepacia pyrC* mutant strains to see if there was any significant difference in the mutant when compared to the wild type. Swimming motility requires flagella, while swarming and twitching motility require type IV pili.

Twitching Motility

Results for twitching motility after 24 h incubation at 37°C are presented in Figure 46. Twitching motility require type IV pili.

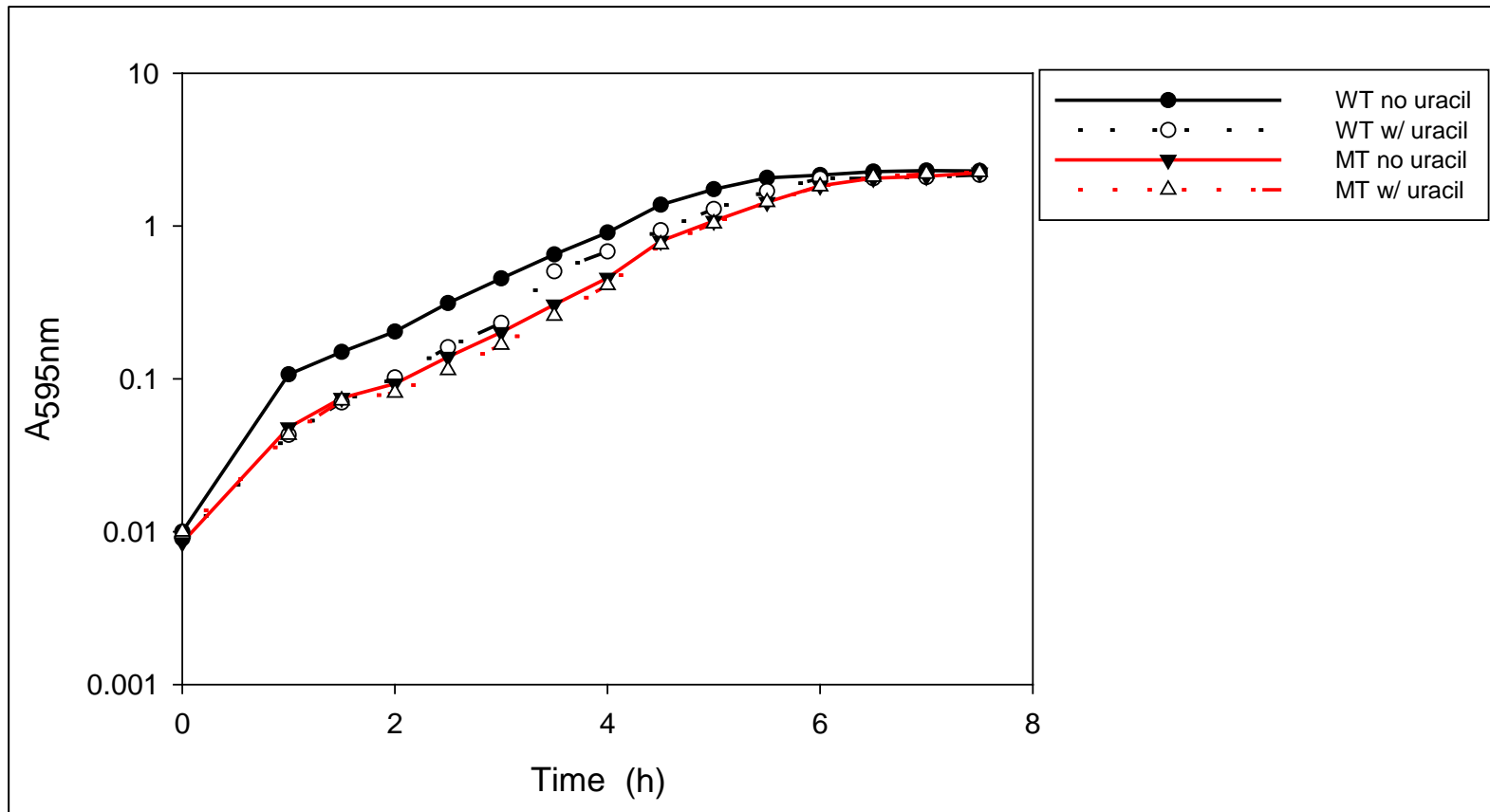


Fig. 45 Growth curve of *B. cepacia* wild type and *pyrC* mutant. WT: wild type, MT: *pyrC* mutant. The data represent the mean value of three experiments and the error bars were removed from graphs for clarity. No difference in growth rate was seen because the *pyrC* strain remained a prototroph.

The results showed that the twitching motility of *B. cepacia pyrC*⁻ mutant strain was apparently reduced to compare with that of wild-type *B. cepacia* after 24 h. However, *B. cepacia* wild type and the *pyrC*⁻ mutant strain did not show significant difference of twitching motility with or without uracil, but in wild type, the addition of uracil slightly decreased. Therefore, the *B. cepacia pyrC*⁻ mutant strain did not recover the normal twitching motility even with exogenous uracil. The phenotypes of wild type were rough growth perimeter while the mutants with decreased twitching motility were smooth growth perimeter.

Swarming Motility

Results for swarming motility after 24 h incubation at 37°C are presented in Figure 47. Swarming motility requires both flagella and type IV pili. Swarming motility results were different from twitching. Swarming was not impaired for the *pyrC*⁻ mutant in plates and also *B. cepacia* wild type and the *pyrC*⁻ mutant strain did not show significant difference of swarming motility with or without uracil. Therefore, the swarming motility of the *pyrC*⁻ mutant strain was not affected even without a functioning of *pyrC* gene.

Swimming Motility

Results for swimming motility after 24 h incubation at 37°C are presented in Figure 48. Swimming motility requires flagella.

The results showed that swimming motility was reduced in the mutant to compare with that of wild type after 24 h. However, *B. cepacia* wild type and the *pyrC*⁻ mutant strain did not show significant difference of swimming motility with or without uracil, but in wild type, the addition of uracil slightly decreased. Even though

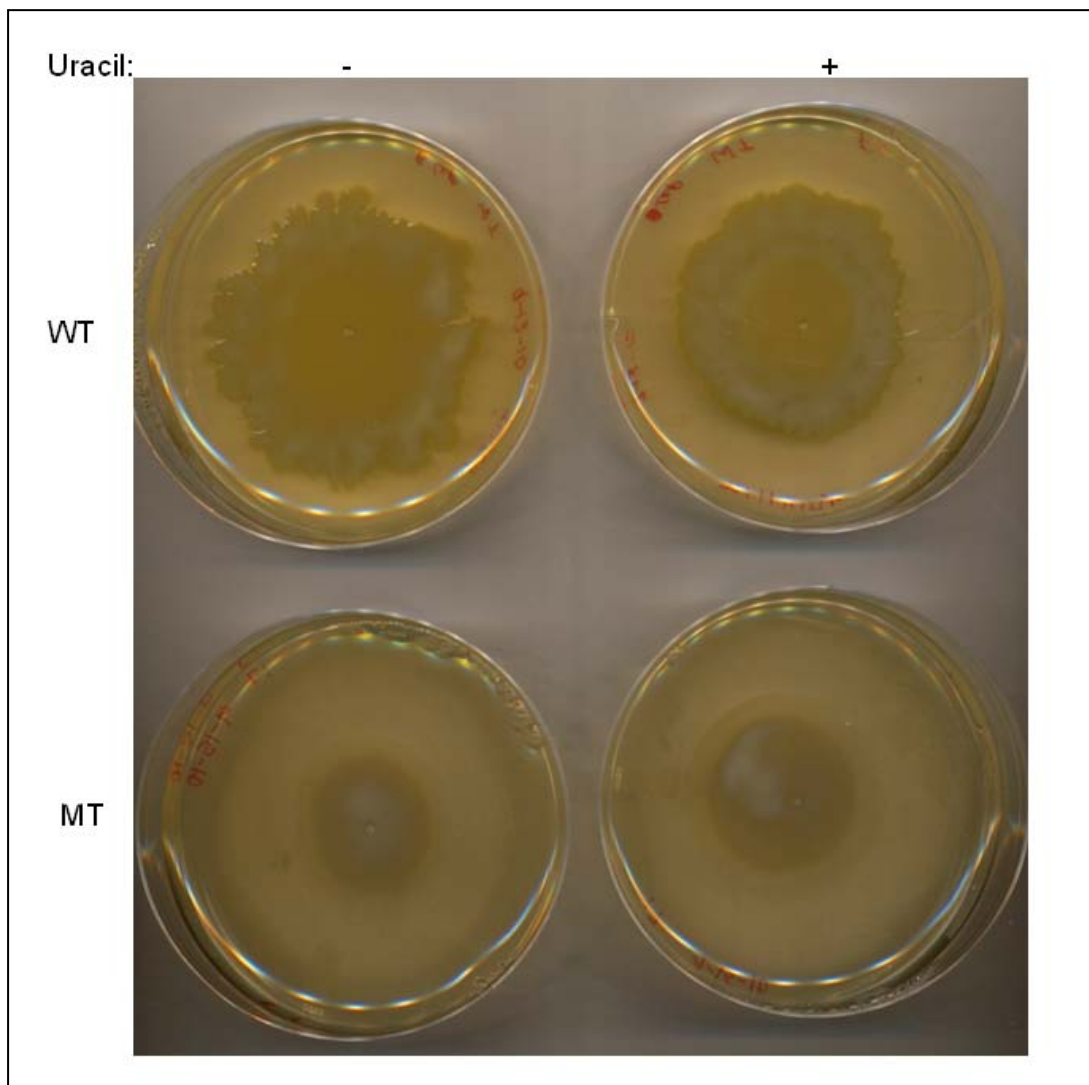


Fig. 46 Twitching motility assay.

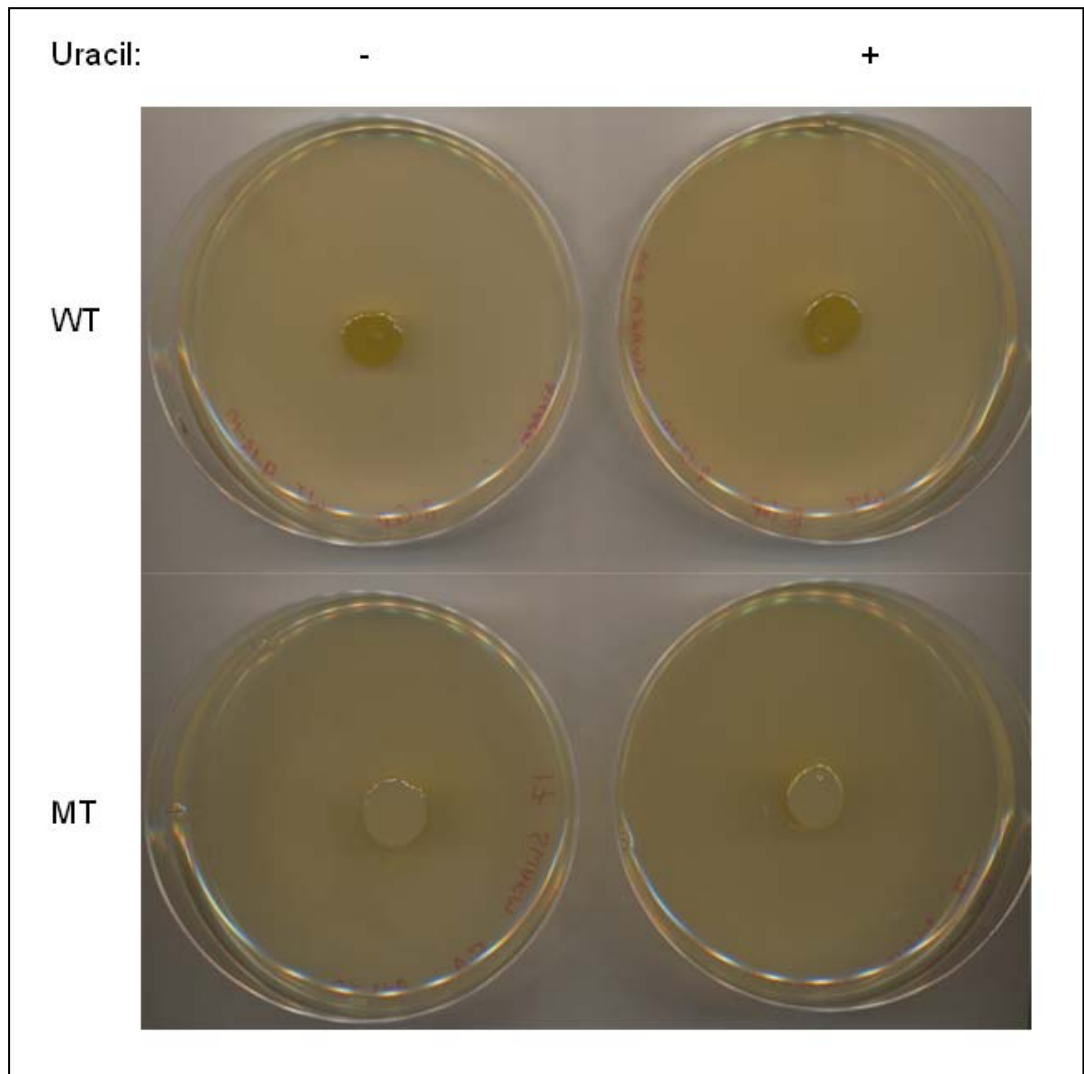


Fig. 47 Swarming motility assay.

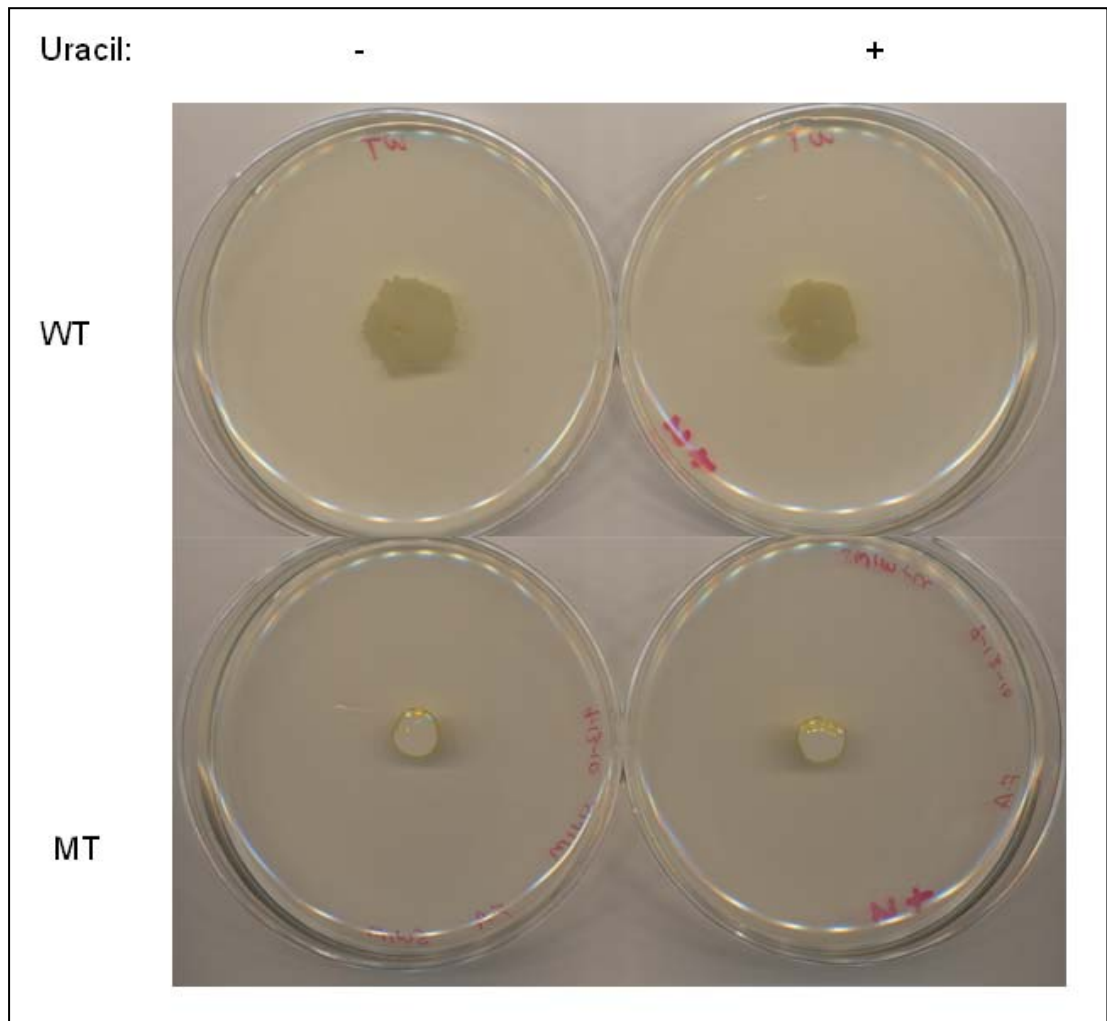


Fig. 48 Swimming motility.

the growth curve for the wild type and the *pyrC*⁻ mutant were nearly identical, this was not the case for the motility studies. Here the *pyrC*⁻ mutant strains failed to produce the wild type levels of twitching and swimming motilities. The residual *pyrC*, here designated *pyrC2* was unable to produce a wild type motility response. A similar result was seen for the biofilm production.

Biofilm Assay

To determine the ability of *B. cepacia* wild type and *B. cepacia pyrC*⁻ mutant strains to attach to abiotic surfaces, two different biofilm assays were carried out as described in Materials and Methods. Thus the wild type and the *pyrC*⁻ mutant strain were compared for biofilm production. The wild type produced a thick biofilm in polystyrene microtiter plates while the mutant did not show any comparable attachment (Figure 49). These results occurred with or without uracil and were observed before it was known that two *pyrC*s were present in *B. cepacia*. Biofilm formation by *B. cepacia* wild type and the *B. cepacia pyrC*⁻ mutant strain was virtually independent of uracil. However, both 48 h cell cultures of wild type and *pyrC*⁻ mutant strains showed more biofilm formation than did the 24 h cell cultures.

The Air-liquid interface coverslip assay also revealed similar results to the Microtiter plate biofilm assay (Figure 50 and 51). Increased and wider biofilm formation in the coverslip of the *B. cepacia* wild type compared to *pyrC*⁻ mutant strain was observed. Both 48 h cell cultures of wild type and *pyrC*⁻ mutant strains showed more biofilm formation than that observed in the 24 h cell cultures. However, exogenous uracil did not significantly affect biofilm yields.

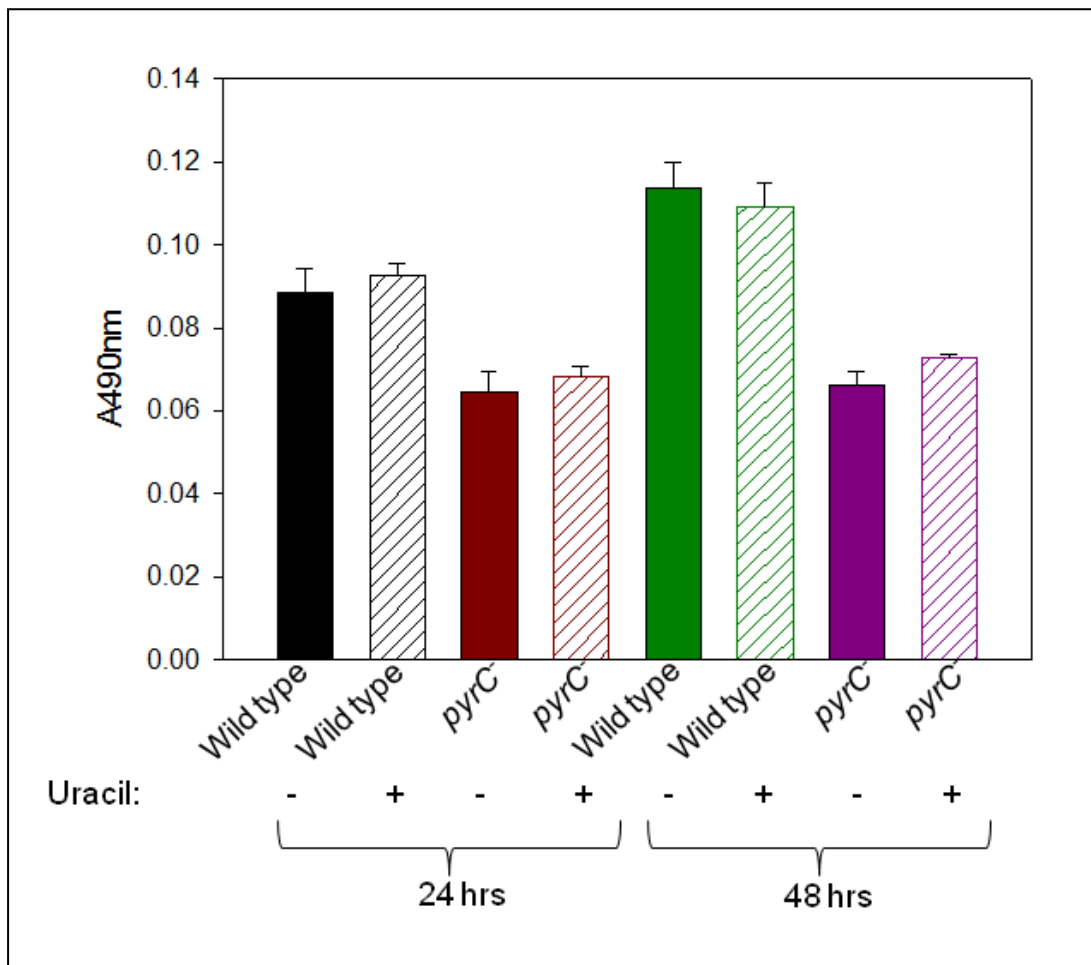
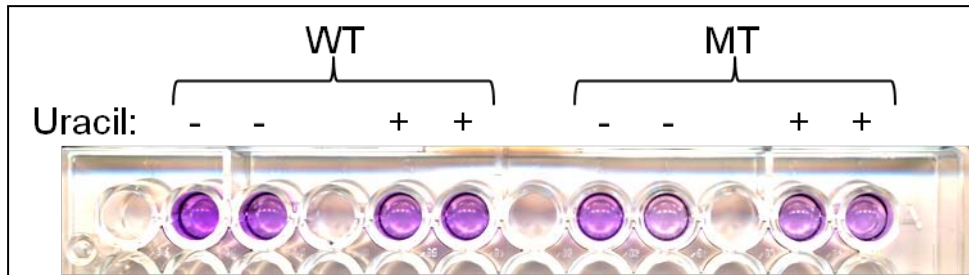


Fig. 49 Microtiter plate biofilm assay.

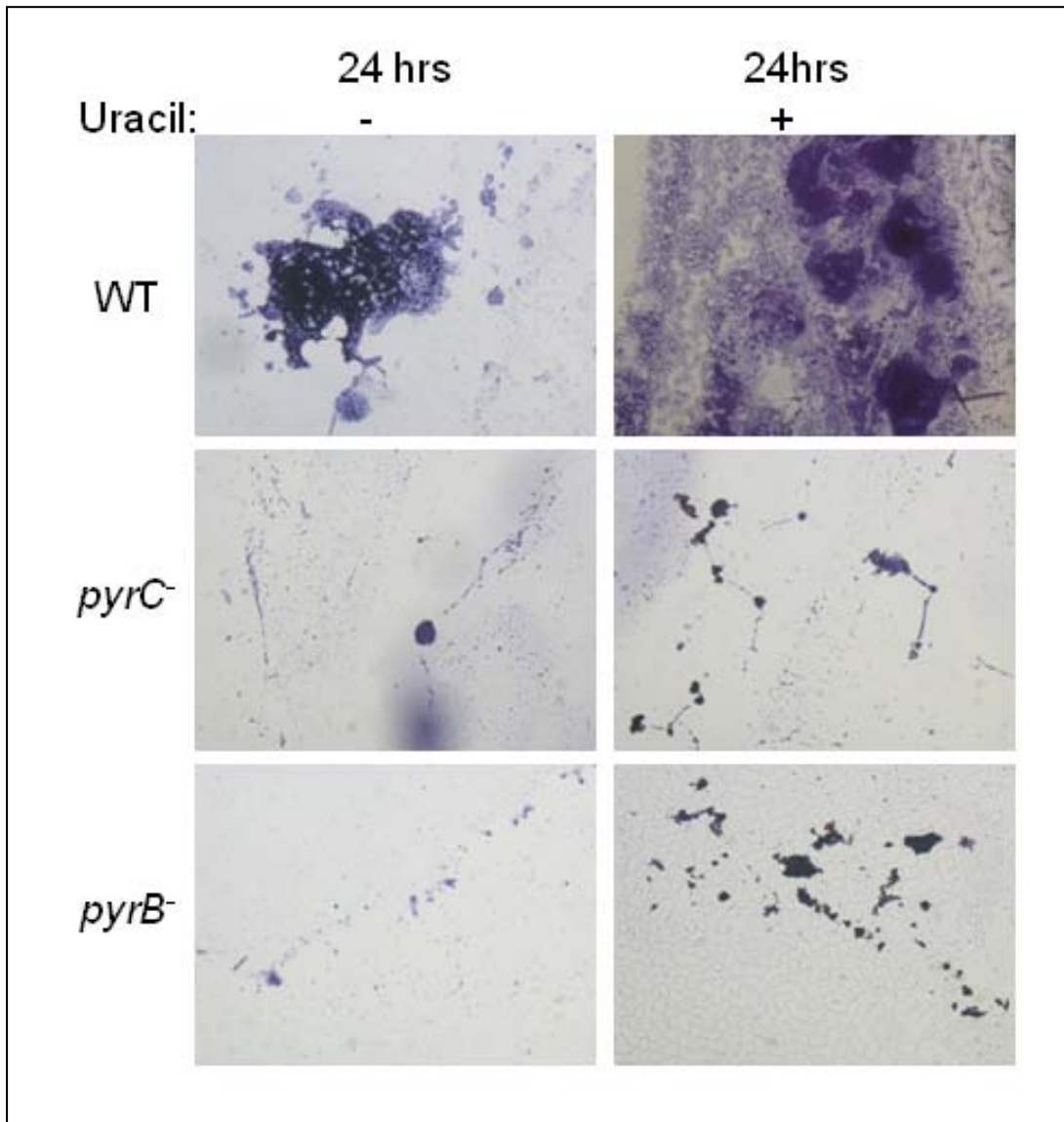


Fig. 50 Air-liquid interface coverslip assay of 24 h cultured cells.

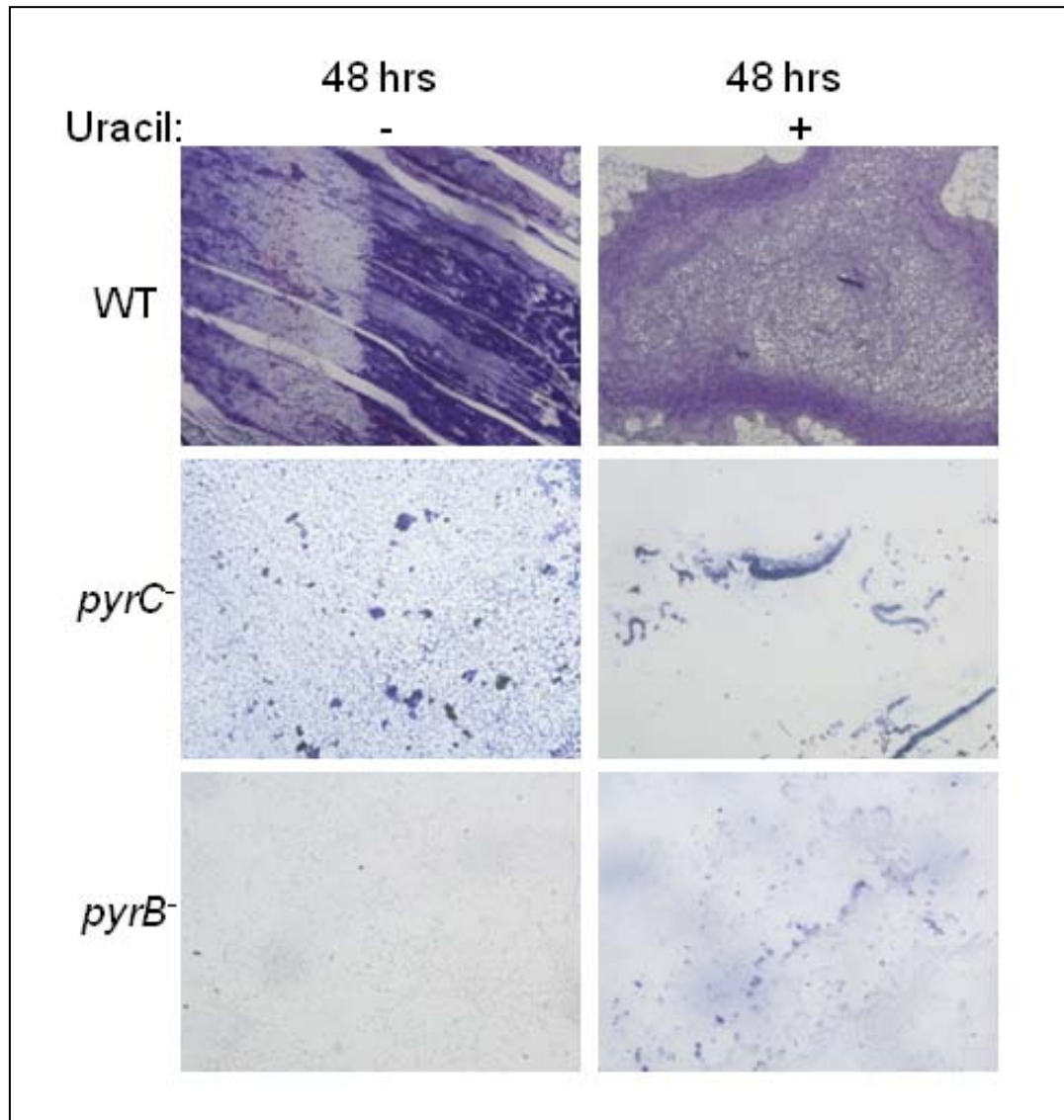


Fig. 51 Air-liquid interface coverslip assay of 48 h cultured cells.

CHAPTER 4

DISCUSSION

The molecular mass and kinetic properties of ATCase have been used to separate bacterial ATCases into three classes along phylogenetic lines (Bethell and Jones 1969). Large bacterial ATCases are found in Class A with molecular masses of 450-500 kDa. All ATCases are inhibited by nucleotide triphosphates and display Michaelis-Menten kinetics. The ATCases of the *Pseudomonas* (*P. putida*, *P. aeruginosa*; Schurr et al. 1995) are typical of this Class. The *Pseudomonas* ATCase contains six copies of the PyrB subunit with a molecular mass of 36.4 kDa and six copies of the larger PyrC' polypeptide with a mass of 44.2 kDa are arranged as a dodecamer (Schurr et al. 1995). The larger PyrC' polypeptide is not active as a DHOase but it has to be present for the ATCase holoenzyme to be active (Schurr et al. 1995). Members of the class A group are seen in column 2 of Table 7.

The three traditional classes A, B, C were extended in 1999 by Hughes et al. (1999) when the ATCase was studied in *Streptomyces griseus*. Here, the *pyrBC* complex, unlike *P. putida* ATCase holoenzyme contains an active DHOase encoded by *pyrC*.

To distinguish between the ATCases with active DHOases from those with inactive DHOases, Hughes suggested the designation Class A₁ for those with active DHOase and Class A₂ for those with inactive DHOase. These are seen in Columns 1 and 2 in Table 7.

The Class B ATCases have a molecular mass of about 300 kDa and are

typified by sigmoidal kinetics. The enzyme from *E. coli* is the most studied ATCase member of Class B. The enzyme is a dodecamer and consists of six catalytic polypeptides encoded by *pyrB* and six regulatory polypeptide encoded by *pyrI*. The PyrB enzyme has a molecular mass of 34kDa and the PyrI, a molecular mass of 17kDa. The catalytic polypeptides line up as two active trimers and three regulatory dimers to form the classic dodecameric holoenzyme. Class B ATCases are found in most enteric bacteria as well as in *Neisseria* and *Pyrococcus* (Purcarea et al. 1994). Members of Class B are seen in Column 3 Table 7.

Class C ATCases are characterized by their small size, lack of inhibition by nucleotides and Michaelis-Menten kinetics for carbamoyl phosphate and aspartate substrates. *Bacillus subtilis* has a typical Class C ATCase. It is a typical Class C ATCase. It is active only as a trimer consisting of three identical polypeptides for a molecular mass of 100 kDa. The Class C enzymes are seen in Column 4 of Table 7.

In this study, the ATCase *pyrBC* complex was purified from *Burkholderia cepacia*. In the course of the purification four different ATCase activities appeared as two dodecameric holoenzymes of 550 kDa and 510 kDa and as two trimeric ATCases (like the trimer of Class C) of 140 kDa and 120 kDa. The 140 kDa trimer consists of 3x47 kDa while the 120 kDa consists of 3x40 kDa. The 40 kDa PyrB arose uniquely by specific cleavage of the 47 kDa polypeptide between Serine 74 and Valine 75. This created a shortened PyrB polypeptide lacking 74 amino acids at its N-terminus. Other Ser/Val sites downstream were not cleaved. Chemical modification of the Ser/Val site prevented cleavage (Kim 2004). In seeking a possible role for the 74 amino acid overhang, the enzyme activities of the two trimers were studied and effector assays with the four nucleotide triphosphates carried out. The holoenzymes were also

studied.

Surprisingly, the 140 kDa enzyme showed significant inhibition while the 120 kDa had much less inhibition. This suggested that the 74 amino acid overhang at the N-terminus of PyrB housed the nucleotide binding site. As mentioned above, this binding site is removable by specific cleavage eliminating inhibition in the larger 550 kDa holoenzyme by UTP and to a lesser extent by ATP. The smaller holoenzyme of 510 kDa, with the 74 amino acid removed, gave much less inhibition. Both holoenzymes contained an active PyrC (DHOase). However, the favorable combination of ATCase and DHOase to form the ATCase holoenzyme is not clear (Figure 52).

Column 5 of Table 7 shows some of the unique features of *B. cepacia* ATCase. *B. cepacia* produces two active large holoenzymes at 550 kDa and 510 kDa. It produces two active trimers of 140 kDa and 120 kDa. The 40 kDa PyrB arose by cleavage of the 47 kDa chain. Both cleaved and uncleaved ATCase make active trimers and these two trimers participate in holoenzymes synthesis. The physiological conditions that allow the cleavage have not yet determined. Since *B. cepacia* ATCase contains atypical characteristics to those seen in Class A (Class A₁ and Class A₂) it seems appropriate to suggest a new class, namely Class D to accommodate the unique *B. cepacia* and *B. cepacia*-like ATCases.

The aim of this study was to clone and characterize the *pyrC* gene in *B. cepacia* 25416 that plays important roles in ATCase holoenzyme formation and the virulence factor production. To verify the composition of the PyrBC holoenzyme complex, the *pyrC* gene encoding *B. cepacia* dihydroorotase (DHOase, subunit size of 45 kDa) was cloned and purified by the pMAL protein fusion and purification system.

In an earlier study in our lab, Linscott (1996) partially purified the ATCases from *B. cepacia* and found that there were two bands at about 600 kDa and 240 kDa respectively, in ATCase activity gel. That was an unusual finding since *B. cepacia* was considered a pseudomonad at that time. Studies from O'Donovan's lab suggested that ATCase could be used as a taxonomic marker (O'Donovan and Shanley 1999).

Pseudomonas ATCases are representative Class A₂ ATCases as mentioned previously. *B. cepacia* ATCase also has been classified as Class A ATCase previously. While purifying the ATCase and DHOase from *B. cepacia*, we discovered the 4 different ATCase activities as mentioned above. It was great questionable phenomenon why this organism possesses 4 different sizes of ATCases. After Kim's discovery, Azad (2005) showed ATCase activity for all phases of growth in the dialyzed cell free extract using 5 different species bacteria including *B. cepacia* grown in rich media. He found that the ATCase of *B. cepacia* yielded two large bands at 550 kDa and 480-500 kDa and one much smaller band at 140 kDa on activity gels (Azad 2005). From his ATCase activity gel, especially for samples from stationary phase and death phase, there was a significant decrease in activity in the larger holoenzyme but the smaller holoenzyme remained partially active in death phase even though activity was decreased (gel picture not shown).

In order to determine more about the roles of the DHOase in *B. cepacia*, the *pyrC* gene was knocked out. *B. cepacia pyrC*⁻ mutant did not exhibit a requirement for pyrimidines and remained a prototroph. Nevertheless, though the *PyrC*⁻ knockout strain is a pyrimidine prototroph, it is not prototrophic for biofilm and virulence factor production.

In growth studies, there was no difference in growth rate between wild type

strain and the knockout mutant indicating that the observed motility defects in this study were not due to delayed growth of mutant. Moreover, the knockout strain did not require uracil.

Even though DNA sequences of *B. cepacia* 25416 are not available so far based on these results and the released sequences of other *Burkholderia* species, we can conclude there is another *pyrC* in this organism.

To characterize the relationship between pyrimidine pathway and virulence factor production, motility tests and biofilm assays were conducted using *pyrC* mutant. It would not be possible to test the *pyrC* mutant for all the possible virulent factors since the genus *Burkholderia* is well known to produce many different factors depending on the species they produce different virulent factors. Biofilm formation is the common characteristic of the genus *Burkholderia* and the pathogenicity of *B. cepacia* is in part due to the ability of biofilm production (Djordjevic et al. 2002). The comparison of ability of biofilm formation between the wild type and the mutant was the great way for these reasons. To develop biofilm, their motility should be involved to attach, once produced, bacteria may undergo significant phenotypic shifts including induction of different metabolic pathways and development of resistance to antibiotic.

Even though no significant difference in growth rates was observed, there were significant differences between the wild type and mutant in biofilm production and other virulence factor. Overall the wild type had significantly greater biofilm formation than did the mutant. This indicates that differences in biofilm formation were due to factors other than the ability to match wild type growth.

Two different biofilm assays were combined for more accurate results. The direct microscopic observation and the quantification using the microtiter plate assay

provided the consistent results for biofilm production. Addition of uracil did not make any significant difference. These assays confirmed that *pyrC* gene was directly or indirectly involved in biofilm formation in *B. cepacia*.

Motility plays a major role in biofilm formation. Swarming behavior of the *pyrC* mutants and the wild-type was not distinguishable, indicating that swarming motility was not required for biofilm production (Figure 47). Huber et al. also reported that swarming motility is not required for biofilm formation in *B. cepacia* H111 (Huber et al. 2001). Swimming and twitching motility were diminished in the mutant strain, therefore *pyrC* mutant may have a problem in the initial cell attachment, but more investigations such as knockout of genes involved in motility would be required to confirm the requirement of these types of motility for the biofilm production.

The results from biofilm production in this study open very important possibility in relationships between the pyrimidine biosynthetic pathway and quorum sensing (QS) system which is the global gene regulation systems in bacteria. As mentioned in the introduction, QS system controls the production not only of other virulence factors but also of biofilm. It could be possible that *pyrC* gene knockout also affects QS system. That is reasonable since the pyrimidine pathway is the essential pathway for the living organisms. More research is needed to investigate these details. In order to know the exact functions of each *pyrC* genes, the goal of this study had been changed to the construction of double knockout of *pyrC* genes. Unfortunately, that was not successful after several trials.

In 2003, the Wellcome Trust Sanger Institute sequenced the first genome of the *Burkholderia* genus, which was *B. cenocepacia* J2315. Recently more sequence information is available than when this study began. But especially for the

identification of another *pyrC*, designated *pyrC2*, required to have more genome sequencing in the future.

During this research, *B. cepacia pyrC* was identified and gene sequence was reported in NCBI data base. A BLAST search using *B. cepacia* PyrC amino acid sequence revealed high homology to *Pseudomonas* spp. PyrC amino acid sequence (Figure 53). The PyrC amino acids homology among *B.cepacia*, *P. aeruginosa*, *P. putida*, and *P. fluorescens* was analyzed using Biology WorkBench (Figure 54) (<http://seqtool.sdsc.edu/CGI/BW.cgi>). *B.cepacia* PyrC amino acid showed about 60 % homology with PyrC of *P. aeruginosa*, *P. putida*, and *P. fluorescens*. Another BLAST search using *B. cepacia* PyrC amino acid sequence was performed. As expected, *B. cepacia* PyrC amino acid sequence showed very high homology to other *Burkholderia* spp. PyrC amino acid sequences (Figure 55). Some *Burkholderia* spp., such as *B. mallei*, have two *pyrC* gene loci in chromosome 1 while other *Burkholderia* spp., such as *B. cenocepacia*, have one *pyrC* in chromosome 1 and another one in chromosome 2. Among them, *B. cepacia* PyrC amino acid sequence matches mostly with *B. cenocepacia* PyrC in chromosome 1 (Figure 56). Therefore, *B. cepacia pyrC* is likely to be found in chromosome 1.

Maksimova *et al.* reported that in a DHOase mutant strain of *P. putida* failed to produce the siderophore pyoverdine, which is one of its virulence factors (Maksimova *et al.* 1993). Brichta (2003) showed that the *pyrC* and *pyrC2* of *P. aeruginosa* are involved in the production of the siderophore pyoverdine and pyocyanin, which are virulence factors. She also reported that *pyrC* was found to be constitutively expressed while *pyrC2* was expressed only in the *pyrC* mutant background. It is possible that similar regulation may occur in *B. cepacia*.

In an earlier study, Kim (2004) showed that the *pyrB1* knockout in *B. cepacia* 25416 had lost its virulence against *Caenorhabditis elegans*. He also showed that there were two *pyrBs* (*pyrB1* and *pyrB2*) in *B. cepacia*.

The research presented here combined two important aspects of use ATCase as a taxonomic tool and a potential therapeutic target. Recently, many different approaches have been performed to discover and control the virulence factors from typical gene inactivation to very recent comparative transcriptomics (Yoder-Himes et al. 2010).

ATCase, an essential enzyme, is found in almost all living organisms and is conserved in its basic characteristics during the evolution. We can deduce that it has originated from a common ancestor. Without this enzyme, organisms can not survive excluding a few natural pyrimidine auxotrophs. The unique ATCase in *B. cepacia* has been classified as Class A₂, but it contains active DHOase like Class A₁ and also contains active trimers of ATCase like Class C. It seems that they carry the mixed characteristics of ATCase from most bacteria. We are not sure of the advantages of carrying several ATCases. But it may be an advantage for adaptation to protection from new environments quickly, and also for their versatile characteristics. The study of ATCase in multichromosomal organisms, such as how organisms keep and develop the genes for their survival, during evolution will provide us invaluable information for the future.

To characterize the relationship between pyrimidine pathway and virulent factor production, some virulent tests and biofilm assay were conducted using *B. cepacia pyrC* mutant. *B. cepacia pyrC* mutant showed diminished twitching motility. This may due to the malfunction of Type IV pili.

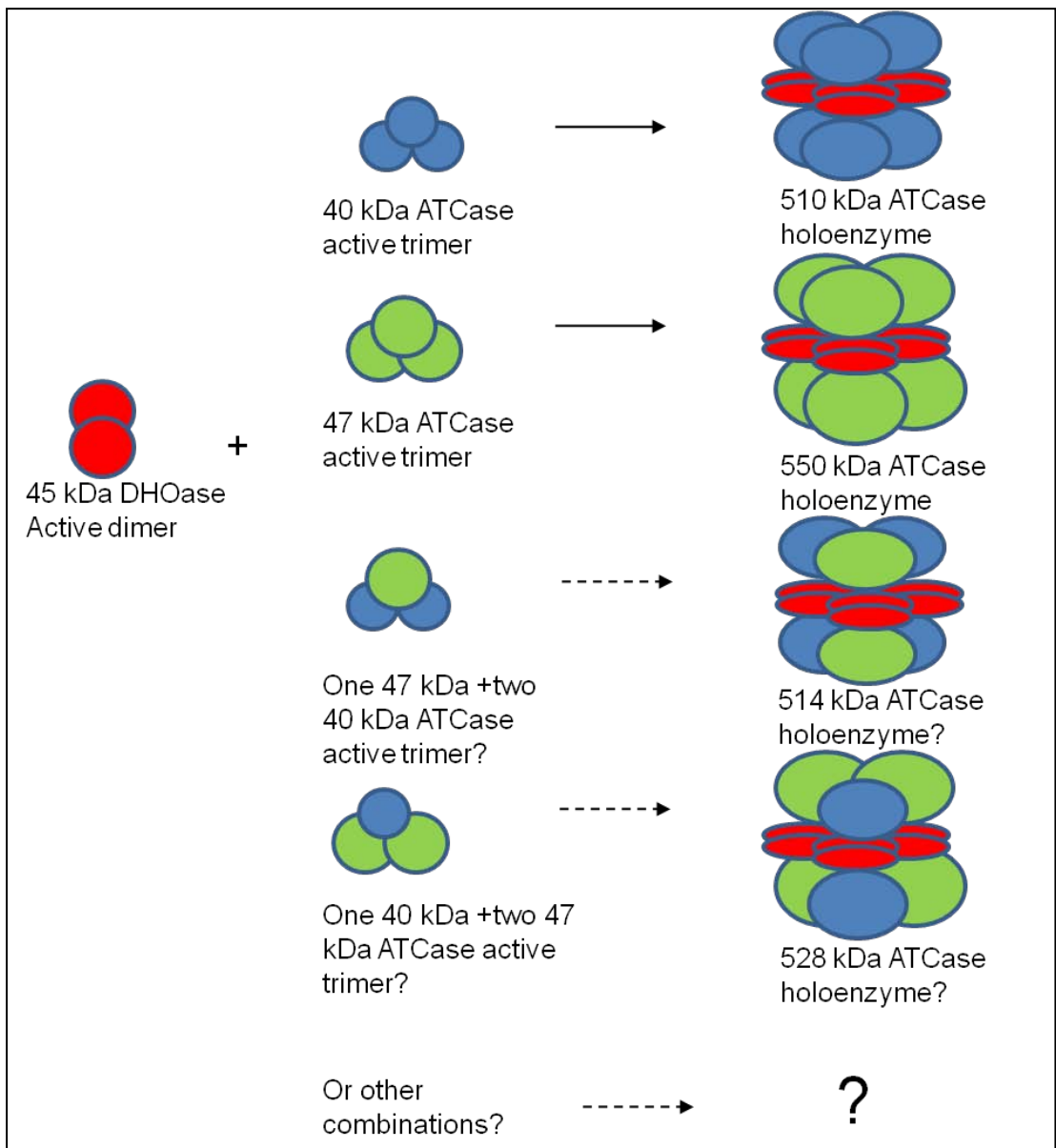


Fig. 52 Feasible combination of DHOase and ATCase to make an ATCase holoenzyme.

```

          *           20           *           40
B. cepacia : MTASNASSPATLSLARPDWHHLHRDGDMLAAVLPHTARQEF : 41
P. aerugin : MSDR-----LTLRPPDDWHIHLRDGAALANTVGDARTF : 34
P. putida   : MSDR-----LTLRPPDDWHIHLRDGAVLPHTVGDVARTF : 34
P. fluores : MSDR-----LTLRPPDDWHIHLRDGAALPHTVADVARTF : 34
          M3dr           L3LIRPDDWH6HLRDGa L t6 d ArtF

          *           60           *           80
B. cepacia : GRAIVMPNLKPPVTTTAQACAYRERILAAAPACMTFEPLMT : 82
P. aerugin : GRAIVMPNLVPPVRNAAEALAYRQRILAAAPAAASFPEPLMV : 75
P. putida   : ARAIIMPNLVPPVRNVTEACAYRERILAAAPAGSRFEPLMV : 75
P. fluores : GRAIIMPNLVPPVRNAAEALAYRQRILAAAPAGSRFEPLMV : 75
          gRAI6MPNLvPPVrn 2A AYR2RILAArPAGsrFEPLMV

          *           100          *           120
B. cepacia : LYLTDNMPFDEIRRARESGFVHGVKLYPAGATTNSDGHVTD : 123
P. aerugin : LYLTDRSTEEIRTAKASGFVHAAKLYPAGATTNSDSGVTR : 116
P. putida   : LYLTDRSTPEIVRAKASGFVHAAKLYPAGATTNSDSGVTS : 116
P. fluores : LYLTDRTCPEEIRTAKASGFVHAAKLYPAGATTNSDSGVTS : 116
          LYLTDRt pee6R A4aSGFVhaaKLYPAGATTNSDsGVT

          *           140          *           160
B. cepacia : LAKCAKTLKLEAMQETGMPLLVHGEVTDASTDLFDREKVFIDR : 164
P. aerugin : IDNTEALEAMAEVGMPLLVHGEVTRAEVDVFDREKQFIDE : 157
P. putida   : IDNTEPAIEALAEVGMPLLVHGEVTRSEIDVFDREKEFIDE : 157
P. fluores : IDKILPAIEAMAEVGMPLLIHGEVTRGVDVDFDREKEFIDE : 157
          6d i a6EA6aEvGMPLL6HGEVTr 6D6FDREK FIDE

          *           180          *           200
B. cepacia : VMTFLRRDFPGLKVVFEHITTDAAADYVRDADAAPGLLGAT : 205
P. aerugin : HLRRVVERFPTLKVVFEHITTDAAQFVREAEAN---VGAT : 195
P. putida   : HMRRVVERFPTLKVVFEHITTDAAQFVTEAEAN---VGAT : 195
P. fluores : HMRRVVERFPTLKVVFEHITTDAAVQFVTEAEAN---VGAT : 195
          h6rr6ve FPtLKVVFEHITT DAAq5V eA An 6GAT

          *           220          *           240
B. cepacia : ITAHLLYNRNMLEVGGIRPHYYCLPVLKRETHRVALVEAA : 246
P. aerugin : ITAHLLYNRNMLEVGGIRPHFYCLPILKRNTHQEALLDAA : 236
P. putida   : ITACHLLYNRNMLEVGGIRPHFYCLPILKRNTHQVALLDAA : 236
P. fluores : ITAHLLYNRNMLEVGGIRPHFYCLPILKRNTHQVALLDAA : 236
          ITAhHLLYNRNh6LVGGIRPH5YCLP6LKRnTHqVAL6dAA

          *           260          *           280
B. cepacia : TSGNPRFFLGTDSAPHARHAKETACGCAGCYTALHALEYLA : 287
P. aerugin : VSGNPKFFLGTDSAPHARHAKETACGCAGCYSAYAAIELYA : 277
P. putida   : TSGNPKFFLGTDSAPHARHAKETACGCAGCYTAYAAIEMYA : 277
P. fluores : TSGNPKFFLGTDSAPHARHAKETACGCAGCYTAAFAIELYA : 277
          tSGNP4FFLGTDSAPHArhAKEaACGCAGCY3A aA6E6YA

          *           300          *           320
B. cepacia : EAFDHAGALDKLEGFASFFGALFYGLPNSAETVTLRREAWE : 328
P. aerugin : EAFEQRNALDKLEGFASLEGPFYGLPNTDRITLVREBWO : 318
P. putida   : EAFEQRNALDKLEGFASLEGPFYGLPANTDTITLVREBWT : 318
P. fluores : EAFEQRNALDKLEGFASINGRPFYGLPANTDRITLVREBWT : 318
          EAFeqrnALDKLEGFAS Gp FYGLP ntd 6TLvRE W

          *           340          *
B. cepacia : LPREIFAGDTPVVPLRGGETTICWKLAE--- : 354
P. aerugin : APASLPFGDFDVVPLRAGETLRWKLLEAGA : 348
P. putida   : APESLPFGDQTVVPLRAGERLRWRLLLEKNA : 348
P. fluores : APASLPFGEELTVIPLRAGETLRWRLLLEESK : 348
          aP s6pfg V6PLRaGET6rW4Lle

```

Fig. 53 Amino acids alignment of *B. cepacia* PyrC with *Pseudomonas* PyrC

Clustal W options and diagnostic messages

```
Alignment type: Protein                Alignment order: aligned

                Pairwise alignment parameters

Method: accurate
Matrix: Gonnet
Gap open penalty: 10.00                Gap extension penalty: 0.10

                Multiple alignment parameters

Matrix: Gonnet                        Negative matrix?: no
Gap open penalty: 10.00                Gap extension penalty: 0.20
% identity for delay: 30               Residue-specific gap penalties: on
Penalize end gaps: on                 Hydrophilic gap penalties: on
Gap separation distance: 0             Hydrophilic residues: GPSNDQEKR

CLUSTAL W (1.81) Multiple Sequence Alignments

Sequence type explicitly set to Protein
Sequence format is Pearson
Sequence 1: P._fluorescens            348 aa
Sequence 2: P.putida_DHOase          348 aa
Sequence 3: P.aeruginosa              348 aa
Sequence 4: B.cepacia_DHOase         354 aa
Start of Pairwise alignments
Aligning...
Sequences (1:2) Aligned. Score: 88
Sequences (1:3) Aligned. Score: 87
Sequences (1:4) Aligned. Score: 63
Sequences (2:3) Aligned. Score: 87
Sequences (2:4) Aligned. Score: 62
Sequences (3:4) Aligned. Score: 65
Time for pairwise alignment: 0.048685

Guide tree      file created:  [../tmp-dir/10091.CLUSTALW.dnd]
Start of Multiple Alignment
There are 3 groups
Aligning...
Group 1: Sequences:  2      Score:7189
Group 2: Sequences:  3      Score:7142
Group 3: Sequences:  4      Score:6200
Time for multiple alignment: 0.119159

Alignment Score 10129
CLUSTAL-Alignment file created  [../tmp-dir/10091.CLUSTALW.aln]
```

Fig. 54 Analysis of amino acids alignment of *B. cepacia* PyrC with Pseudomonad PyrC using Biology WorkBench.

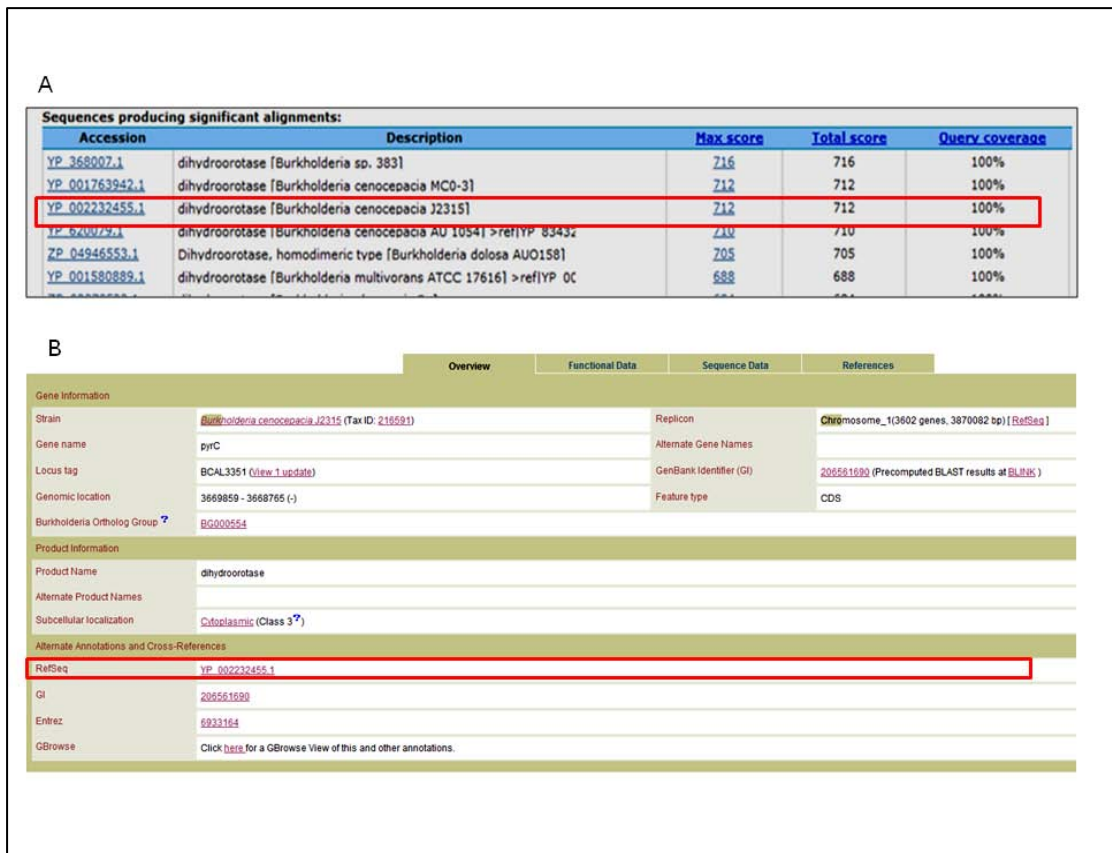
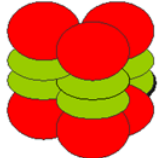
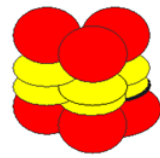
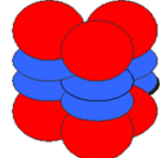
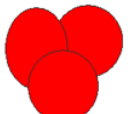
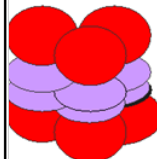
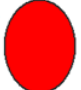






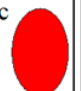



Fig. 55 Expected locus of *B. cepacia pyrC*. The red boxes show highly homologous *pyrC* between *B. cepacia* and *B. cenocepacia*. A. Gene blast result using *B. cepacia pyrC*. B. *pyrC* gene locus of *B. cenocepacia*

B. cepacia pyrC mutant also showed the reduction of biofilm formation. Quorum sensing regulates biofilm production, which is mediated by hormone-like N-acyl homoserine lactones. These molecules control the production not only of biofilm matrix material but also of virulence factors such as proteases, flagellae, and fimbriae. Recent research has found that *B. cepacia* shares the same quorum-sensing molecules as *P. aeruginosa*; thus, these organisms potentially enhance each other's virulence (Huber *et al.* 2001). Therefore, *B. cepacia pyrC* mutant may have a problem in the regulation of initial cell attachment, or in the control of the maturation of the biofilm. These results provide the evidence that twitching motility of *B. cepacia* is quorum-sensing-regulated, possibly through the control of biosurfactant production.

As a result, we propose the new classification of *B. cepacia* ATCase as Class D ATCase (Table 7). *B. cepacia* contains two *pyrC* genes, one locating at chromosome 1. The *B. cepacia* pyrimidine pathway has a relationship to virulence factor production and biofilm formation. In addition to that, since *B. cepacia* has characteristic of plant promoter and bioremediation, this research will help to make *B. cepacia* as a bio-agent in agriculture and anti-pollution industry. Moreover, it will pave the way to generate the vaccine to prevent the deadly infection to CF patient.

Table 7 Proposed new class of ATCase, class D, for *B. cepacia*

Classes	Class A1	Class A2	Class B	Class C	Class D
Structure					
Subunit Structure	<p>PyrB catalytic 34 kDa </p> <p>PyrC active 45 kDa </p>	<p>PyrB catalytic 34 kDa </p> <p>PyrC' inactive 45 kDa </p>	<p>PyrB catalytic 34 kDa </p> <p>PyrI regulatory 17 kDa </p>	<p>PyrB catalytic 34 kDa </p> <p>active as trimer No holoenzyme</p>	<p>PyrB catalytic 47 kDa or 40 kDa </p> <p>PyrC active 45 kDa </p>
Organism	<i>Streptomyces griseus</i> <i>S.coelicolor</i> <i>Mycobacterium smegmatis</i> <i>Thermus aquaticus</i>	<i>Pseudomonas putida</i> <i>P. aeruginosa</i> <i>Burkholderia cepacia</i>	<i>E. coli</i> <i>Salmonella typhimurium</i> <i>Neisseria meningitidis</i> <i>Pyrococcus abyssi</i>	<i>Bacillus subtilis</i> <i>B. caldolydicus</i> <i>Streptococcus pyogenes</i>	<i>Burkholderia cepacia</i>
Size of Holoenzyme	450 kDa	480 kDa	310 kDa	No holoenzyme Trimer only 100 kDa	550 kDa or 510 kDa

REFERENCES

- Abdelal AT, Bussey L, Vickers L (1983) Carbamoylphosphate synthetase from *Pseudomonas aeruginosa*. Subunit composition, kinetic analysis and regulation. Eur J Biochem 129:697-702
- Aguilar C, Bertani I, Venturi V (2003) Quorum-sensing system and stationary-phase sigma factor (rpoS) of the onion pathogen *Burkholderia cepacia* genomovar I type strain, ATCC 25416. Appl Environ Microbiol 69:1739-1747
- Allardet-Servent A, Michaux-Charachon S, Jumas-Bilak E, Karayan L, Ramuz M (1993) Presence of one linear and one circular chromosome in the *Agrobacterium tumefaciens* C58 genome. J Bacteriol 175:7869-7874
- Anderson PM (1983) CTP synthetase from *Escherichia coli*: an improved purification procedure and characterization of hysteretic and enzyme concentration effects on kinetic properties. Biochemistry 22:3285-3292
- Anderson PM, Meister A (1965) Evidence for an activated form of carbon dioxide in the reaction catalyzed by *Escherichia coli* carbamyl phosphate synthetase. Biochemistry 4:2803-2809
- Azad KN (2005) Pyrimidine enzyme specific activity at four different phases of growth in minimal and rich media, and concomitant evaluation of virulence

factor production in *Pseudomonas aeruginosa*. Ph.D. dissertation, University of North Texas, Denton, Texas.

Baldwin A, Mahenthiralingam E, Drevinek P, Vandamme P, Govan JR, Waine DJ, LiPuma JJ, Chiarini L, Dalmastrì C, Henry DA, Speert DP, Honeybourne D, Maiden MC, Dowson CG (2007) Environmental *Burkholderia cepacia* complex isolates in human infections. *Emerg Infect Dis* 13:458-461

Baldwin A, Mahenthiralingam E, Thickett KM, Honeybourne D, Maiden MC, Govan JR, Speert DP, Lipuma JJ, Vandamme P, Dowson CG (2005) Multilocus sequence typing scheme that provides both species and strain differentiation for the *Burkholderia cepacia* complex. *J Clin Microbiol* 43:4665-4673

Beck DA (1995) Pyrimidine salvage enzymes in microorganisms: Labyrinths of enzymatic diversity. Ph.D. dissertation, University of North Texas, Denton

Beck DA, O'Donovan GA (2008) Pathways of pyrimidine salvage in *Pseudomonas* and former *Pseudomonas*: detection of recycling enzymes using high-performance liquid chromatography. *Curr Microbiol* 56:162-167

Beckwith JR, Pardee AB, Austrian R, Jacob F (1962) Coordination of the synthesis of the enzymes in the pyrimidine pathway of *E. coli*. *J Mol Biol* 5:618-634

Bergh ST, Evans DR (1993) Subunit structure of a class A aspartate transcarbamoylase from *Pseudomonas fluorescens*. *Proc Natl Acad Sci U S A* 90:9818-9822

- Bethell MR, Jones ME (1969) Molecular size and feedback-regulation characteristics of bacterial aspartate transcarbamylases. *Arch Biochem Biophys* 134:352-365
- Bontemps C, Elliott GN, Simon MF, Dos Reis Junior FB, Gross E, Lawton RC, Neto NE, de Fatima Loureiro M, De Faria SM, Sprent JI, James EK, Young JP (2010) *Burkholderia* species are ancient symbionts of legumes. *Mol Ecol* 19:44-52
- Bothwell M, Schachman HK (1974) Pathways of assembly of aspartate transcarbamoylase from catalytic and regulatory subunits. *Proc Natl Acad Sci U S A* 71:3221-3225
- Brabson JS, Switzer RL (1975) Purification and properties of *Bacillus subtilis* aspartate transcarbamylase. *J Biol Chem* 250:8664-8669
- Brichta DM (2003) Construction of a *Pseudomonas aeruginosa* dihydroorotase mutant and the discovery of a novel link between pyrimidine biosynthetic intermediates and the ability to produce virulence factors. Ph.D. dissertation, University of North Texas, Denton, Texas
- Burkholder WH (1948) Bacteria as plant pathogens. *Annu Rev Microbiol* 2 (1 vol.):389-412
- Caiazza NC, O'Toole GA (2004) SadB is required for the transition from reversible to irreversible attachment during biofilm formation by *Pseudomonas aeruginosa*

PA14. J Bacteriol 186:4476-4485

Chain PS, Denev VJ, Konstantinidis KT, Vergez LM, Agullo L, Reyes VL, Hauser L, Cordova M, Gomez L, Gonzalez M, Land M, Lao V, Larimer F, LiPuma JJ, Mahenthiralingam E, Malfatti SA, Marx CJ, Parnell JJ, Ramette A, Richardson P, Seeger M, Smith D, Spilker T, Sul WJ, Tsoi TV, Ulrich LE, Zhulin IB, Tiedje JM (2006) *Burkholderia xenovorans* LB400 harbors a multi-replicon, 9.73-Mbp genome shaped for versatility. Proc Natl Acad Sci U S A 103:15280-15287

Chernish RN, Aaron SD (2003) Approach to resistant gram-negative bacterial pulmonary infections in patients with cystic fibrosis. Curr Opin Pulm Med 9:509-515

Christopherson RI, Jones ME (1979) Interconversion of carbamoyl-L-aspartate and L-dihydroorotate by dihydroorotase from mouse Ehrlich ascites carcinoma. J Biol Chem 254:12506-12512

Chu CP, West TP (1990) Pyrimidine biosynthetic pathway of *Pseudomonas fluorescens*. J Gen Microbiol 136:875-880

Coenye T, Vandamme P (2003) Diversity and significance of *Burkholderia* species occupying diverse ecological niches. Environ Microbiol 5:719-729

- Coenye T, Vandamme P, Govan JR, LiPuma JJ (2001) Taxonomy and identification of the *Burkholderia cepacia* complex. J Clin Microbiol 39:3427-3436
- Coleman PF, Suttle DP, Stark GR (1977) Purification from hamster cells of the multifunctional protein that initiates *de novo* synthesis of pyrimidine nucleotides. J Biol Chem 252:6379-6385
- Condon S, Collins JK, O'Donovan G A (1976) Regulation of arginine and pyrimidine biosynthesis in *Pseudomonas putida*. J Gen Microbiol 92:375-383
- Conway BA, Venu V, Speert DP (2002) Biofilm formation and acyl homoserine lactone production in the *Burkholderia cepacia* complex. J Bacteriol 184:5678-5685
- Cooper VS, Vohr SH, Wrocklage SC, Hatcher PJ (2010) Why genes evolve faster on secondary chromosomes in bacteria. PLoS Comput Biol 6:e1000732
- Couturier E, Rocha EP (2006) Replication-associated gene dosage effects shape the genomes of fast-growing bacteria but only for transcription and translation genes. Mol Microbiol 59:1506-1518
- Darling P, Chan M, Cox AD, Sokol PA (1998) Siderophore production by cystic fibrosis isolates of *Burkholderia cepacia*. Infect Immun 66:874-877
- Davidson JN, Chen KC, Jamison RS, Musmanno LA, Kern CB (1993) The

evolutionary history of the first three enzymes in pyrimidine biosynthesis. *Bioessays* 15:157-164

Djordjevic D, Wiedmann M, McLandsborough LA (2002) Microtiter plate assay for assessment of *Listeria monocytogenes* biofilm formation. *Appl Environ Microbiol* 68:2950-2958

Eaton KA, Morgan DR, Krakowka S (1992) Motility as a factor in the colonisation of gnotobiotic piglets by *Helicobacter pylori*. *J Med Microbiol* 37:123-127

el-Banna N, Winkelmann G (1998) Pyrrolnitrin from *Burkholderia cepacia*: antibiotic activity against fungi and novel activities against streptomycetes. *J Appl Microbiol* 85:69-78

Ellis KJ, Morrison JF (1992) Buffers of constant ionic strength for studying pH-dependent processes. *Methods Enzymol* 87:405-26

Estrada-De Los Santos P, Bustillos-Cristales R, Caballero-Mellado J (2001) *Burkholderia*, a genus rich in plant-associated nitrogen fixers with wide environmental and geographic distribution. *Appl Environ Microbiol* 67:2790-2798

Faure M, Camonis JH, Jacquet M (1989) Molecular characterization of a *Dictyostelium discoideum* gene encoding a multifunctional enzyme of the pyrimidine pathway. *Eur J Biochem* 179:345-358

- Feldman M, Bryan R, Rajan S, Scheffler L, Brunnert S, Tang H, Prince A (1998)
Role of flagella in pathogenesis of *Pseudomonas aeruginosa* pulmonary
infection. *Infect Immun* 66:43-51
- Fields CJ, Brichta DM, Shepherdson M, Farinha M, O'Donovan GA (1999)
Phylogenetic analysis and classification of dihydroorotases: a complex history
for a complex enzyme. *Paths to Pyrimidines. An International
Newsletter*:7:49-63
- Fiore A, Laevens S, Bevivino A, Dalmastrì C, Tabacchioni S, Vandamme P, Chiarini
L (2001) *Burkholderia cepacia* complex: distribution of genomovars among
isolates from the maize rhizosphere in Italy. *Environ Microbiol* 3:137-143
- FitzSimmons S (1998) Cystic Fibrosis Foundation.. Patient registry 1997 annual data
report. In. Cystic Fibrosis Foundation, Bethesda
- Freund JN, Jarry BP (1987) The rudimentary gene of *Drosophila melanogaster*
encodes four enzymic functions. *J Mol Biol* 193:1-13
- George AM, Jones PM, Middleton PG (2009) Cystic fibrosis infections: treatment
strategies and prospects. *FEMS Microbiol Lett* 300:153-164
- Gerhart JC, Pardee AB (1962) The enzymology of control by feedback inhibition. *J
Biol Chem* 237:891-896

- Gerhart JC, Pardee AB (1964) Aspartate Transcarbamylase, an Enzyme Designed for Feedback Inhibition. *Fed Proc* 23:727-735
- Ginther CL, Ingraham JL (1974) Nucleoside diphosphokinase of *Salmonella typhimurium*. *J Biol Chem* 249:3406-3411
- Govan JR (2000) Infection control in cystic fibrosis: methicillin-resistant *Staphylococcus aureus*, *Pseudomonas aeruginosa* and the *Burkholderia cepacia* complex. *J R Soc Med* 93 Suppl 38:40-45
- Govan JR, Hughes JE, Vandamme P (1996) *Burkholderia cepacia*: medical, taxonomic and ecological issues. *J Med Microbiol* 45:395-407
- Govan JR, Vandamme P (1998) Agricultural and medical microbiology: a time for bridging gaps. *Microbiology* 144 (Pt 9):2373-2375
- Grogan DW, Gunsalus RP (1993) *Sulfolobus acidocaldarius* synthesizes UMP via a standard de novo pathway: results of biochemical-genetic study. *J Bacteriol* 175:1500-1507
- Hayashi S, Abe M, Kimoto M, Furukawa S, Nakazawa T (2000) The dsbA-dsbB disulfide bond formation system of *Burkholderia cepacia* is involved in the production of protease and alkaline phosphatase, motility, metal resistance, and multi-drug resistance. *Microbiol Immunol* 44:41-50

- Herve G (1981) Is the association of concerted homotropic cooperative interactions and local heterotropic effects a general basis feature of regulatory enzymes? *Biochimie* 63:103-105
- Holm L, Sander C (1997) Decision support system for the evolutionary classification of protein structures. *Proc Int Conf Intell Syst Mol Biol* 5:140-146
- Holmes A, Govan J, Goldstein R (1998) Agricultural use of *Burkholderia (Pseudomonas) cepacia*: a threat to human health? *Emerg Infect Dis* 4:221-227
- Hoover TA, Roof WD, Foltermann KF, O'Donovan GA, Bencini DA, Wild JR (1983) Nucleotide sequence of the structural gene (*pyrB*) that encodes the catalytic polypeptide of aspartate transcarbamoylase of *Escherichia coli*. *Proc Natl Acad Sci U S A* 80:2462-2466
- Huber B, Feldmann F, Kothe M, Vandamme P, Wopperer J, Riedel K, Eberl L (2004) Identification of a novel virulence factor in *Burkholderia cenocepacia* H111 required for efficient slow killing of *Caenorhabditis elegans*. *Infect Immun* 72:7220-7230
- Huber B, Riedel K, Hentzer M, Heydorn A, Gotschlich A, Givskov M, Molin S, Eberl L (2001) The *cep* quorum-sensing system of *Burkholderia cepacia* H111 controls biofilm formation and swarming motility. *Microbiology* 147:2517-2528

- Hughes LE, Hooshdaran MZ, O'Donovan GA (1999) *Streptomyces aspartate* transcarbamoylase is a dodecamer with dihydroorotase activity. *Curr Microbiol* 39:175-179
- Isaac JH, Holloway BW (1968) Control of pyrimidine biosynthesis in *Pseudomonas aeruginosa*. *J Bacteriol* 96:1732-1741
- Isles A, Maclusky I, Corey M, Gold R, Prober C, Fleming P, Levison H (1984) *Pseudomonas cepacia* infection in cystic fibrosis: an emerging problem. *J Pediatr* 104:206-210
- Karibian D, Couchoud P (1974) Dihydro-orotate oxidase of *Escherichia coli* K12: purification, properties, and relation to the cytoplasmic membrane. *Biochim Biophys Acta* 364:218-232
- Kedzie KM (1987) Characterization of the *pyrB* Gene of *Serratia marcescens* and hybrid gene formation with the *pyrB* Gene of *Escherichia coli*, leading to the production of chimerical ATCases. Ph.D. Dissertation, Texas A&M University, College Station, Texas
- Khan AI, Chowdhry BZ, Yon RJ (1999) Wheat-germ aspartate transcarbamoylase: revised purification, stability and re-evaluation of regulatory kinetics in terms of the Monod-Wyman-Changeux model. *Eur J Biochem* 259:71-78

- Kim S (2004) Purification and Characterization of ATCase from *Burkholderia cepacia*. Ph.D. dissertation, University of North Texas, Denton, Texas
- Kooi C, Corbett CR, Sokol PA (2005) Functional analysis of the *Burkholderia cenocepacia* ZmpA metalloprotease. *J Bacteriol* 187:4421-4429
- Larsen JN, Jensen KF (1985) Nucleotide sequence of the *pyrD* gene of *Escherichia coli* and characterization of the flavoprotein dihydroorotate dehydrogenase. *Eur J Biochem* 151:59-65
- Lawlor MS, O'Connor C, Miller VL (2007) Yersiniabactin is a virulence factor for *Klebsiella pneumoniae* during pulmonary infection. *Infect Immun* 75:1463-1472
- Lessie TG, Hendrickson W, Manning BD, Devereux R (1996) Genomic complexity and plasticity of *Burkholderia cepacia*. *FEMS Microbiol Lett* 144:117-128
- Levitzki A, Koshland DE, Jr. (1972) Ligand-induced dimer-to-tetramer transformation in cytosine triphosphate synthetase. *Biochemistry* 11:247-253
- Lewenza S, Conway B, Greenberg EP, Sokol PA (1999) Quorum sensing in *Burkholderia cepacia*: identification of the *LuxRI* homologs *CepRI*. *J Bacteriol* 181:748-756
- Lewenza S, Sokol PA (2001) Regulation of ornibactin biosynthesis and N-acyl-L-

homoserine lactone production by *CepR* in *Burkholderia cepacia*. J Bacteriol
183:2212-2218

Lieberman I, Kornberg A (1954) Enzymatic synthesis and breakdown of a pyrimidine,
orotic acid. I. Dihydroorotic acid, ureidosuccinic acid, and 5-
carboxymethylhydantoin. J Biol Chem 207:911-924

Linscott AJ (1996) Regulatory divergence of aspartate transcarbamoylase from the
pseudomonads. Ph. D. dissertation, University of North Texas, Denton, Texas

Lipscomb WN (1994) Aspartate transcarbamylase from *Escherichia coli*: activity and
regulation. Adv Enzymol Relat Areas Mol Biol 68:67-151

Long C, Koshland DE, Jr. (1978) Cytidine triphosphate synthetase. Methods Enzymol
51:79-83

Long CW, Pardee AB (1967) Cytidine triphosphate synthetase of *Escherichia coli* B.
I. Purification and kinetics. J Biol Chem 242:4715-4721

MacKenzie FM, Gould IM, Chapman DG, Jason D (1994) Comparison of
methodologies used in assessing the postantibiotic effect. J Antimicrob
Chemother 34:223-230

Mahenthiralingam E, Baldwin A, Dowson CG (2008) *Burkholderia cepacia* complex
bacteria: opportunistic pathogens with important natural biology. J Appl

Microbiol 104:1539-1551

Mahenthiralingam E, Baldwin A, Vandamme P (2002) *Burkholderia cepacia* complex infection in patients with cystic fibrosis. J Med Microbiol 51:533-538

Mahenthiralingam E, Urban TA, Goldberg JB (2005) The multifarious, multireplicon *Burkholderia cepacia* complex. Nat Rev Microbiol 3:144-156

Mahenthiralingam E, Vandamme P (2005) Taxonomy and pathogenesis of the *Burkholderia cepacia* complex. Chron Respir Dis 2:209-217

Maksimova NP, Blazhevich OV, Fomichev Iu K (1993) [The role of pyrimidines in the biosynthesis of the fluorescing pigment pyoverdine Pm in *Pseudomonas putida* M]. Mol Gen Mikrobiol Virusol:22-26

Malott RJ, Baldwin A, Mahenthiralingam E, Sokol PA (2005) Characterization of the cciIR quorum-sensing system in *Burkholderia cenocepacia*. Infect Immun 73:4982-4992

Mandel M, Higa A (1970) Calcium-dependent bacteriophage DNA infection. J Mol Biol 53:159-162

McClellan S, Callaghan M (2009) *Burkholderia cepacia* complex: epithelial cell-pathogen confrontations and potential for therapeutic intervention. J Med Microbiol 58:1-12

- McFarland WC, Stocker BA (1987) Effect of different purine auxotrophic mutations on mouse-virulence of a Vi-positive strain of *Salmonella dublin* and of two strains of *Salmonella typhimurium*. *Microb Pathog* 3:129-141
- Meyer JM, Hohnadel D, Halle F (1989) Cepabactin from *Pseudomonas cepacia*, a new type of siderophore. *J Gen Microbiol* 135:1479-1487
- Meyer JM, Van VT, Stintzi A, Berge O, Winkelmann G (1995) Ornibactin production and transport properties in strains of *Burkholderia vietnamiensis* and *Burkholderia cepacia* (formerly *Pseudomonas cepacia*). *Biometals* 8:309-317
- Michaux S, Paillisson J, Carles-Nurit MJ, Bourg G, Allardet-Servent A, Ramuz M (1993) Presence of two independent chromosomes in the *Brucella melitensis* 16M genome. *J Bacteriol* 175:701-705
- Navre M, Schachman HK (1983) Synthesis of aspartate transcarbamoylase in *Escherichia coli*: transcriptional regulation of the pyrB-pyrI operon. *Proc Natl Acad Sci U S A* 80:1207-1211
- Noureddini H, Gao X, Philkana RS (2005) Immobilized *Pseudomonas cepacia* lipase for biodiesel fuel production from soybean oil. *Bioresour Technol* 96:769-777
- O'Donovan GA, Gerhart JC (1972) Isolation and partial characterization of regulatory mutants of the pyrimidine pathway in *Salmonella typhimurium*. *J Bacteriol* 109:1085-1096

- O'Donovan GA, Neuhard J (1970) Pyrimidine metabolism in microorganisms. *Bacteriol Rev* 34:278-343
- O'Donovan GA, Shanley M (1999) Pyrimidine Metabolism in *Pseudomonas*. Paths to Pyrimidines. *An International Newsletter*:7:49-63
- Ornston LN, Stanier RY (1966) The conversion of catechol and protocatechuate to beta-ketoadipate by *Pseudomonas putida*. *J Biol Chem* 241:3776-3786
- Pardee AB, Yates RA (1956) Pyrimidine biosynthesis in *Escherichia coli*. *J Biol Chem* 221:743-756
- Parke JL, Gurian-Sherman D (2001) Diversity of the *Burkholderia cepacia* complex and implications for risk assessment of biological control strains. *Annu Rev Phytopathol* 39:225-258
- Patel MV (2000) The regulatory roles of PyrR and Crc in pyrimidine metabolism in *Pseudomonas aeruginosa*. Ph.D. dissertation, University of North Texas, Denton, Texas
- Payne GW, Ramette A, Rose HL, Weightman AJ, Jones TH, Tiedje JM, Mahenthiralingam E (2006) Application of a recA gene-based identification approach to the maize rhizosphere reveals novel diversity in *Burkholderia* species. *FEMS Microbiol Lett* 259:126-132

Porter TN, Li Y, Raushel FM (2004) Mechanism of the dihydroorotase reaction.
Biochemistry 43:16285-16292

Pratt LA, Kolter R (1999) Genetic analyses of bacterial biofilm formation. Curr Opin
Microbiol 2:598-603

Prescott LM, Jones ME (1969) Modified methods for the determination of carbamyl
aspartate. Anal Biochem 32:408-419

Purcarea C, Herve G, Ladjimi MM, Cunin R (1997) Aspartate transcarbamylase from
the deep-sea hyperthermophilic archaeon *Pyrococcus abyssi*: genetic organization,
structure, and
expression in *Escherichia coli*. J Bacteriol 179 (13): 4143-57

Rashid MH, Kornberg A (2000) Inorganic polyphosphate is needed for swimming,
swarming, and twitching motilities of *Pseudomonas aeruginosa*. Proc Natl
Acad Sci U S A 97:4885-4890

Rashid MH, Rumbaugh K, Passador L, Davies DG, Hamood AN, Iglewski BH,
Kornberg A (2000) Polyphosphate kinase is essential for biofilm development,
quorum sensing, and virulence of *Pseudomonas aeruginosa*. Proc Natl Acad
Sci U S A 97:9636-9641

Reddy M (1997) Status on commercial development of *Burkholderia cepacia* for

biological control of fungal pathogens and growth enhancement of conifer seedlings for a global market. In: US Forest service general technical report PNW. US Forest service Washington, pp p. 235-244

Rodley PD, Romling U, Tummler B (1995) A physical genome map of the *Burkholderia cepacia* type strain. Mol Microbiol 17:57-67

Saiman L, Cacalano G, Prince A (1990) *Pseudomonas cepacia* adherence to respiratory epithelial cells is enhanced by *Pseudomonas aeruginosa*. Infect Immun 58:2578-2584

Sajjan SU, Forstner JF (1992) Identification of the mucin-binding adhesin of *Pseudomonas cepacia* isolated from patients with cystic fibrosis. Infect Immun 60:1434-1440

Samant S, Lee H, Ghassemi M, Chen J, Cook JL, Mankin AS, Neyfakh AA (2008) Nucleotide Biosynthesis Is Critical for Growth of Bacteria in Human Blood. PLoS Pathog

Sambrook J, Fritsch EF, Maniatis T (1989) Molecular Cloning. A Laboratory Manual. 2nd Edition.

Scapin G, Sacchettini JC, Dessen A, Bhatia M, Grubmeyer C (1993) Primary structure and crystallization of orotate phosphoribosyltransferase from *Salmonella typhimurium*. J Mol Biol 230:1304-1308

- Schurr MJ, Vickrey JF, Kumar AP, Campbell AL, Cunin R, Benjamin RC, Shanley MS, O'Donovan GA (1995) Aspartate transcarbamoylase genes of *Pseudomonas putida*: requirement for an inactive dihydroorotase for assembly into the dodecameric holoenzyme. *J Bacteriol* 177:1751-1759
- Schwyn B, Neilands JB (1987) Universal chemical assay for the detection and determination of siderophores. *Anal Biochem* 160(1): 47-56.
- Serino G, Maliga P (1997) A negative selection scheme based on the expression of cytosine deaminase in plastids. *Plant J* 12:697-701
- Shepherdson M, McPhail D (1993) Purification of aspartate transcarbamoylase from *Pseudomonas syringae*. *FEMS Microbiol Lett* 114:201-205
- Sim SH, Yu Y, Lin CH, Karuturi RK, Wuthiekanun V, Tuanyok A, Chua HH, Ong C, Paramalingam SS, Tan G, Tang L, Lau G, Ooi EE, Woods D, Feil E, Peacock SJ, Tan P (2008) The core and accessory genomes of *Burkholderia pseudomallei*: implications for human melioidosis. *PLoS Pathog* 4:e1000178
- Simmer JP, Kelly RE, Scully JL, Grayson DR, Rinker AG, Jr., Bergh ST, Evans DR (1989) Mammalian aspartate transcarbamylase (ATCase): sequence of the ATCase domain and interdomain linker in the CAD multifunctional polypeptide and properties of the isolated domain. *Proc Natl Acad Sci U S A* 86:4382-4386

- Sokol PA (1986) Production and utilization of pyochelin by clinical isolates of *Pseudomonas cepacia*. *J Clin Microbiol* 23:560-562
- Sokol PA, Lewis CJ, Dennis JJ (1992) Isolation of a novel siderophore from *Pseudomonas cepacia*. *J Med Microbiol* 36:184-189
- Souciet JL, Nagy M, Le Gouar M, Lacroute F, Potier S (1989) Organization of the yeast URA2 gene: identification of a defective dihydroorotase-like domain in the multifunctional carbamoylphosphate synthetase-aspartate transcarbamylase complex. *Gene* 79:59-70
- Sousa SA, Ramos CG, Leitao JH (2010) *Burkholderia cepacia* Complex: Emerging Multihost Pathogens Equipped with a Wide Range of Virulence Factors and Determinants. *Int J Microbiol* 2011
- Stephan H, Freund S, Beck W, Jung G, Meyer JM, Winkelmann G (1993) Ornibactins--a new family of siderophores from *Pseudomonas*. *Biometals* 6:93-100
- Thompson JD, Gibson TJ, Plewniak F, Jeanmougin F, Higgins DG (1997) The CLUSTAL_X windows interface: flexible strategies for multiple sequence alignment aided by quality analysis tools. *Nucleic Acids Res* 25:4876-4882
- Tomich M, Herfst CA, Golden JW, Mohr CD (2002) Role of flagella in host cell invasion by *Burkholderia cepacia*. *Infect Immun* 70:1799-1806

- Tuanyok A, Leadem BR, Auerbach RK, Beckstrom-Sternberg SM, Beckstrom-Sternberg JS, Mayo M, Wuthiekanun V, Brettin TS, Nierman WC, Peacock SJ, Currie BJ, Wagner DM, Keim P (2008) Genomic islands from five strains of *Burkholderia pseudomallei*. *BMC Genomics* 9:566
- Tumapa S, Holden MT, Vesaratchavest M, Wuthiekanun V, Limmathurotsakul D, Chierakul W, Feil EJ, Currie BJ, Day NP, Nierman WC, Peacock SJ (2008) *Burkholderia pseudomallei* genome plasticity associated with genomic island variation. *BMC Genomics* 9:190
- Turnbough CL, Jr., Hicks KL, Donahue JP (1983) Attenuation control of pyrBI operon expression in *Escherichia coli* K-12. *Proc Natl Acad Sci U S A* 80:368-372
- Turnbough CL, Jr., Switzer RL (2008) Regulation of pyrimidine biosynthetic gene expression in bacteria: repression without repressors. *Microbiol Mol Biol Rev* 72:266-300, table of contents
- Van Haute E, Joos H, Maes M, Warren G, Van Montagu M, Schell J (1983) Intergeneric transfer and exchange recombination of restriction fragments cloned in pBR322: a novel strategy for the reversed genetics of the Ti plasmids of *Agrobacterium tumefaciens*. *EMBO J* 2:411-417
- Vandamme P, Mahenthiralingam E (2003) Strains from the *Burkholderia cepacia* Complex: Relationship to Opportunistic Pathogens. *J Nematol* 35:208-211

- Vandamme P, Opelt K, Knochel N, Berg C, Schonmann S, De Brandt E, Eberl L, Falsen E, Berg G (2007) *Burkholderia bryophila* sp. nov. and *Burkholderia megapolitana* sp. nov., moss-associated species with antifungal and plant-growth-promoting properties. *Int J Syst Evol Microbiol* 57:2228-2235
- Vanlaere E, Baldwin A, Gevers D, Henry D, De Brandt E, LiPuma JJ, Mahenthiralingam E, Speert DP, Dowson C, Vandamme P (2009) Taxon K, a complex within the *Burkholderia cepacia* complex, comprises at least two novel species, *Burkholderia contaminans* sp. nov. and *Burkholderia lata* sp. nov. *Int J Syst Evol Microbiol* 59:102-111
- Vanlaere E, Lipuma JJ, Baldwin A, Henry D, De Brandt E, Mahenthiralingam E, Speert D, Dowson C, Vandamme P (2008) *Burkholderia latens* sp. nov., *Burkholderia diffusa* sp. nov., *Burkholderia arboris* sp. nov., *Burkholderia seminalis* sp. nov. and *Burkholderia metallica* sp. nov., novel species within the *Burkholderia cepacia* complex. *Int J Syst Evol Microbiol* 58:1580-1590
- Vickrey JF, Herve G, Evans DR (2002) *Pseudomonas aeruginosa* aspartate transcarbamoylase. Characterization of its catalytic and regulatory properties. *J Biol Chem* 277:24490-24498
- Visca P, Ciervo A, Sanfilippo V, Orsi N (1993) Iron-regulated salicylate synthesis by *Pseudomonas* spp. *J Gen Microbiol* 139:1995-2001
- Wang YR, Xiao XZ, Huang SN, Luo FJ, You JL, Luo H, Luo ZY (1996) Heat shock

pretreatment prevents hydrogen peroxide injury of pulmonary endothelial cells and macrophages in culture. *Shock* 6:134-141

Washabaugh MW, Collins KD (1986) Dihydroorotase from *Escherichia coli*. Sulfhydryl group-metal ion interactions. *J Biol Chem* 261:5920-5929

Whitby PW, Vanwagoner TM, Springer JM, Morton DJ, Seale TW, Stull TL (2006) *Burkholderia cenocepacia* utilizes ferritin as an iron source. *J Med Microbiol* 55:661-668

Wigley P, Burton NF (2000) Multiple chromosomes in *Burkholderia cepacia* and *B. gladioli* and their distribution in clinical and environmental strains of *B. cepacia*. *J Appl Microbiol* 88:914-918

Wild JR, Foltermann KF, Roof WD, O'Donovan GA (1981) A mutation in the catalytic cistron of aspartate carbamoyltransferase affecting catalysis, regulatory response and holoenzyme assembly. *Nature* 292:373-375

Wild JR, Loughrey-Chen SJ, Corder TS (1989) In the presence of CTP, UTP becomes an allosteric inhibitor of aspartate transcarbamoylase. *Proc Natl Acad Sci U S A* 86:46-50

Womack JE, O'Donovan GA (1978) Orotic acid excretion in some wild-type strains of *Escherichia coli* K-12. *J Bacteriol* 136:825-827

Yabuuchi E, Kosako Y, Oyaizu H, Yano I, Hotta H, Hashimoto Y, Ezaki T, Arakawa M (1992) Proposal of *Burkholderia* gen. nov. and transfer of seven species of the genus *Pseudomonas* homology group II to the new genus, with the type species *Burkholderia cepacia* (Palleroni and Holmes 1981) comb. nov. *Microbiol Immunol* 36:1251-1275

Yoder-Himes DR, Konstantinidis KT, Tiedje JM (2010) " Identification of potential therapeutic targets for *Burkholderia cenocepacia* by comparative transcriptomics." *PLoS One* 5 (1): e8724

Zientz E, Dandekar T, Gross R (2004) Metabolic interdependence of obligate intracellular bacteria and their insect hosts. *Microbiol Mol Biol Rev* 68:745-770